

Interactions between tetraalkylammonium ions and silicates

Citation for published version (APA):

Donck, van der, J. C. J. (1992). *Interactions between tetraalkylammonium ions and silicates*. [Phd Thesis 1 (Research TU/e / Graduation TU/e), Chemical Engineering and Chemistry]. Technische Universiteit Eindhoven. <https://doi.org/10.6100/IR384131>

DOI:

[10.6100/IR384131](https://doi.org/10.6100/IR384131)

Document status and date:

Published: 01/01/1992

Document Version:

Publisher's PDF, also known as Version of Record (includes final page, issue and volume numbers)

Please check the document version of this publication:

- A submitted manuscript is the version of the article upon submission and before peer-review. There can be important differences between the submitted version and the official published version of record. People interested in the research are advised to contact the author for the final version of the publication, or visit the DOI to the publisher's website.
- The final author version and the galley proof are versions of the publication after peer review.
- The final published version features the final layout of the paper including the volume, issue and page numbers.

[Link to publication](#)

General rights

Copyright and moral rights for the publications made accessible in the public portal are retained by the authors and/or other copyright owners and it is a condition of accessing publications that users recognise and abide by the legal requirements associated with these rights.

- Users may download and print one copy of any publication from the public portal for the purpose of private study or research.
- You may not further distribute the material or use it for any profit-making activity or commercial gain
- You may freely distribute the URL identifying the publication in the public portal.

If the publication is distributed under the terms of Article 25fa of the Dutch Copyright Act, indicated by the "Taverne" license above, please follow below link for the End User Agreement:

www.tue.nl/taverne

Take down policy

If you believe that this document breaches copyright please contact us at:

openaccess@tue.nl

providing details and we will investigate your claim.

**INTERACTIONS BETWEEN
TETRAALKYLAMMONIUM IONS
AND SILICATES**

J.C.J. van der Donck

INTERACTIONS BETWEEN TETRAALKYLAMMONIUM IONS AND SILICATES

PROEFSCHRIFT

ter verkrijging van de graad van doctor aan de
Technische Universiteit Eindhoven, op gezag van
de Rector Magnificus, prof. dr. J.H. van Lint,
voor een commissie aangewezen door het College
van Dekanen in het openbaar te verdedigen op
dinsdag 17 november 1992 om 16.00 uur

door

Jacques Cor Johan van der Donck
geboren te Oranjestad (Aruba)

Dit proefschrift is goedgekeurd door de promotoren

prof. dr. H.N. Stein

en

prof. dr. R.A. van Santen

voor Angela

CONTENTS.

CHAPTER I	INTRODUCTION.	1
	References.	6
CHAPTER II	VISCOSITY OF SILICATE SOLUTIONS.	8
2.1	Introduction.	8
2.2	Theory: The Jones-Dole coefficients.	11
2.2.1	The A coefficient.	11
2.2.2	The B coefficient.	14
2.2.2.1	The addition of B coefficients.	16
2.2.2.2	Splitting of B coefficients into ionic contributions.	16
2.2.3	The D coefficient.	18
2.2.4	Viscosities of silicate solutions.	20
2.3	Experimental.	21
2.3.1	Determination of Nernstian behaviour.	21
2.3.1.1	Materials.	21
2.3.1.2	Procedure.	22
2.3.2	Viscosity measurements.	22
2.3.2.1	Materials.	23
2.3.2.2	Procedure.	23
2.4	Results.	24
2.5	Discussion.	28
2.5.1	The B coefficient.	28
2.5.2	The A coefficient.	29
2.5.3	The D coefficient.	33
2.6	Conclusions.	34
	References.	34

CHAPTER III	COACERVATION IN AQUEOUS SOLUTIONS OF TAA BROMIDES AND SODIUM SILICATE.	37
3.1	Introduction.	37
3.2	Theory.	40
3.3	Experimental.	50
3.3.1	Materials.	50
3.3.2	Analyses of the coexisting phases.	51
3.3.3	Titration method.	52
3.4	Results and discussion.	53
3.4.1	Analyses of the coexisting phases.	53
3.4.2	Titration method.	58
3.4.3	Combination of the analyses of the coexisting phases and titration.	63
3.4.3.1	Contribution of the activity coefficients.	63
3.4.3.2	Comparison of the experiments with the calculated binodals.	65
3.4.3.3	Constants of the excess Gibbs free energy.	71
3.5	Conclusions.	76
	References.	77
CHAPTER IV	ADSORPTION OF TAA BROMIDE ON SILICA.	80
4.1	Introduction.	80
4.2	Theory.	82
4.2.1	The electrical double layer.	82
4.2.2	Adsorption models.	86
4.2.2.1	The Stern model.	86
4.2.2.2	The Site binding model.	88
4.2.2.3	The surface-ligand model.	89

4.2.2.4	Stimulated adsorption	91
4.2.2.5	Model of hydrophobic monolayer/hydrophilic bilayer.	93
4.2.2.6	Adsorption of TAA according to Rutland and Pashley.	95
4.3	Experimental.	98
4.3.1	Materials.	98
4.3.2	Measurement of the ζ potential.	98
4.3.3	Determination of the surface charge.	100
4.3.4	Adsorption of TAA ions on silica.	101
4.4	Results and discussion.	101
4.4.1	ζ potentials of silica.	101
4.4.2	Surface charge of silica.	106
4.4.3	Adsorption of TAA ions on silica.	117
4.5	Conclusions.	132
	References.	133
CHAPTER V	CONCLUSIONS.	136
Appendix A	Viscosity of silicate solutions.	143
Appendix B	Molar fractions of electrolytes.	146
Appendix C	Calculations with the G-function.	149
Summary		150
Samenvatting		152
Curriculum Vitae		154
Dankwoord		155

CHAPTER I:

INTRODUCTION

Silicate chemistry is comparable to carbon chemistry when we consider its tremendous complexity. An enormous quantity of silicate compounds exists. Every silicate compound is in equilibrium with other silicates. In the solid phase reactions will be quite slow but in aqueous solution reactions are fast. This impedes purification and identification of silicate compounds in solutions. Nowadays silicates can be identified with ^{29}Si -NMR. As chemical equilibria are not disturbed with this technic it is very suitable for the determination of silicate ions in solutions. Recently work in this field was published by Wijnen [1] and McGormick [2].

At present zeolite synthesis has become an important field of research in silicate chemistry. Zeolites are crystalline, microporous structures which contain mainly silica and alumina. They are used as additives in washing machine detergents, as drying agents and form selective supports for catalysts and many other purposes.

In the last decades the number of synthetic zeolites has been extended. Usually zeolite syntheses follows a general scheme:

A silica source, usually a gel, is dissolved in a base. Depending on the kind of zeolite required an alumina source is added. The reaction mixture is hydrothermally treated. It is thought that in the solution large silicate ions are present which are the primary building units of the zeolite. These units are joined together and a zeolite is formed. Under hydrothermal conditions some zeolites are not stable. After some time quartz is formed by decomposition of the zeolite.

Chapter I

In the beginning zeolites were prepared by treating aluminosilicate gels with alkali and alkaline earth metal hydroxides. But nowadays frequently templates are used. Templates are organic molecules or ions. A wide variety of substances is used as templates (TABLE 1.1).

TABLE 1.1: Templates used in zeolite syntheses

	Structure	Reference
TMA	Sodalite	3,4
TEA	ZSM-8	5
	ZSM-12	6
	ZSM-20	7
	Mordenite	8,9
TPA	ZSM-5	10
TBA	ZSM-11	11
Methyltriethylammonium	ZSM-12	12
n-Propylamine	ZSM-5	13,14
Choline	ZSM-38	15,16
	ZSM-34	17
	ZSM-43	18
	CZH-5	19
Pyrrolidine	ZSM-35	20
	ZSM-21	15,16
	ZSM-23	21
$H_2N-(CH_2)_n-NH_2$		
n=2-6	ZSM-5	22,23,24,25
n=7-10	ZSM-11	26,27
n=2	ZSM-21	15,16
n=2, 3, 4	ZSM-35	20,22,23,24
n=8	ZSM-48	26,27

TMA is Tetramethylammonium, TEA is tetraethylammonium, TPA is tetrapropylammonium and TBA is tetrabutylammonium.

Chapter I

TABLE I doesn't claim to be a complete list of templates. A large quantity of compounds can be used for this purpose. For some zeolites mixtures of templates are used. Examples of this are mixtures of templates as TMA and TEA [28,29] and TMA and n-Propylamine [28,29,30,31] or mixtures of templates with alkali metal cations as TMA with sodium [32,33].

As is very clear in TABLE I a large number of zeolites can be formed with the use of templates. Some zeolites can be synthesised with several kinds of templates, and with some templates several kinds of zeolites can be obtained.

During the synthesis the template influences a lot of processes on molecular scale.

At first the dissolution of the silica is influenced. Wijnen [1] shows that the dissolution rate is dependent on the base cation. Potassium hydroxide dissolves the silica fast while TMA hydroxide has a low dissolution rate.

In the solution formed a lot of different kinds of silicate ions are formed. The cation present has a large influence on the distribution of the silicate over the different structures. For the anorganic bases only subtle changes have been found in silicate distribution but for the organic bases the silicate distribution is strongly influenced by the kind of organic cation present. In the presence of TMA Hoebbel et.al. [34,35,36] found the cubic octameric silicate ion $\text{Si}_8\text{O}_{20}^{8-}$. For TEA they found the hexagonal prismatic $\text{Si}_6\text{O}_{15}^{6-}$ and for TPA they found the pentagonal $\text{Si}_{10}\text{O}_{25}^{10-}$. These larger silicate ions are sometimes present in sodium or potassium silicate solutions but never in the quantities as found for the tetraalkylammonium (TAA) ions. These large double ring silicate ions are thought to be the primary building units of the zeolite.

Chapter I

The large silicate ions are joined together to form the zeolite. This process is also influenced by the TAA ions. By comparing the synthesis of the ZSM-5 zeolite with TPA as template the reaction rate is much higher than with TEA as template. The difference can only be explained by differences in the joining rate of the large silicate ions. Knight et.al. [37] found an unexpected slow approach to thermodynamic equilibrium of the silicate anion in aqueous TMA silicate solutions. This may favour side reactions as the coupling of the primary building units.

When inorganic bases are used the zeolite is not the most stable form. The zeolite reacts further to quartz. When organic bases are used this is not observed. According to Jansen and van Beckum [38] the organic cation is present in the cavities of the zeolite. The presence of the template in the cavities of the zeolite is expected to prohibit the zeolite-quartz rearrangement. This is thought to be another important role of the organic cation as a template.

A special group of templates are the symmetrical quaternary ammonium ions. They are used for the syntheses of sodalite, silicalite, ZSM-5 [3,4] and many others. The kind of zeolite formed depends on the kind of base, the silica/alumina ratio, the silica/base ratio and the temperature. The differences in structure are probably due to differences in interactions between the ionic species. In all steps of the synthesis differences in behaviour are found depending on the kind of cation. This means that in every step of the synthesis interactions between the cation and the silica take place which have a large influence on the formation of the zeolite.

In this thesis we want to investigate the processes which take place on a molecular scale. The systems encountered in the zeolite syntheses have a

Chapter I

quite complicated composition therefore we rather study model systems. A good model system is a solution of a quaternary ammonium salt which is in contact with solid silica. By investigating the adsorption behaviour information can be obtained about the interaction of the template with a silica surface. Another system which can serve as a model system is a solution of a quaternary ammonium silicate. The dependence of the silicate composition on the kind of cation, as found by Hoebbel [34,35,36], shows that even in homogeneous solutions specific interactions between the ions are present. These systems are typical colloid chemical model systems and by means of colloid chemical methods it should be possible to obtain information about these interactions. Although many research efforts have been spent on the zeolite syntheses, until now hardly anything is known about the colloid chemistry of systems containing silica and quaternary ammonium ions.

In the next chapters attention will be paid to viscosities of silicate solutions (chapter II) and adsorption of quaternary ammonium ions on silica surfaces (chapter IV). The viscosity of a solution is determined by the interactions that take place in solutions. These interactions are for instance: solvent-solvent interactions, solvent-solute interactions and solute-solute interactions. In chapter II we want to obtain insight in processes on a molecular scale.

During the research an interesting phenomena was observed: coacervation. This is demixing of the homogeneous aqueous solutions into two aqueous phases. Usually coacervation takes place in solutions which contain interionic interactions. It is likely that these interactions are the same as those encountered in the zeolite syntheses. Therefore the research was extended to coacervating systems (chapter III).

Chapter I

References.

- [1] P. Wijnen, thesis, Eindhoven, 1990.
- [2] A.V. McGormick, thesis, Berkeley, 1987.
- [3] C. Baerlocher and W.M. Meier, *Helv. Chim. Acta*, 52(1969)1853.
- [4] C. Baerlocher and W.M. Meier, *Helv. Chim. Acta*, 53(1970)1285.
- [5] Mobil Oil Corp., *Neth. Pat.* 7 014 807 (1971).
- [6] E.J. Rosinski and M. Rubin, *US Pat.* 3 832 449 (1974).
- [7] J. Ciric, *US Pat.* 3 972 983 (1976).
- [8] P. Chu, *US Pat.* 3 766 093 (1973).
- [9] C.D. Chang, W.H. Lang and A.J. Silvestri, *US Pat.* 3 894 104 (1975).
- [10] R.J. Argauer and G.R. Landolt, *US Pat.* 3 702 886 (1972).
- [11] P. Chu, *US Pat.* 3 979 (1973).
- [12] P. Chu and G.H. Kuehl, *Eur. Pat. Appl.* 18 038 (1980).
- [13] M. Rubin, E.J. Rosinski and C.J. Plank, *US Pat.* 4 151 489 (1979)
- [14] G.F. Dwyer and P. Chu, *Eur. Pat. Appl.* 11 362 (1980).
- [15] C.J. Plank, M. Rubin and E.J. Rosinski, *US Pat.* 4 105 541 (1987).
- [16] C.J. Plank, E.J. Rosinski and M. Rubin, *US Pat.* 4 046 859 (1977).
- [17] M. Rubin, E.J. Rosinski and C.J. Plank, *US Pat.* 4 086 186 (1987).
- [18] M. Rubin, E.J. Rosinski and C.J. Plank, *US Pat.* 4 247 728 (1981).
- [19] D.A. Hickson, *UK Pat. Appl.* 2 079 735 (1982).
- [20] C.J. Plank, E.J. Rosinski and M. Rubin, *US Pat.* 4 016 245 (1977).
- [21] M. Rubin, C.J. Plank and E.J. Rosinski, *US Pat.* 4 104 151 (1987).
- [22] D.A. Hickson *BE Pat.* 8 886 833 (1981).
- [23] L.D. Rollmann, *US Pat.* 4 296 083 (1981).
- [24] L. Marosi, M. Scharzmann and J. Stabenow, *Eur. Pat. Appl.* 49 386 (1982).

Chapter I

- [25] L.D.Rollmann and E.W.Valyocsik, US Pat. 4 139 600 (1979).
- [26] L.D.Rollmann and E.W.Valyocsik, US Pat. 4 108 881 (1978).
- [27] L.D.Rollmann and E.W.Valyocsik, Eur.Pat.Appl. 15 132 (1980).
- [28] F.G.Dwyer and E.E.Jenkins, US Pat. 4 287 166 (1981).
- [29] B.G.Pelgrine, US Pat. 4 259 306 (1981).
- [30] P.Chu, Eur.Pat,Appl. 0 023 089 (1981).
- [31] C.C.Chu, US Pat. 4 260 843 (1981).
- [32] R.Aiello and R.M.Barrer, J.Chem.Soc.A, (1970)1470.
- [33] R.M.Barrer and P.J.Denny, J.Chem.Soc., (1961)971.
- [34] D.Hoebbel, G.Garzó, G.Engelhardt und A.Vargha, Z.anorg.allg. Chem., 494(1982)31.
- [35] D.Hoebbel, A.Vargha, G.Engelhardt und K Ujszászy, Z.anorg.allg. Chem., 509(1984)85.
- [36] D.Hoebbel, A.Vargha, B.Fahlke und G.Engelhardt, Z.anorg.allg. Chem., 521(1985)61.
- [37] C.T.G.Knight, R.J.Kirkpatrick and E.Oldfield, J.Chem.Soc., Chem. Commun., 1986 66-67
- [38] J.C.Jansen and H. van Bekkum, I²-Procestechnologie, 9(1985)5.22

CHAPTER II:

VISCOSITIES OF

SILICATE SOLUTIONS

2.1 Introduction

Interactions in solutions play an important role in the deformation behaviour under shear. This results in a high viscosity for solvents with strong intermolecular interactions and a low viscosity for solvents with weak intermolecular interactions. Solute molecules can change interactions between the solvent molecules and will have interactions with other solute molecules. Therefore the presence of dissolved compounds will have an influence on the viscosity. These interactions can be electrical interaction, hydrodynamical interaction and many others. In this chapter we will discuss the influence of electrolytes, in particular silicates, on the viscosity.

In 1847 Poiseuille [1] was one of the first who studied the influence of electrolytes on the viscosity of water. In the same century Arrhenius [2] developed one of the first theories about the viscosity of electrolyte solutions:

$$\eta_r = \frac{\eta}{\eta^o} = A^c \quad (2.1)$$

In this equation η_r is the relative viscosity, η the viscosity of the electrolyte solution, η^o the viscosity of water and A a constant.

Chapter II

In 1929 Jones and Dole [3,4] found an empirical relation which describes the viscosity of solutions as a function of the electrolyte concentration:

$$\eta_r = 1 + A\sqrt{c} + Bc \quad (2.2)$$

In which c is the molar concentration and A and B are the Jones-Dole coefficients.

This equation was in agreement with experimental data for concentrations up to 0.05 M. For higher concentrations Kaminsky [5] added a term proportional to the square of the concentration: Dc^2 .

$$\eta_r = 1 + A\sqrt{c} + Bc + Dc^2 \quad (2.3)$$

In these equations the coefficients have the following meaning:

A describes long range electrostatic interactions.

B describes solute-solvent interactions.

D describes solute-solute interactions other than electrostatic interactions.

This division is not quite accurate since higher order terms of the two first mentioned effects are incorporated in the D coefficient.

Other equations describe the dependence of the viscosity on the temperature. The viscosity of water is strongly temperature dependent. At high temperature the viscosity is lower than at low temperature. Sepulveda and Gamboa [6] give an exponential relation between viscosity and temperature:

Chapter II

$$\ln (\eta_r) \propto \frac{1}{T} \quad (2.4)$$

T is the temperature in K.

They attributed the slope of this curve to the activation energy for the creation of a hole in the liquid. Electrolytes have an influence on flow by influencing these holes as is described in work of Werblan [7], Feakins et.al [8] and Crudden et.al.[9,10]. This mechanism is usually called activated flow.

For describing viscosity data as a function of concentration the Jones-Dole equation and the activated flow theories are available. The Jones-Dole equation seems to be most useful, because it describes the viscosity in terms of interaction parameters. These parameters are supported by quantitative and semi quantitative theories by work of Falkenhagen [11,12,13], Onsager [14], Stokes and Mills [15] and Palma and Morel [16]. The theories about activated flow are still in an empirical stage. The molecular view of the activated flow model is not completely satisfactorily. In addition, in activated flow mechanism only the influence of solute-solvent interactions are considered, while Jones and Dole clearly show that other interactions (for instance long range electrostatic interactions) are not negligible. Therefore the mechanism of activated flow cannot describe all aspects of viscous behaviour. As the Jones-Dole B coefficient describes solute-solvent interactions, the mechanism of activated flow can possibly contribute to the theoretical back-

Chapter II

ground of this parameter. The Jones-Dole equation is fit for describing the viscosity of electrolyte solutions and is a first step for the interpretation of viscosity data to processes on a molecular scale.

In this chapter the Jones-Dole A, B and D coefficients are reported for solutions of TMA silicate, sodium silicate, potassium silicate and mixtures of TMA and alkali silicate solutions. These values were compared with each other and with the coefficients of other electrolytes. Most theories for the Jones-Dole equation are only valid for strong electrolytes. Since, recently, McGormic [17] showed that in solutions of sodium silicate ion association may take place, deviation from Nernstian behaviour is investigated by means of ion selective electrodes for sodium and potassium ions.

2.2 Theory: The Jones-Dole coefficients.

At first the Jones-Dole equation (equations 2.2 and 2.3) was empirical. However, it did not take long to obtain insight in the physical meaning of these coefficients. In this paragraph the coefficients will be quantified as much as possible and different theories about these coefficients will be discussed.

2.2.1 The A coefficient.

Shortly after the papers by Jones and Dole, Falkenhagen (1929) [11,12,13] and Onsager [14] gave a physical background to the A coefficient. The A coefficient describes the contribution of the long range electrostatic interactions to the viscosity. The main backgrounds will be summarised below.

Chapter II

In solutions of strong electrolytes the behaviour of the ion cloud is described by the Debye-Hückel theory. The Debye-Hückel theory describes a spherical distribution of counter ions around a central ion. Under the influence of shear the charge distribution will become distorted. This causes a gradient in counter ion concentration, and thus a potential difference (disturbed potential), in the shear direction (see Figure 2.1). The counter ions will move back towards their equilibrium position. Because of the size of the ions there will be a drag force present working on the ions and on the solution. This will cause an increase in viscosity.

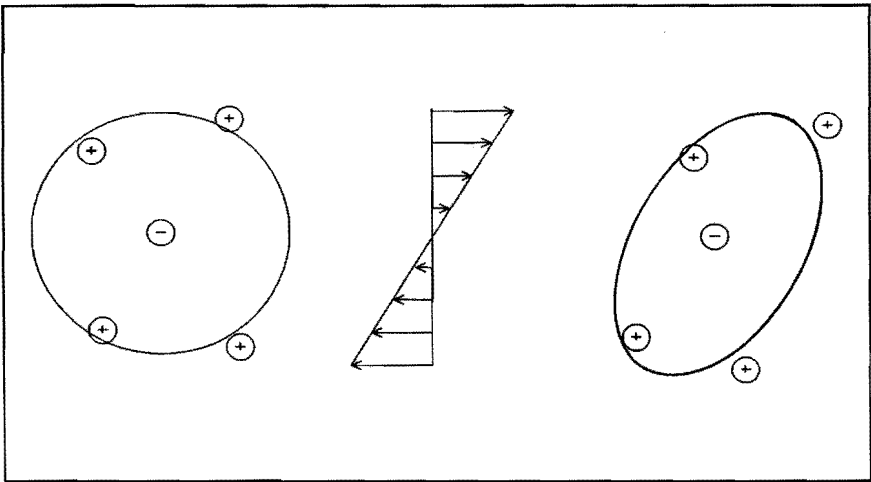


Figure 2.1: Distortion of a charge distribution by shear.

In 1929 an equation was presented by Falkenhagen for symmetrical electrolytes with equal mobilities of cat- and anions [11], but in 1932 the complete formula was available for asymmetrical electrolytes with different

Chapter II

mobilities [13].

In this calculation the products of the concentration of counter ions with the distorted potential are integrated over the ion cloud. At a close distance the distortion is small and the concentration of counter ions large and at large distance the distortion is larger and the counter ion concentration smaller.

The equation for the A coefficient given by Falkenhagen en Vernon [13] is as follows:

$$A = 1.45 \frac{\sqrt{\nu_1 z_1}}{(z_1 + z_2) \eta^\circ \sqrt{D^\circ} T} \phi \quad (2.5)$$

$$\phi = \frac{l_1 z_1^2 + l_2 z_1^2}{4 l_1 l_2} - \frac{(z_2 l_1 - z_1 l_2)^2}{l_1 l_2 \left(\sqrt{l_1 + l_2} + \sqrt{l_1 z_2 + l_2 z_1} \frac{\sqrt{z_1 + z_2}}{\sqrt{z_1 z_2}} \right)^2}$$

In this equation are:

l_1 and l_2 mobilities of ions of types 1 and 2, respectively

z_1 and z_2 valencies of ions of types 1 and 2, respectively

ν_1 number of ions 1 per molecule

η° viscosity of solvent

D° dielectric constant of solvent

T temperature

Chapter II

According to some authors [15,18] the effect of the A coefficient is negligible at higher concentrations. The main reason for this is that in some cases the contribution of the A coefficient will be much smaller than the contribution of the B coefficient. Although at high concentrations the A coefficient will not very accurately reflect electrostatic interactions, because of deviations from Debye-Hückel behaviour, this is no reason to exclude the effect. The distortion of the ion cloud will take place at all concentrations. Therefore it is better to bring the A coefficient into account over the whole concentration range, although we realize that the Debye-Hückel theory is only a rough guide in the more concentrated concentration range.

Equation (2.5) is only valid for strong electrolytes. Weak electrolytes have a less pronounced charge distribution than strong electrolytes. Quintana et.al. [19] gives for the contribution of the electrostatic interactions of a weak electrolyte to the viscosity:

$$A_{Falkenhagen} \sqrt{(1-\alpha)c} \quad (2.6)$$

Here $A_{Falkenhagen}$ is the A coefficient calculated with equation (2.5) and α is the degree of association.

2.2.2 The B coefficient.

As the B coefficient is proportional to the concentration it is widely believed that the B coefficients describe the effect of the solute on its direct environment, the solvent. It is analogous to the viscosity relation of Einstein for dilute suspensions [20] which describes the hydrodynamical interaction of a sphere with the solvent:

Chapter II

$$\eta_r = 1 + 2.5\phi \quad (2.7)$$

in which ϕ is the volume fraction.

Several theories have been reported in order to describe the B coefficient. Some of them consider solute-solvent interactions as being the main cause of the B coefficient [7,8,9,10,21]. Out [22] shows that both hydrodynamics and solute-solvent interactions contribute to the B coefficient.

In 1965 Stokes and Mills [15] presented a semi quantitative theory including both hydrodynamical effects and solute-solvent interactions:

$$B = B_h + B_{orient} + B_{str} \quad (2.8)$$

B_h is the hydrodynamical contribution which originates from the Einstein viscosity relation (equation 2.7), B_{orient} is a positive contribution due to the orientation of the dipoles of the solvent when a solvent molecule is moving past the ion and B_{str} is a term which brings into account the structure breaking or building properties of the solute.

Krumgalz [23] added a positive term B_{reinf} to equation 2.8 for the reinforcement of structure which is caused by hydrophobic hydration. Although hydrophilic hydration (B_{str}) and hydrophobic hydration (B_{reinf}) are of a different origin, as is suggested by Frank and Wen [24], they both describe the influence of the solute on the solvent structure. Therefore it is probably better to combine these terms, similar to Out [22] and Krumgalz [25]. They give for the B coefficient:

Chapter II

$$B = B_h + B_{str} \quad (2.9)$$

B_{str} is a temperature dependent term which mainly involves the structure breaking and building effects. B_{orient} in equation 2.8 is most probably incorporated in B_{str} . For hydrophobic hydration and structure builders the water surrounding the ion is more or less ice-like. At high temperatures the ice-like hydration structure "melts down". The term B_{str} diminishes and may approach zero at high temperatures. If the ion present is a structure breaker the B_{str} is negative. This means that the hydration structure is less ordered than the bulk solvent. At high temperatures the bulk solvent becomes less ordered. The difference in structure between hydration structure and bulk water decreases and B_{str} approaches to zero.

2.2.2.1 The addition of B coefficients.

The B coefficient describes the solute-solvent interactions. In order to obtain this term, it is supposed to be additively composed of contributions of every single ion in solution. As a consequence of this the B coefficients of mixtures can be calculated by summing the B coefficients of the pure components. Dordick [26] showed that the additivity rule for the B coefficients is valid in the case of alkali halogenides.

2.2.2.2 Splitting of B coefficients into ionic contributions.

A salt is a mixture of cations and anions. It is not very likely that both ions have the same contribution to the viscosity. Every ion will have a characteristic size and influence on the water structure. For the determination of the influence of an ion on the water structure at first the B coefficients found in different salt solutions should be split up into their ionic contri-

Chapter II

butions. Because of the additivity rule, as proved by Dordick, the overall B coefficient will be the sum of the two ionic B coefficients. Two methods are described in the literature for water as solvent.

In 1957 Kaminsky [27] described a suitable method for the splitting of B coefficients. By measuring the electric conductivity it had been found that the effective radius of the potassium ion was nearly equal to that of the chloride ion. Kaminsky supposed that, because of the same valency, the solute-solvent interaction were the same as well. This leads to the conclusion:

$$B_{K^+} = B_{Cl^-} \quad (2.10)$$

In 1979 Desnoyers [28] suggested that Kaminsky's method was not completely accurate. Desnoyers supposed that a better approximation should be that the tetraethylammonium ion in water neither behaves as a structure builder nor as a structure breaker. The ionic B coefficient could be well described with the hydrodynamical term. The hydrodynamical term is calculated with the Einstein relation for viscosity (equation 2.7). The volume fraction, ϕ , was calculated by multiplication of the concentration with the molar volume.

$$\phi = V_m c \quad (2.11)$$

The differences between ionic B coefficients calculated with Kaminsky's method and with Desnoyers method are quite small. Out [22] used Kaminsky's method to calculate the ionic B coefficients. For the ionic B coefficient of the tetraethylammonium ion he found an important temperature

Chapter II

dependent term. Even when calculated with Desnoyers method this temperature dependent term is present. This indicates that the tetraethylammonium ion is a structure builder. This is confirmed by Heuvelsland [29] who measured enthalpies of dissolution (solvation). He calculated the hydrophobic hydration of quaternary ammonium ions. He found that even tetramethylammonium is hydrophobically hydrated. This means that the approximation of Desnoyers [28] is not valid and that in this case there is no alternative for Kaminsky's method.

2.2.3 The D coefficient.

The Jones-Dole equation comprising only the A and B coefficients is found to be valid for concentrations up to 0.05 M. In 1957 Kaminsky [5] added a third term, proportional to the square of the concentration, just like Thomas [30] did with regard to the Einstein equation for viscosity (equation 2.12). In the beginning these D-values were quite inaccurate, but in 1972 Desnoyers and Perron [28] were among the first who published accurate D coefficients. They denoted this term as a mixture term which contains solute-solute interactions; in addition higher order terms of the A and B coefficient are incorporated in the D coefficient. Out calculated the contribution of the higher order term of the B coefficient with the higher order term of the hydrodynamical relation for suspensions which was presented by Thomas [30]:

Chapter II

$$\eta_r = 1 + 2.5\phi + 10.05\phi^2 \quad (2.12)$$

According to Batchelor [31] the coefficient of the ϕ^2 term should be 6.2 because ions can be considered as small particles where Brownian motion plays a role.

Out [22] found that the D coefficient is proportional to the square of the B coefficient of quaternary ammonium salts. Therefore he described the D coefficient in terms of hydrodynamical interactions. For the B coefficient a difference is made for the hydrodynamical contributions and the influence of the solute on the solvent (equation 2.8 and 2.9). For the hydrodynamical contributions for the D coefficient this should be the same. The proportionality of the D coefficient with the square of the B coefficient, as found by Out, cannot be a consequence of hydrodynamics. In solutions of TAA ions large contributions of the solute solvent interactions to the B coefficient are present. The linear correlation between the D coefficient and the square of the B coefficient shows rather that the effect that causes the B coefficient has a quadratic effect on the D coefficient. The B coefficients for the TAA bromides, as found by Out, show a nearly linear dependence on the chain length and the D coefficients show a linear dependence on the square of the chain length. The molar volumes of the TAA ions are not linearly dependent on the chain length. Therefore other interactions than hydrodynamical interactions are the main cause of the B and D coefficients for these ions.

In 1979 Palma and Morel [16] drew a parallel with the work of Frank and Evans [32]. Frank and Evans described the B coefficient in terms of solvent entropy. Palma and Morel calculated for every electrolyte the charac-

Chapter II

teristic solute-solute pair interaction entropy. This entropy gave a linear connection with the D coefficients found in mixtures of TAA bromides with tertiary butanol.

Palma and Morel's work does not give a complete theory describing the D coefficient. A number of effects contribute to this coefficient. In solutions of normal electrolytes, e.g. alkali metal halogenides, the solute-solute interactions are thus small that the high order terms of the A and especially the B coefficient form the principal contribution to the D coefficient. In Palma and Morel's approach for the D coefficient some restrictions have to be mentioned. Probably the high order terms of long range electrostatic interactions and solute solvent interactions have to be subtracted from the experimental D coefficient before relating it to the electrolyte-electrolyte pair interaction entropy. Until now the size of these high order terms is not known. Therefore the use of this theory is restricted.

2.2.4 Viscosity of silicate solutions.

Most of the theories presented until now are only suitable for strong electrolytes. These systems are precisely defined. Silicate systems are far more complicated. Silica can be present in several forms, for instance monomers, dimers, trimers and so on, and the pH of the solutions is high. This means that a considerable amount of hydroxylic ions is present in solution. Therefore the charge on the silica cannot be calculated accurately and a mixture of ions is present. This can have consequences for the coefficients of the Jones-Dole equation.

The behaviour of the A coefficient in mixtures has not been investigated until now. But it is very likely that the ions with the highest mobility

Chapter II

will have the highest influence on the A coefficient. The hydroxylic ions have a very high mobility and therefore they will have a large influence on the A coefficient. In order to avoid complications arising from differences in mobility between the different ions present, we have determined A values from measurements on systems with reasonably constant silicate compositions. These A values will be compared with A values found for other electrolytes. Hoebbel [33,34,35] showed that the number of silicate types is dependent on the concentration, the kind of cation and the silica / base ratio. We have to choose a concentration and silica / base ratio which has a reasonably constant silicate composition.

For the B coefficients of mixtures the additivity rule of Dordick [26] will be used (see section 2.2.2.1).

The situation for the D coefficient can be compared with the A coefficient. A reliable theory about D coefficients of mixtures has not been presented yet. The values can only be used in comparison with other values.

2.3 Experimental.

2.3.1 Determination of Nernstian behaviour.

2.3.1.1 Materials.

Sodium hydroxide, ex Merck Titrisol.

Sodium chloride, PA., ex Merck.

Potassium hydroxide, ex Merck Titrisol.

Potassium bromide, PA., ex Merck.

Precipitated silica, ultra pure, ex Merck.

twice distilled water .

Chapter II

2.3.1.2 Procedure.

Potentials were measured with a Corning Sodium Selective Electrode for the sodium salts and a Philips Potassium Selective Electrode for the potassium salts against an Orion Double Junction Reference Electrode. The potential as function of the concentration for the bromide, hydroxide and silicate salts of sodium and potassium was determined by means of the Orion Autochemistry System 940/960, with the "serial calibration" standard option. Therefore in this chapter the curves of the potential versus the logarithm of the concentration are called "electrode calibration curves". In order to expand the concentration range, solutions with concentration of 2 and .1 M were used to determine the calibration curves. For the silicate solutions the alkali metal / silicate molar ratio was 2:1. All experiments were carried out at 20 °C.

2.3.2 Viscosity measurements.

High precision viscosity measurements were carried out with an automated Ubbelohde capillary viscometer. Viscosities were calculated from the following equation:

$$\eta_r = \frac{t \rho}{t^o \rho^o} SC \quad (2.13)$$

Here t and t^o are the flow times of sample and water respectively, corrected for loss of kinetic energy [36,37]. ρ and ρ^o are the densities of sample and water, respectively. SC is the surface tension correction as given by [38]. Surface tension corrections were calculated from:

Chapter II

$$SC = 1 + K \left(\frac{\sigma^0}{\rho^0} - \frac{\sigma}{\rho} \right) \quad (2.14)$$

where K is a factor which contains geometrical constants of the viscometer, σ^0 and σ are the surface tensions of water and sample, respectively and ρ^0 and ρ are the densities of water and sample, respectively.

2.3.2.1 Materials.

TMA bromide, Merck, >99 %.

TMA hydroxide pentahydrate , 97%, ex Janssen Chimica.

sodium hydroxide, ex Merck Titrisol.

potassium hydroxide, ex Merck Titrisol.

precipitated silica, > ultra pure, ex Merck.

twice distilled water

2.3.2.2 Procedure.

The viscosities of TMA bromide solutions were measured for comparison with literature values in order to check our experimental procedure.

For the silicate solutions stock solutions were made with a base to silica ratio of 2:1. The cation composition was expressed as the molar fraction TMA of all cations. For mixtures of sodium and TMA silicate TMA fractions of 0, 0.25, 0.5, 0.7 and 1 were used and for mixtures of TMA and potassium silicate TMA fractions of 0, 0.25, 0.5, 0.75 and 1. Eight solutions of TMA bromide and of each stock solution were prepared in the concentration range $0.02 \leq c \leq 0.7$ M based on the cation concentration. At the

Chapter II

highest concentration the composition of the silicate ions was determined by a method described by Groenen [39]. No significant differences in silicate composition were found for sodium and TMA silicate solutions. Viscosities were measured using a Schott Ubbelohde viscometer 0a and a Schott Viscosity Measuring unit AVS 310 (± 0.01 s). The temperature was fixed at 25 °C with a LKB 7600 A precision thermostat (± 0.001 °C). Densities were measured with an Anton Paar DMA Calculating Precision Density Meter (± 0.00001 g/ml). Measurements of the surface tensions were carried out with the Krüss tensiometer KT 10 (± 0.1 mN/m) using the Wilhelmy plate method. Surface tensions were found to be dependent on time. This is thought to be due to slow approach to equilibrium. As the liquid in the Ubbelohde viscometer is moving, the surface is not in equilibrium. Therefore the initial surface tension was used in equation 2.14.

2.4 Results.

At first the results of our measurements of TMA bromide are compared with the results obtained by Out [22]. In Figure 2.2 the viscosity of TMA bromide solutions as a function of the concentration is compared with Out's data. The Jones-Dole coefficients obtained from our data were: $A=0.0063$, $B=0.0772$ and $D=0.0581$. The differences between our data and Out's coefficients ($A=0.0063$, $B=0.076$, $D=0.059$) are minimal.

Figure 2.3 gives the electrode calibration curves of the sodium salts (Figure 2.3a) and of the potassium salts (Figure 2.3b). The curves are shifted in vertical direction, by approximately 20 and 40 mV, to emphasize the Nernstian behaviour. If any association of silicate and alkali metal ions takes place, this will be visible as a decrease in slope with increasing

Chapter II

concentration.

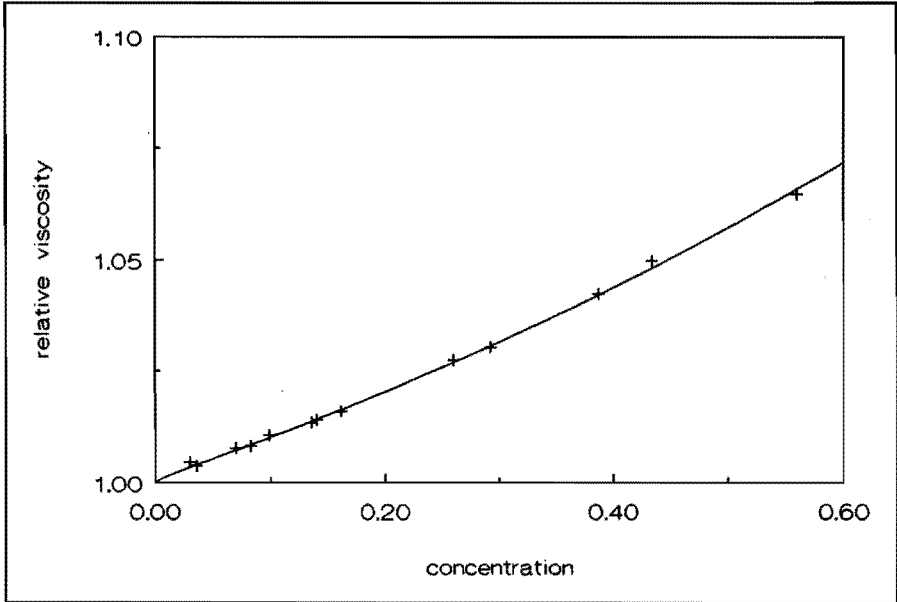


Figure 2.2: Viscosity of TMA bromide as function of the concentration (+ measurements, drawn line Out's results).

Figure 2.4a gives the coefficients of the extended Jones-Dole equation, for the five ratios of TMA silicate and Na silicate. Figure 2.4b gives the Jones-Dole coefficients for the mixtures of TMA and potassium silicate. On the horizontal axis is the fraction of TMA of all cations. These coefficients were obtained, by fitting the experimental data with a method provided by Press et.al. [40], to the extended Jones-Dole equation (equation 2.3). The viscosities are listed in appendix A. The total cation concentration was used

Chapter II

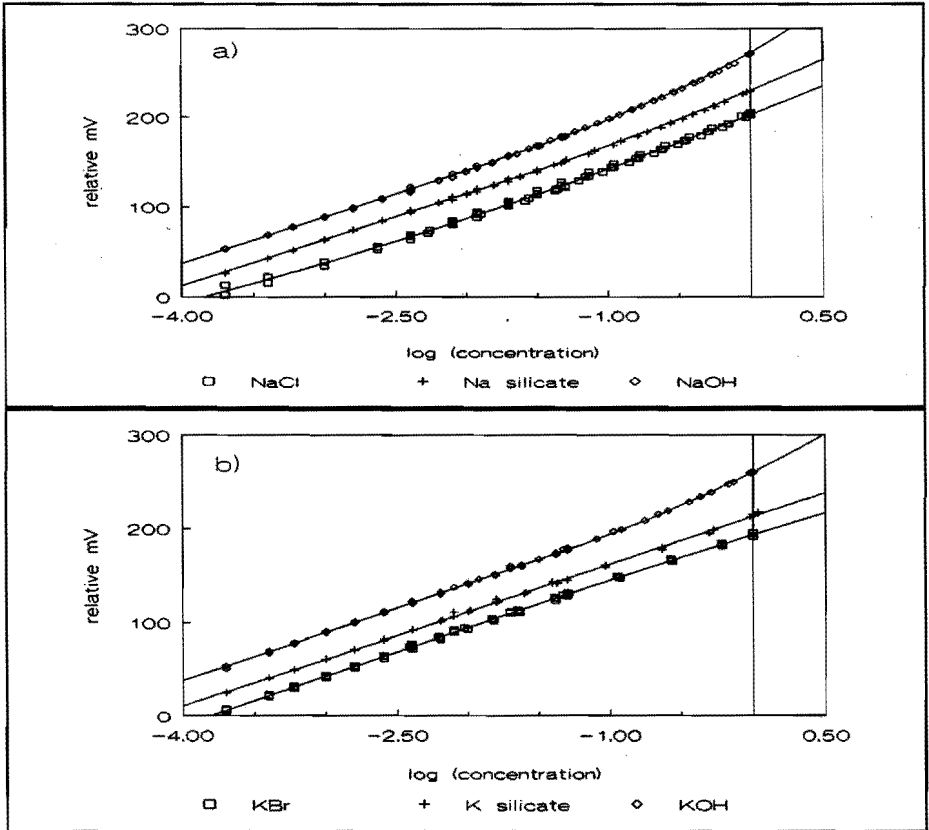


Figure 2.3: Calibration curves of a) sodium salts b) potassium salts.

in the fitting procedure instead of the silica concentration. As a result of this we have to divide literature A coefficients of bivalent electrolytes by $\sqrt{2}$ to adjust them to the concentration scale we used. Because of the additivity rule for the B coefficients, literature values of the B coefficient can be used. The concentration scale we used is particularly convenient for comparison of the A, B and D coefficients of the silicate solutions with those of sodium chloride and TMA bromide. The influence of the silicate ions on the coeffi-

Chapter II

icients is shown most clearly by keeping all other variables constant while the bromide is replaced by the silicate.

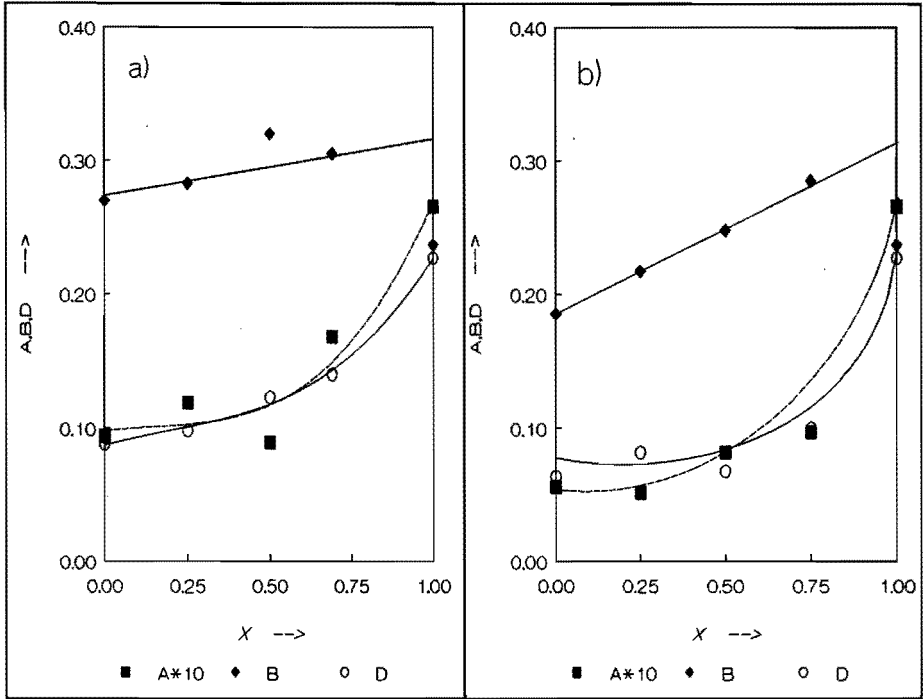


Figure 2.4: Jones-Dole coefficients of silicate solutions as function of the TMA fraction ($10 \cdot A$, B , D), a) sodium-TMA, b) potassium-TMA.

The uncertainties in the viscosities are less than 0.01 %. The uncertainties caused by the fitting procedure, provided by Press et.al. [40], in the A coefficients are about 5 % and in the B and D coefficients are approximately 1 %. The straight lines through the B coefficients are the theoretical lines based on Dordick's [26] additivity rule calculated with data provided by Out [22] (equation 2.15).

Chapter II

2.5 Discussion.

The precision of the coefficients permits to conclude that in Figure 2.4 the curves of the A and D coefficients are significantly convex towards the X-axis. For ratios up to 0.7 the B coefficients can be described as straight lines.

2.5.1 The B coefficient.

The B coefficients were in the range of 0.24 - 0.32 dm³ mole⁻¹ for mixtures of sodium and TMA silicate and for mixtures of potassium and TMA silicate they were in the range of 0.18 - 0.29 dm³ mole⁻¹. Out [22] found for sodium chloride 0.078 dm³ mole⁻¹, for potassium bromide -0.0468 dm³ mole⁻¹ and for TMA bromide 0.076 dm³ mole⁻¹. The difference in B coefficients between the halogenides and the silicates indicates that the contribution of the silicates to the B coefficient is large. As silicate ions have a hydrophilic hydration, the large B coefficient is most probably due to a large B_{str} in equation 2.9. This means that silicate ions have large structured hydration regions and can therefore be considered as structure builder.

According to the additivity of the B coefficients, the curve for sodium TMA mixtures should have been a straight line, described by:

$$B(X) = B_{Na_2SiO_4} + X(B_{TMA} - B_{Na}) \quad (2.15)$$

where B_{TMA} and B_{Na} are the ionic B coefficients of the TMA and sodium ions and X is the fraction of TMA of all cations. One could expect a factor 2 in

Chapter II

the second term because the base/silicate ratio is 2. This factor is not used because the concentrations used in the fit are the total cation concentration and not the silicate concentration. The slope can be calculated from B coefficients found by Out [22], and from these data is expected to be $0.044 \text{ dm}^3 \text{ mole}^{-1}$. This was found for molar fractions up to 0.7.

For mixtures of potassium and TMA silicates a slope can be calculated in a similar way and is expected to be $0.123 \text{ dm}^3 \text{ mole}^{-1}$. Similarly for sodium-TMA mixtures the slope does agree with the experimental B-values for ratios up to 0.75. The exceptionally small B coefficient found for TMA silicate, does not conform with the additivity rule.

An explanation for the small B coefficient of TMA silicate is the difference in hydration of the ions. Silicate ions are hydrophillic structure builders and TMA is a hydrophobic structure builder. Frank and Evans [32] suggested that these two hydration types are of a different origin. Therefore these different structured regions do not overlap. The small B coefficient of TMA silicate can then be explained by the assumption that at points of contact of hydrophillically induced and hydrophobically induced solvent regions structure breakdown occurs.

2.5.2 The A coefficient.

The A coefficients of TMA, sodium and potassium silicate found in this investigation were 0.0266, 0.0099 and $0.0056 \text{ l}^{0.5} \text{ mole}^{-0.5}$ respectively. Out [22] calculated with the Falkenhagen equation (equation 2.5) for sodium chloride, TMA bromide and potassium bromide 0.0061, 0.0063 and $0.0050 \text{ l}^{0.5} \text{ mole}^{-0.5}$. The difference between chloride and bromide ions is of no importance, because they have the same mobility. Stokes and Mills [11]

Chapter II

mention 0.0142, 0.0092, 0.0113, 0.0106, 0.0117 and 0.0118 $l^{0.5} \text{ mole}^{-0.5}$ for barium chloride, cadmium chloride, cobalt chloride, iron (II) chloride, magnesium chloride and lithium sulfate respectively. These values are corrected for the concentration scale we used. The A coefficient of sodium silicate is comparable with the value of other 2:1 electrolytes. The A coefficient of potassium silicate is much smaller. The A coefficient of TMA silicate was $2\frac{1}{2}$ times higher than that of sodium silicate. As the A coefficients of sodium chloride and TMA bromide have nearly the same value, the difference in A coefficient of the silicates cannot be explained with the Falkenhagen theory. According to Quintana [15] the small values of the A coefficient can be caused by ion association. However, if this would be the main reason for the difference between the A coefficients of TMA silicate and sodium silicate then, according to equation 2.6, 86% of the sodium ions should have been associated to silicate ions. McGormic [13] showed that in solutions of sodium and silicate ions association can take place. This association should strongly influence the electrode calibration curves shown in Figure 2.3. An association percentage of 86% would cause a potential drop of 51 mV with respect to the value observed in completely dissociated salt solutions. The calibration curve in Figure 2.3a shows a nearly Nernstian behaviour for silicate solutions. The difference in slope between the three sodium salts is negligible compared to the pronounced change in slope which should occur if association takes place. This indicates that the large difference in A coefficient cannot be explained in terms of association of sodium silicate.

Calculating the A coefficient of sodium monosilicate with the Falkenhagen equation, we found an A coefficient of $0.016 l^{0.5} \text{ mole}^{-0.5}$. However, application of the Falkenhagen equation to our results is interfered by the

Chapter II

consideration that silicate solutions are mixtures of different silicate ions and hydroxide ions, and that even the charge of the silicate ions is not very well known. The charge on the silicate ions is limited by the base to silica ratio and its average value therefore cannot exceed two charges per silicate ion. The high pH of the solution indicates that the charge is lower than the maximum charge. The pH of the solutions is between pH=12 and pH=13.5; therefore the charge is expected to be between $-1\frac{1}{2}$ and -2 per silicate ion. The uncertainties in charge and the presence of the very mobile hydroxide ions can cause a smaller A coefficient. This may explain the differences between the experimental value for sodium silicate ($0.0099 \text{ l}^{0.5} \text{ mole}^{-0.5}$) and the calculated one ($0.016 \text{ l}^{0.5} \text{ mole}^{-0.5}$). This is not the case with TMA silicate. Based on Falkenhagens equation the A coefficients of TMA silicate and sodium silicate should be the same (conform Out's [22] calculations for the halogenides). According to Frank and Evans [32] the presence of large structured solvent regions around ions can cause a deformation of the Debye-Hückel ion cloud. The hydration shell will cause a hindrance in the approach of the counter ions. In fact the deformation of the ion cloud, caused by the structured region, is an increase in average ion-counterion distance. This means that the attraction between TMA and silicate ions is, on the average, less than would be expected on the basis of the charge and dimensions of the ions themselves. The increase in average ion-counterion distance is in agreement with the results of the coacervation (chapter III). The influence of this enlarged ion-counterion distance on the A coefficient is large. As the distance between ion and counter ion is large the shielding will be diminished. A consequence of this is that the potential does not drop as fast with the distance as for the Debye-Hückel ion cloud in the absence of structured regions around the ions. At large distance from the ion the

Chapter II

deformation of the ion cloud in a shear field is more pronounced. As the potential is large, compared to the Debye-Hückel ion cloud, the disturbed potential is also large. In solutions of TMA silicate the counter ions are present at a larger distance from the central ion than for sodium silicate. At large distances from the central ion the disturbance of the potential is larger than close to the central ion thus the product of counter ion concentration with the disturbed potential is larger as well.

Thus the large A coefficient of TMA silicate can be explained by an enlarged TMA-silicate distance because of the different hydration regions of TMA and silicate which do not overlap. This is supported by the form of the curve in figure 2.3a. The curve, convex to the X-axis, shows a large influence of sodium on the A coefficient. The TMA-silicate distance is larger than the sodium-silicate distance. In mixtures of TMA and sodium, the effect of the TMA is small because sodium can approach the silicate closer than TMA. The mean ionic distribution does not differ much from sodium silicate and gives rise to an A coefficient which is in the same range as the A coefficient of sodium silicate.

The A coefficient of potassium silicate is distinctly smaller than the A coefficient of sodium silicate. The electrode calibration curve for potassium silicate, as shown in Figure 2.3b, is perfectly parallel with the curves of potassium bromide and potassium hydroxide. Ionic association would have been visible as a decrease in slope. The Nernstian behaviour for potassium silicate excludes significant association. As potassium has a higher mobility than sodium the difference in A coefficient between potassium and sodium silicate is conform the Falkenhagen equation. The curve of the A coefficients in Figure 2.4b can be explained with the same mechanism as for mixtures of sodium and TMA silicate. The curvature is

Chapter II

more pronounced for potassium-TMA silicate mixtures than for sodium-TMA silicate mixtures. A coefficients will be higher for electrolytes with the same mobilities for cation and anion than for electrolytes with the same mean mobility but different mobility for cation and anion. Very mobile potassium ions will have more influence on the A coefficient than ions with lower mobility in decreasing the A coefficient.

2.5.3 The D coefficient.

For the curve of the D coefficient as a function of the cation composition we find the same general form as for the curve of the A coefficient. The D coefficients of sodium silicate and potassium silicate (0.087 and $0.064 \text{ l}^2 \text{ mole}^{-2}$) are comparable with those of TMA bromide ($0.059 \text{ l}^2 \text{ mole}^{-2}$), sodium chloride ($0.013 \text{ l}^2 \text{ mole}^{-2}$), potassium bromide ($0.01 \text{ l}^2 \text{ mole}^{-2}$) and other common electrolytes found by Out [22]. The D coefficient of TMA silicate is much higher ($0.220 \text{ l}^2 \text{ mole}^{-2}$) and a curve convex towards the X-axis is found for the mixed compositions.

The high value of the D coefficient for TMA silicate indicates the presence of additional interionic interactions. These interactions do not occur between two TMA or two silicate ions because for solutions of TMA bromide, sodium silicate and potassium silicate low D coefficients are found. The additional interactions in TMA silicate solutions therefore occur between TMA and silicate ions. The form of the curve in Figure 2.4 can be explained by the difference in equilibrium distance of the cation with the silicate ions. The sodium ions can move closer to the silicate than TMA and swamp the effect of the TMA. This supports the analysis of the A and B coefficients.

Chapter II

2.6 Conclusions.

By comparing A, B and D coefficients with each other and with literature data information is obtained about interactions that take place between ions in solutions containing TMA ions and silicate ions. The large B coefficients indicate that silicate ions are structure builders. For mixtures of TMA and alkali metal silicates the B coefficients are additive for TMA fractions up to 0.75. The large D coefficient found for TMA silicate, compared to the D coefficients of TMA bromide, sodium silicate and potassium silicate, shows the presence of strong solute-solute interactions between TMA and silicate ions. The analysis of the B and D coefficients supports the explanation for the large A coefficient found for TMA silicate. In the absence of specific hydration effects the A coefficient of TMA silicate should have been the same for TMA and sodium silicate. The large A coefficient can be ascribed to the deformation of the Debye-Hückel ion cloud as a result of strong hydration shells around the silicate and the TMA which do not overlap.

References

- [1] J.L.Poisseeuille, *Ann.Chim.Phys.*, 21(1847)76.
- [2] S.Arrhenius, *Z.Physik.Chem.*, 1(1887)285.
- [3] G.Jones and M.Dole, *J.Am.Chem.Soc.*, 51(1929)2950.
- [4] G.Jones and S.K.Talley, *J.Am.Chem.Soc.*, 55(1932)4124.
- [5] M.Kaminsky, *Z.Phys.Chem.*, 12(1957)206-231.
- [6] L.Sepulveda and C.Gamboa. *J.Colloid Interface Sci.*, 118(1987)87-90.
- [7] L.Weblan, *Bull.Acad.Pol.Sci.*, 27(1979)873-890.
- [8] D.Feakins, W.E.Waghorne and K.G.Lawrence, *J.Chem.Soc.*, Faraday

Chapter II

Trans 1., 82(1986)563-568.

- [9] J.Crudden, G.M.Delany, D.Feakins, P.J.O'Reilly, W.E.Waghorne and K.C.Lawrence, *J.Chem.Soc., Faraday Trans 1.*, 82(1986)2195-2206.
- [10] J.Crudden, G.M.Delany, D.Feakins, P.J.O'Reilly, W.E.Waghorne and K.C.Lawrence, *J.Chem.Soc., Faraday Trans 1.*, 82(1986)2207-2219.
- [11] H.Falkenhagen and M.Dole, *Phys.Z.*, 33(1929)611-622.
- [12] H.Falkenhagen, *Phys.Z.*, 32(1931)745-764.
- [13] H.Falkenhagen and E.L.Vernon, *Phys.Z.*, 33(1932)140.
- [14] L.Onsager and R.M.Fuoss, *J.Phys.Chem.*, 36(1932)2689-2778.
- [15] R.H.Stokes and R.Mills, "Viscosity of electrolytes and related properties", Pergamon Press, New York, 1965, p11.
- [16] M.Palma and J.P.Morel, *J.Sol.Chem.*, 1, 3(1979)767-777.
- [17] A.V.McGormick, thesis, Berkeley, 1987, chapter V.
- [18] S.Mohanty and P.B.Das, *Thermochim.Acta*, 48(1981)219-223.
- [19] C.Quintana, M.L.Llorente, M.Sanches and A.Vivo, *J.Chem.Soc., Faraday Trans.*, 1, 82(1986)3307-3314.
- [20] A.Einstein, *Ann.Phys.*, 19(1906)289.
- [21] N.Gorsky, *Z.Phys.Chemie, Leipzig*, 264(1983)640-644.
- [22] D.J. Out, thesis, Amsterdam, 1979.
- [23] B.S.Krumgalz, *J.Phys.Chem.*, 83,6(1979)763-765.
- [24] H.S.Frank and W.Y.Wen, *Disc.Faraday Soc.*, 24(1957)133.
- [25] B.S.Krumgalz, *J.Chem.Soc., Faraday I*, 76(1980)1275-1276.
- [26] R.S.Dordick and W.Drost-Hansen, *J.Phys.Chem.*, 85(1981)1086-1088.
- [27] M.Kaminsky, *Disc.Faraday Soc.*, 24(1957)171.

Chapter II

- [28] J.E.Desnoyers and G.Perron, *J.Sol.Chem.*, 1,3(1972)199-212.
- [29] W.J.M.Heuvelsland, Thesis, 1980, Amsterdam, p27.
- [30] D.G.Thomas, *J.Colloid Sci.*, 20(1965)267.
- [31] G.K.Batchelor, *J.Fluid Mech.*, 83(1977)97.
- [32] H.S.Frank and M.W.Evans, *J.Chem.Phys.*, 13, 11, (1945) 507-531.
- [33] D.Hoebbel, G.Garzo, G.Engelhardt and A.Vargha, *Z.anorg.allg.-Chem.*, 494(1982) 31-42.
- [34] D.Hoebbel, A.Vargha, G.Engelhardt and K.Üjszászy., *Z.anorg.allg. Chem.*, 509(1984)85-94.
- [35] D.Hoebbel, A.Vargha, B.Fahlke und G.Engelhardt, *Z.anorg.allg. Chem.*, 521(1985) 61-68.
- [36] H.L.Dryden, F.D.Murnaghan and H.Bateman, "Hydrodynamics", Dover Publications, Inc., 1956, p.105.
- [37] G.Barr, "A monograph of viscosity", Oxford University Press, London, 1931.
- [38] American National Standard (ASTM), 1979, D 446-79.
Deutsche Normen, March 1981, DIN 53012.
- [39] E.J.J.Groenen, A.G.T.G.Kortbeek, M.Mackay and Sudmeyer, *Zeolites*, 6(1986)403.
- [40] W.H.Press, B.P.Flannery, S.A.Teukolsky and W.T.Vetterling, "Numerical recipes", Cambridge University Press, Cambridge, 1988, chapter 14.

CHAPTER III: COACERVATION IN AQUEOUS SOLUTIONS OF TAA BROMIDE AND SODIUM SILICATE.

3.1 Introduction.

The demixing of oil and water is a well known phenomenon. In some cases a comparable behaviour is found in aqueous solutions: the liquid separates into two layers. This was observed, e.g., for solutions of gelatin or casein with sulphates [1] and gelatin with sulphosalicylic acid [2]. According to Bungenberg de Jong and Kruyt [3] demixing in aqueous solutions is different from partial miscibility. In both layers water is the continuous phase. As a consequence of this the phase rule does not hold. Therefore they introduced the term coacervation. Kruyt described coacervation in colloid rich systems [4]. These systems have a particular disperse phase. He assumed that coacervation and flocculation are closely related phenomena.

According to Kruyt [4] two types of coacervation are observed: simple and complex coacervation. Coacervation is called simple coacervation when the phase separation is induced by the non-ionized groups in the solute molecules. A general characteristic is the water deficit in the total system. Upon dilution the coacervate disappears.

Chapter III

Complex coacervation occurs when to a solution of a charged colloid, a second colloidal species is added which is oppositely charged to the one which is already present in solution. The charges on the macromolecules which are concerned induce the formation of salt bonds. In both coacervate types colloids are involved. Voorn [5] described complex coacervation of polyelectrolytes in terms of electrostatic interactions and entropy.

In early literature coacervation was mostly observed in the presence of colloids. These colloids are usually proteins or macromolecules but also ionic systems can be taken into account. Coacervation was also observed in solutions of quaternary ammonium compounds as described by Mugnier de Trobriant [6,7,8] and Lucas [9,10,11]. In these systems the coacervation is classified as simple coacervation. They supposed that the demixing was caused by the limited amount of water. At high concentrations formation of dimers and micelles of TAA ions was assumed to take place. The amount of water in hydration shells around the dissolved species diminishes and the water coming free can be used to dissolve other ions. In this way two kinds of regions are formed, one with the quaternary ammonium compound and one with the other salt. Quantitative support for this theory was not advanced however. Other ionic systems in which coacervation takes place are surfactant systems. Several investigators have studied the solution properties of a number of coacervating anionic and cationic soap systems extensively [12,13,14]. These systems are mainly classified as simple coacervation. Other work by Thalberg et.al. [15,16,17,18] on coacervation deals with interactions between polymers and oppositely charged surfactants. Because of the electrostatic interactions and the interactions between the hydrophobic parts of the polymer and the surfactant a special phase separation behaviour occurs. Although only one type of polymer is present this is an example of

Chapter III

complex coacervation in ionic systems. Dissolved silicate ions can be considered partially as a small type of anorganic polymer and the quaternary ammonium ions mostly have surface active properties. This could lead to the conclusion that coacervation in systems of TAA bromide- sodium silicate-water is due to complex coacervation.

We found coacervation in solutions of sodium silicate with quaternary ammonium bromide starting from TMA (bromide). Previously reported data refer only to quaternary ammonium ions with larger alkyl groups. The TMA bromide solutions formed coacervates with other silicate salts but not with other sodium salts up to saturation. No coacervation was found for systems which contained sodium bromide-sodium silicate, TMA bromide-TMA silicate, TMA bromide-sodium bromide or TMA silicate-sodium silicate. For coacervation the presence of TMA halogenide-alkali metal silicate is necessary. This suggests that the silicate plays an active role in the coacervation. Interactions between TAA and silicate seem to be the cause of the demixing behaviour. In the systems of Mugnier de Trobriant [6,7,8] and Lucas [9,10,11] simple coacervation is observed. If an active role is played by silicate ions, complex coacervation may occur in our systems. The type of interaction between the silicate and TAA ions will determine the correct classification.

In this chapter we will discuss the separation of solutions of quaternary ammonium bromides and sodium silicate into two aqueous layers. The composition of the coacervates and the concentration region where coacervation takes place will be determined. The coacervation will be described in terms of thermodynamical parameters. If these parameters can be connected to characteristics of the TAA ions, e.g. the chain length, they can give indications about the mechanism of the coacervation.

Chapter III

3.2 Theory.

For the description of the coacervation two questions arise: i) how are the ions distributed over the two aqueous layers, and ii) in what concentration range does the demixing phenomenon occur.

The distribution can be expressed in terms of a distribution coefficient as used by Lucas [9,10,11] and Mugnier the Trobriand [6,7,8].

$$D = \frac{c_u}{c_l} \quad (3.1)$$

In which D is distribution coefficient and c_u and c_l are the concentrations in the upper and lower layer, respectively.

For the concentration range at which coacervation occurs the concentrations of all compounds must be known. As a consequence of this at least six concentrations have to be taken into account. This does complicate the understanding of the system. The system can be simplified to three compounds by taking salt concentrations instead of ionic concentrations. The salts are chosen by combination of the ions which show comparable demixing behaviour (the majority of both ions are present in the same phase). In this way the coacervate could be treated as a ternary system. In order to describe the concentration range where demixing occurs some objective criteria have to be developed. For this thermodynamics can be of great use. Although differences are present between coacervation and partial miscibility the system can be considered as a mixture of two partially miscible fluids. Therefore theories about partial miscibility will be used to describe the

Chapter III

coacervation.

Demixing phenomena will occur when a maximum in the Gibbs free energy as a function of concentrations is present. Consequently we write the Gibbs free energy of the system. For binary systems the Gibbs free energy is:

$$G = x\mu_1^0 + (1-x)\mu_2^0 + RT\{x\ln\gamma_1x + (1-x)\ln\gamma_2(1-x)\} \quad (3.2)$$

The Gibbs free energy in a ternary system can be expressed as:

$$G = x_1\mu_1^0 + x_2\mu_2^0 + x_3\mu_3^0 + RT\{x_1\ln\gamma_1x_1 + x_2\ln\gamma_2x_2 + x_3\ln\gamma_3x_3\} \quad (3.3)$$

In these equations μ_i^0 is the thermodynamical potential of species i in standard state (e.g., at an activity of 1), x_i is its molar fraction and γ_i is its activity coefficient. The molar fractions, as used in equation 3.2, are usually referring to nonelectrolytes. Therefore the molar fractions have to be defined such as to take into account the dissociation of the electrolytes. The molar fraction becomes:

$$x_i = \frac{\nu_i n_i}{\sum_{i=1}^3 \nu_i n_i} \quad (3.4)$$

n_i is the amount of compound i present (in moles) and ν_i the number of ions

Chapter III

in one mole i . For the solvent ν_1 is 1.

In this chapter all molar fractions of electrolytes will be calculated according to equation 3.4. The activity coefficients however are the normal stoichiometric activity coefficients, γ_{\pm} . In appendix B the Gibbs free energy is derived with the molar fractions, as described in equation 3.4, and the stoichiometric activity coefficients, γ_{\pm} .

The activity coefficients, as used in equation 3.2 and 3.3, can be transformed into an excess Gibbs free energy. In this energy all kinds of interactions which cause a deviation from ideality can be taken into account. This can vary from Debye-Hückel type activity coefficients to incomplete dissociation and hydration effects. Excess Gibbs free energies can be calculated from activity coefficients using equation 3.5.

$$G^E = RT(x_1 \ln \gamma_1 + x_2 \ln \gamma_2 + x_3 \ln \gamma_3) \quad (3.5)$$

In this equation the molar fractions are corrected for the dissociation of the electrolytes and the activity coefficients are the stoichiometric activity coefficients, γ_{\pm} .

The excess Gibbs free energy in equation 3.5 can be described in various mathematical forms. It is assumed here that it is possible to split the excess Gibbs free energy into pair interactions:

$$G^E = x_1 x_2 E_a + x_1 x_3 E_b + x_2 x_3 E_c \quad (3.6)$$

In this equation the pair interactions are expressed in terms of the product of the molar fractions with a constant. x_1 , x_2 and x_3 are the molar

Chapter III

fractions of the water, TMA bromide and sodium silicate respectively and E_a , E_b and E_c are constants. In view of the excess Gibbs free energy leading to coacervation only in solutions which contain both TAA and silicate ions, we assume that there is a predominant contribution to G^E from the interaction between these ions. Therefore the last term of equation 3.6 will describe the cause of the coacervation. The other terms are the interactions of the pure electrolytes with water. In first approximation, the first two terms in equation 3.6 can be described by the stoichiometric activity coefficients of the electrolytes in solution which are then supposed to be only slightly influenced by the presence of the third component. In that case the excess function can be described by using the third term of equation 3.6 together with the contributions of the activity coefficients of the separate salts:

$$G^E = x_2 x_3 E + G^\gamma \quad (3.7)$$

E is a constant which will be dependent on the kind of quaternary ammonium compound and the base / silica ratio and G^γ is the contribution of the activity coefficients of separate salts to the Gibbs free energy.

The contributions of the activity coefficients of the separate salts to the Gibbs free energy can be incorporated in several ways. The best way is splitting the activity coefficients into its various contributions.

$$\log \gamma_{\pm i} = -A\sqrt{I} + BI + R(m_i) \quad (3.8)$$

In this equation I is the total ionic strength, m_i is the molality of component i , A the Debye-Hückel limiting slope, B takes into account the effects of incomplete hydration and $R(m_i)$ is an additional function which describes

Chapter III

other contributions to the activity coefficient, such as association. The Debye-Hückel effect and the contribution of incomplete hydration are dependent on the total ionic strength. The additional function $R(m_i)$ can be considered as approximately dependent on the molality of component i only. The complete contributions of the activity coefficients to the Gibbs free energy can be expressed as:

$$G^{\gamma} = 2.303RT \sum_{i=2}^3 [-x_i (A_i \sqrt{I} + B_i I + R_i(m_i))] \quad (3.9)$$

The Debye-Hückel limiting slope is theoretically known. By using literature activity coefficients the B and R values can be determined.

By using an excess Gibbs free energy as described by equation 3.7 the complete G -function will be:

$$G = x_1 \mu_1^0 + x_2 \mu_2^0 + x_3 \mu_3^0 + RT \{x_1 \ln x_1 + x_2 \ln x_2 + x_3 \ln x_3\} + x_2 x_3 E + G^{\gamma} \quad (3.10)$$

The molar fractions are the ones described in equation 3.4. The dissociation behaviour of the electrolytes is incorporated in the Gibbs free energy by using molar fractions as described in equation 3.4.

In the theory of ternary liquid-liquid equilibria the binodal and the spinodal are important properties. The spinodal is the line where spontaneous demixing into regions with small concentration differences occurs and the binodal describes the equilibrium compositions of the separate phases. For a two component system the spinodal points are the bending points in the $G(x)$ -curve (x : the molar fraction of one of the components). This means that the second derivative of the Gibbs free energy to the composition coordinate

Chapter III

should be zero on the spinodal. According to Prigogine and Defay [19] the following criterium should lead to the spinodal in ternary systems:

$$\frac{\partial^2 G}{\partial x_2^2} \frac{\partial^2 G}{\partial x_3^2} - \left(\frac{\partial^2 G}{\partial x_2 \partial x_3} \right)^2 = 0 \quad (3.11)$$

By using equation 3.10 for the G-function and on neglecting the activity coefficients of the separate salts, which are assumed to have a minor influence, equation 3.11 leads to the following expression for the spinodal:

$$x_3 = \frac{1}{x_2} \left(\frac{RT}{E} \right)^2 \quad (3.12)$$

The binodal gives the equilibrium composition of the coexisting phases. The spinodal and the binodal have one intersection point. This is the plait point or (isothermal) critical point [20]. It can give us important information about the excess function, because the G function should be chosen in such a way that the experimental plait point is described by it.

By using equation 3.7 for the excess Gibbs free energy the spinodal and binodal will be symmetric towards the line: $x_2 = x_3$ (Figure 3.1) and their intersection point, the plait point, will be at the maximum water content.

In this figure the activity coefficients of the electrolytes are neglected.

This can be a good description for some systems but in most cases this will not describe the situation satisfactorily. For systems with polydispersity asymmetric binodals are found [21]. The critical point is shifted towards the component with the highest polydispersity. In these cases another expression for the excess Gibbs free energy has to be used. Redlich and Kister [22]

Chapter III

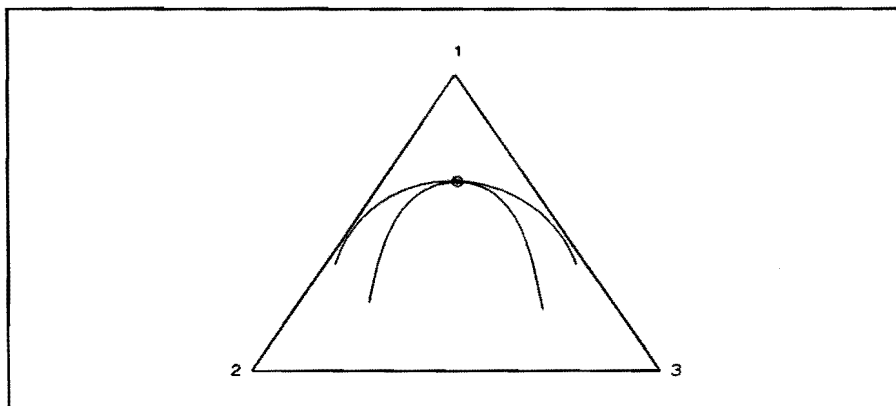


Figure 3.1: Binodal-spinodal (upper and lower curve respectively)

extended the pair wise contribution to the excess Gibbs free energy as used in equation 3.7 to:

$$G^E = x_2 x_3 (E_0 + (x_2 - x_3)E_1 + (x_2 - x_3)^2 E_2 + \dots) + G^Y \quad (3.13)$$

The Redlich-Kister equation is usually employed for nonelectrolytes. This equation can be used for electrolyte solutions when interactions are considered which are not primarily determined by electrostatic interactions. In the systems described in this chapter the coacervation is thought to be caused by interactions between TAA- and silicate- ions. These ions are found in different phases and thus electrostatic interactions can not be regarded as a cause of coacervation and therefore the Redlich-Kister equation can be applied. In the present approach only the first extension of the Redlich-Kister equation is used.

Equation 3.13 will not lead to an easy description of the spinodal. Another approach in finding E_0 and E_1 will be described below. A key role

Chapter III

will be played by the plait point. It is a part of the binodal and the spinodal. The plait point is often situated on the line through the mid points of the conodes [23].

A complication is the fact that the system involved is a ternary system. In ternary systems the analytical criteria for the binodal are more complicated than for binary systems. By treating the system as a quasi binary system it is easier to define these criteria. The reduction of a ternary system to a binary system is accomplished as follows:

For a two component system liquid-liquid separation equilibria are determined by the $G(x)$ curve and the plait point is the point where equation 3.14 has only one solution.

$$\frac{\partial^2 G}{\partial x^2} = 0 \quad (3.14)$$

Thus, we draw a tangential on the L_1 - L_2 binodal line passing through the plait point; the second derivative of the G -curve to the composition coordinate on that line should be zero at the plait point. The tangential concerned is regarded as a line from the binary mixture of components 1 and 2 with molar fraction $x_2 = x_{2,0}$ to the binary mixture of 1 and 3 with molar fraction $x_3 = x_{3,0}$ (Figure 3.2).

This line can be described in parameter form:

$$x_1 = 1 - x_{2,0} + i(x_{2,0} - x_{3,0}); \quad x_2 = (1 - i)x_{2,0}; \quad x_3 = ix_{3,0} \quad (3.15)$$

In this description i is the distance parameter with values between 0 and 1.

By substituting the parameters of the tangential in equation 3.10 in

Chapter III

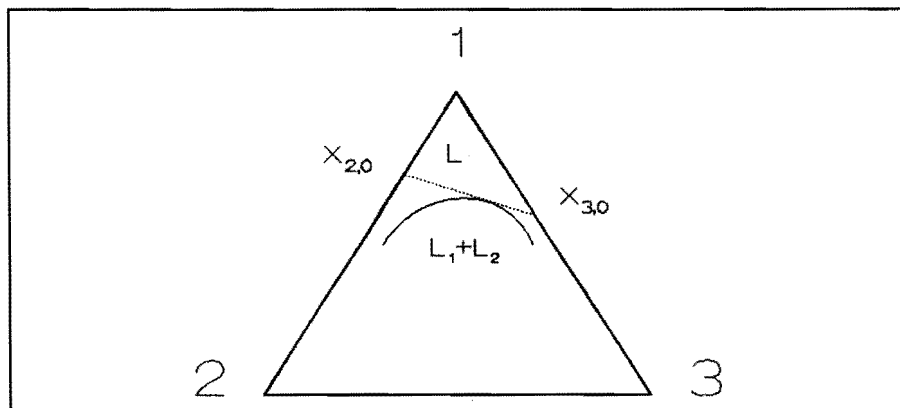


Figure 3.2: Tangential through plait point.

combination with the first extension of equation 3.13 for the excess Gibbs free energy the G-function on the tangential becomes:

$$\begin{aligned}
 G(i) = & (1-x_{2,0})\mu_1^z + x_{2,0}\mu_2^0 + \\
 & i\{-x_{2,0}\mu_2^0 + x_{3,0}\mu_3^0 + (x_{2,0}-x_{3,0})\mu_1^z\} + \\
 & RT\{(1-i)x_{2,0}\ln[(1-i)x_{2,0}] + \\
 & [1-x_{2,0}+i(x_{2,0}-x_{3,0})]\ln[1-x_{2,0}+i(x_{2,0}-x_{3,0})] \\
 & + ix_{3,0}\ln[ix_{3,0}]\} + \\
 & x_{2,0}x_{3,0}(i-i^2)(E_0+(1-i(x_{2,0}+x_{3,0})))E_1 + G^y(i)
 \end{aligned} \tag{3.16}$$

On the tangential described by equation 3.15 the following expressions are valid at the plait point:

$$\frac{\partial^2 G}{\partial i^2} = 0; \quad \frac{\partial^3 G}{\partial i^3} = 0 \tag{3.17}$$

Chapter III

The second derivative of the G-function will be zero because the plait point is on the spinodal. For lines parallel to the tangential but at higher electrolyte concentration two bending points in the G-curve are found. At lower electrolyte concentrations no bending point is present in the G-function. Therefore the second derivative must have an extreme at the plait point and the third derivative has to be zero too.

With the help of the third derivative of the Gibbs free energy and the plait point E_1 can be determined:

$$\frac{E_1}{RT} = \frac{\frac{(x_{2,0} - x_{3,0})^3}{x_1^2} - \frac{x_{2,0}^3}{x_2^2} + \frac{x_{3,0}^3}{x_3^2} - \frac{d^3 G^\gamma(i)}{di^3}}{6(x_{2,0}^2 x_{3,0} + x_{2,0} x_{3,0}^2)} \quad (3.18)$$

In this equation x_1 , x_2 and x_3 are the molar fractions in the plait point. $x_{2,0}$ and $x_{3,0}$ have the same meaning as in figure 3.2. The E_1 calculated with equation 3.18 can be used to calculate the E_0 from the second derivative of the Gibbs free energy:

$$\frac{E_0}{RT} = \frac{\frac{(x_{2,0} - x_{3,0})^2}{x_1} + \frac{x_{2,0}^2}{x_2} + \frac{x_{3,0}^2}{x_3} + \frac{d^2 G^\gamma(i)}{di^2}}{2x_{2,0} x_{3,0}} \quad (3.19)$$

$$\frac{6x_3 x_{2,0} (x_{2,0} + x_{3,0}) + 2x_{2,0} x_{3,0} (2x_{2,0} + x_{3,0}) E_1}{2x_{2,0} x_{3,0}}$$

When the values of E_0 and E_1 are known all important constants of equation 3.16 are known. For demixing the values of Gibbs free energies of

Chapter III

the pure components and of the pure components in the standard state are of no importance. The intercepts of the double tangent with the G-function do not change when a function, linear to i , is added to the G-function (see Appendix C). The rest of the phase diagram can be calculated from the G-curve. The system was treated as quasi binary to simplify the equilibrium criteria. The following procedure was followed:

By drawing a line along a conode the composition of the binary mixtures on the axis can be determined. Using these values in equation 3.16 the G-function along that line can be calculated and the intersection points of the double tangent can be calculated. This gives the composition of the coexisting phases. By calculating intersection points at different concentrations the complete binodal can be found.

3.3 Experimental.

The coacervation behaviour was investigated with two different kinds of experiments: i) For the distribution of the ions over both aqueous layers a coacervate was prepared and both layers were analyzed. ii) For the determination of the binodal a titration procedure was used.

3.3.1 Materials.

sodium silicate solution, den Hertog, 10.1% NaOH, 27.8% SiO₂.

sodium hydroxide, Merck, Pro Analysi.

sodium hydroxide, Merck Titrisol 0.1 M and 1 M.

sodium tetraphenylborate, Janssen Chimica, 98 %.

TMA bromide, Merck, >99%.

Chapter III

TMA bromide, Janssen, >99%.

TEA bromide, Merck, >99%.

TPA bromide, Janssen, >98%.

TPA bromide, Merck, >99%.

silver nitrate, Merck Titrisol, 0.1 M.

Silicium tetrachloride in sodium hydroxide, Merck Titrisol, 1 gr/ml.

nitric acid, Merck, 65%.

ammonium heptamolybdate, Merck, Pro Analyti, >99%.

twice distilled water.

3.3.2 Analyses of the coexisting phases.

Coacervates were prepared with constant TAA bromide / sodium silicate ratio but different water contents. The coacervates were shaken overnight at 25 °C . The phases were separated and the density was determined by weighing a known volume. TAA- and bromide- concentrations were determined using an Orion autochemistry system 940/960. For the TAA concentration a potentiometric titration with sodium tetraphenylborate and a TAA sensitive electrode, developed by Holten and Stein [24], was used. The bromide was determined by a potentiometric titration with silver nitrate and a Philips bromide sensitive electrode (IS 550). Sodium concentrations were determined with AES (Perkin Elmer 4995 AA Spectro-photometer). Silicate concentrations were determined with the molybdate method.

The following procedure was used for the molybdate method [25]:

1 ml silicate solution (0-50 mg/l SiO₂) was added to 2 ml molybdate solution (8% ammonium molybdate, 4% sodium hydroxide) and 1 ml nitric acid (20%). A yellow coloured compound was formed. After 13 minutes the

Chapter III

extinction was measured at 370 nm with a Zeiss spectrophotometer MM12, PMQ II.

3.3.3 Titration method.

An amount of quaternary ammonium bromide was dissolved in an amount of sodium silicate solution, with known concentration, until a coacervate was formed. The stirred coacervate was opaque. Water was added until the opaqueness disappeared. The limit of the coacervation region at a given TAA bromide/sodium silicate ratio, was taken to be that composition where coacervate became transparent upon addition of one droplet of water. By weighing the solution the amount of added water was determined. By adding new quaternary ammonium bromide to that solution a coacervate was formed again and water was added until the coacervate disappeared. This method was repeated several times. A large part of the binodal can be determined in this way. All experiments were carried out at room temperature.

The titration procedure was performed with several kinds of sodium silicate solutions and TAA bromides. For TMA bromide five sodium/silicate ratios were used, 0.82:1, 1:1, 1.5:1, 2:1 and 3:1, and for TEA and TPA bromide a 2:1 sodium silicate ratio.

The silicate solution was prepared by adding sodium hydroxide (Merck Titrisol) to the sodium silicate (den Hertog) solution until the desired sodium/silicate ratio was obtained.

Chapter III

3.4 Results and Discussion.

3.4.1 Analyses of the coexisting phases.

The results of the analyses can be represented in two ways. The distribution of the ions over the aqueous layers can be expressed in terms of distribution coefficients (equation 3.1) or the composition of both phases can be expressed in terms of molar fractions. By using molar fractions a quasi ternary system is considered. For this the compounds of the systems should be water and the two salts which consist of ions with comparable distribution behaviour.

In the figures 3.3 to 3.7 the distribution coefficients are shown of coacervates of TMA bromide with sodium silicate with ratios of 0.82:1, 1:1 and 2:1 and of coacervates of TEA and TPA bromide with a 2:1 sodium silicate.

In all cases the quaternary ammonium bromide was mainly dissolved in the upper phase and the sodium silicate was present in the lower phase. For equation 3.7 an interaction between the TAA and the silicate ions leading to coacervation was assumed. The fact that the TAA and the silicate ions are present in different phases can be considered as an indication on the presence of a repulsive interaction between the TAA and the silicate ions. This is in agreement with the results of chapter II. The demixing behaviour of the sodium and bromide ions can be regarded as an effect of the electroneutrality of both layers. Therefore the system can be considered as two partially miscible solutions of TAA bromide and sodium silicate. This justifies the use of the quasi ternary system: TAA bromide - sodium silicate -

Chapter III

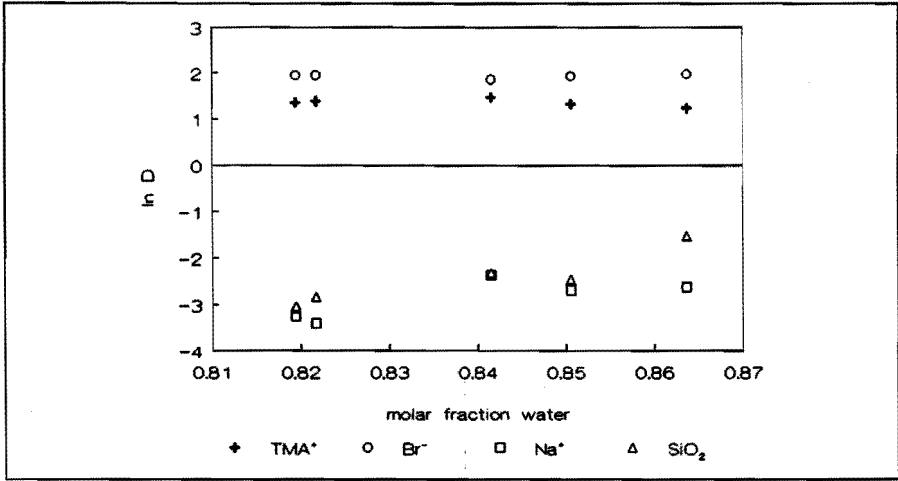


Figure 3.3: Distribution coefficients of TMA bromide and 0.82:1 sodium silicate.

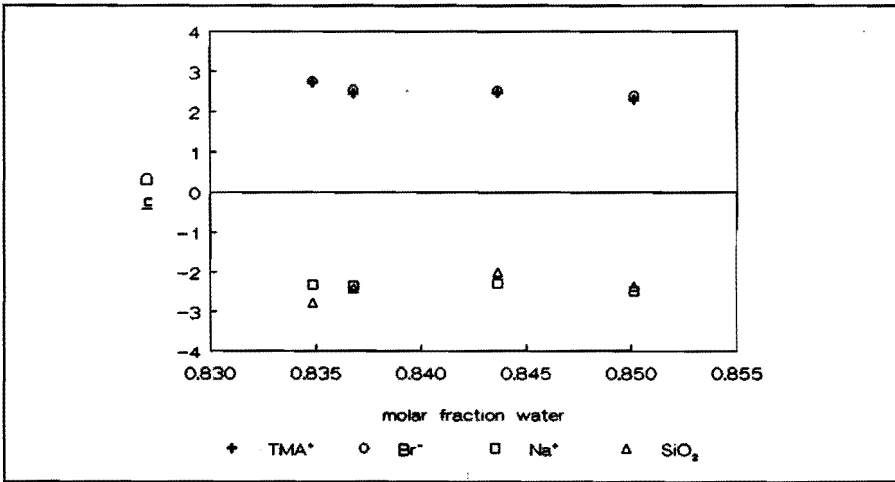


Figure 3.4: Distribution coefficients of TMA bromide and 1:1 sodium silicate.

Chapter III

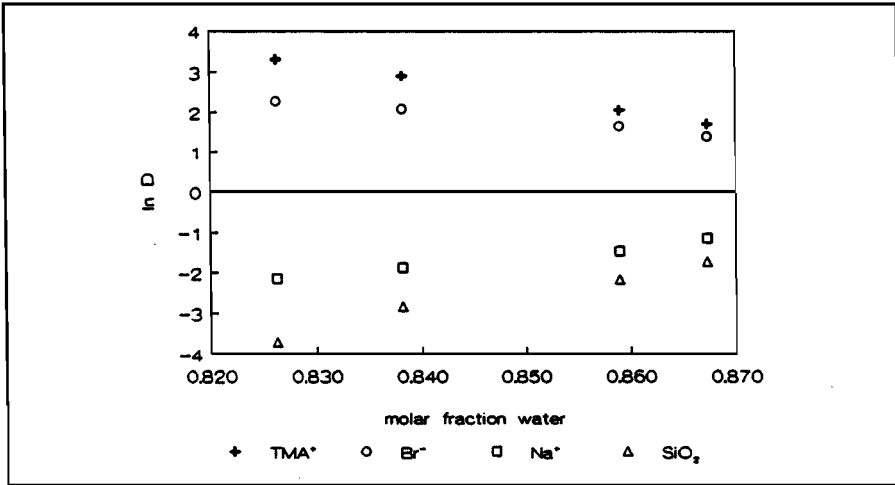


Figure 3.5: Distribution coefficients of TMA bromide and 2:1 sodium silicate.

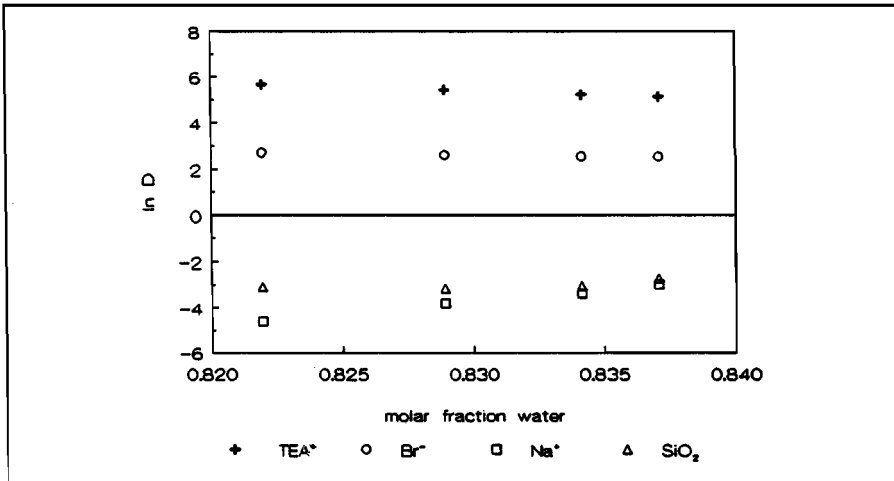


Figure 3.6: Distribution coefficients of TEA bromide and 2:1 sodium silicate.

Chapter III

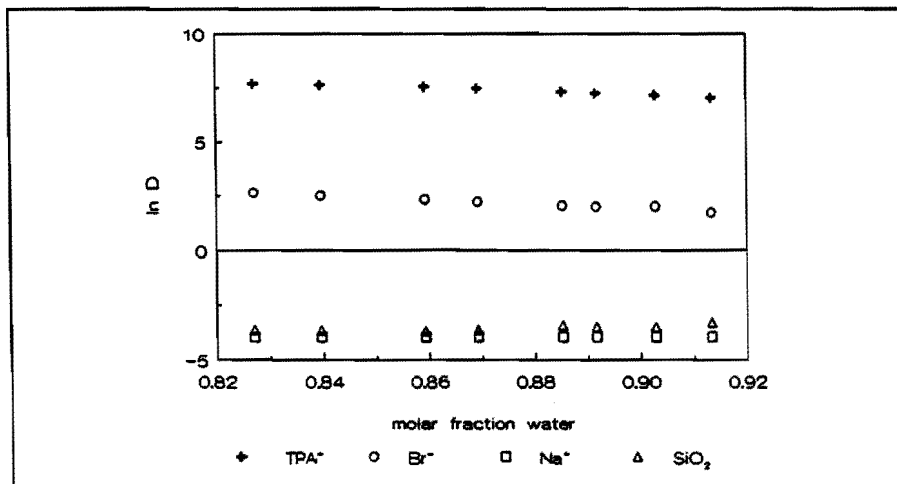


Figure 3.7: Distribution coefficients of TPA bromide and 2:1 sodium silicate.

water and the definition of the excess Gibbs free energy in equation 3.7.

As is to be expected the distribution coefficients show a tendency towards unity at higher molar fractions of water. This effect is most clear for the TMA bromide coacervates because their compositions are quite close to the binodal. For TEA and TPA bromide coacervates the differences in water contents of the coacervates were quite small compared to the difference in water contents of the coacervates and the binodal. This explains the small changes in distribution coefficients for these coacervates. In most cases the distribution coefficients of the cation and the anion of one component are slightly different. The only exception are the coacervates of TMA bromide - 1:1 sodium silicate. In these coacervates the distribution coefficients for TMA equals the coefficient of bromide and also the distribution coefficients for sodium and silicate are equal within the accuracy of the measurement.

Chapter III

For the coacervate TMA bromide - 2:1 sodium silicate the distribution of the silicate over both layers is more extreme than that of the sodium ions. The coacervate TMA bromide - 0.82:1 sodium silicate shows the opposite effect. From these results, we arrive at the following tentative mechanism for coacervation:

TAA and silica have a repulsive interaction. In solutions which contain only TAA and silicate ions, as in the systems described in chapter II, the electrostatic interaction will prevent the ions from migrating too far from each other. In systems which contain additional ions the situation has changed. Because of the repulsion the TAA- and silicate- ions will move apart. The electrostatic interactions of a TAA ion will be accounted for preferably by other ions than silicate ions and those of the silicate ions will be accounted for preferably by other ions than TAA. The sodium will surround the silica and the bromide the TAA. In this way two kinds of regions are formed in solution: a sodium silicate rich region and a TAA bromide rich one. At higher concentrations these regions will form macroscopic droplets and due to the density difference a coacervate is formed.

The TAA bromide solutions behave like normal electrolytes. The situation for the silicate solution is different. Several complications play a role for these compounds. In solutions silicate ions can polymerise to various kinds of oligomers. It can be dissolved as a monomer but oligomers will be present too. The ratio between oligomer and monomer will be dependent on the amount of base and on the kind of cation present. If the cation is an alkali metal ion (e.g. sodium) then the silicate ions will be mainly present as monomer. If TAA ions are present the silicate will form double ring structures as described by Hoebbel [26,27,28]. In order to be dissolved the silicate ions will need a certain amount of base. In general the rule applies that with

Chapter III

increasing base / silica ratio, the fraction of silica which is present as monomer increases. The distribution of the sodium and the silicate ions between both phases is not necessarily the same. Therefore in coacervates the sodium / silicate ratio in one phase is not fixed. In the silica rich layer of the coacervate the sodium / silicate ratio will change to its most favourable value. In the coacervates TMA bromide - 1:1 sodium silicate the distribution coefficients of sodium equals that of the silicate (Figure 3.4). The sodium / silicate ratio is in both layers the same. For the other coacervates with TMA bromide the sodium / silicate ratio in the two layers are different. As most of the sodium silicate is present in the lower phase, the sodium / silicate ratio shifts to its most favourable ratio. In the lower phase the sodium / silicate ratio shifts towards 1:1. For sodium silicate the most favourable ratio appears to be 1:1. This does not hold for TEA and TPA. In the upper phase the sodium silicate ratio was lower than in the lower phase. An explanation is the formation of silicate double ring structures in these solutions. The higher quaternary ammonium ions are found to induce more specifically larger silicate ions than TMA ions. Therefore the total silicate concentration in the upper phase will be higher than would be expected in the case of monomers. As a result the distribution coefficients of the silicate ions are higher than those of the sodium ions.

3.4.2 Titration method.

The results of the analyses of the coexisting phases show clearly that the bromide ions distribute in the same way as the quaternary ammonium ions and the sodium as the silicate ions. Therefore the description of the coacervate in terms of a quasi ternary system of water, TAA bromide and

Chapter III

sodium silicate is possible. In Figure 3.8 the binodals found with the titration method are shown for TMA bromide - sodium silicate with sodium/silicate ratios of 0.82:1 and 1:1. In Figure 3.9 the binodals of TMA bromide - sodium silicate with ratios 1.5:1 and 2:1 are given. In Figure 3.10 the binodal of TMA bromide with 3:1 sodium silicate is shown. The binodals of TMA, TEA and TPA bromide - 2:1 sodium silicate are shown in Figure 3.11.

In the Figures 3.8 to 3.11 the binodals found with the titration method are shown. The Figures 3.8, 3.9 and 3.10 show the influence of the sodium / silicate ratio on the binodal and Figure 3.11 shows the influence of the chain length of the TAA ions on the binodals.

The binodals show a completely different behaviour from that found by Thalberg et.al. [15,16,17,18] for cationic surfactants and an anionic polymer. These authors found demixing into a gel phase and a water phase. The surfactant and the polymer were present in the gel phase. This is quite the opposite to what was found by the analyses of the layers as described in section 3.4.1. This can be explained by the interactions present between the surfactant and the polymer. Two kinds of interactions known from literature are relevant here: an electrostatic attraction and a hydrophobic attraction. In our situation only the electrostatic interaction is present and an interaction which drives the TAA and the silicate apart. No hydrophobic attraction is present because monomeric silicate ions are strongly hydrophilic (see chapter II). This leads us to the conclusion that the role of the silica is different from the role of the polymer in Thalberg's case.

For the 0.82:1 sodium silicate the titration method tends to show

Chapter III

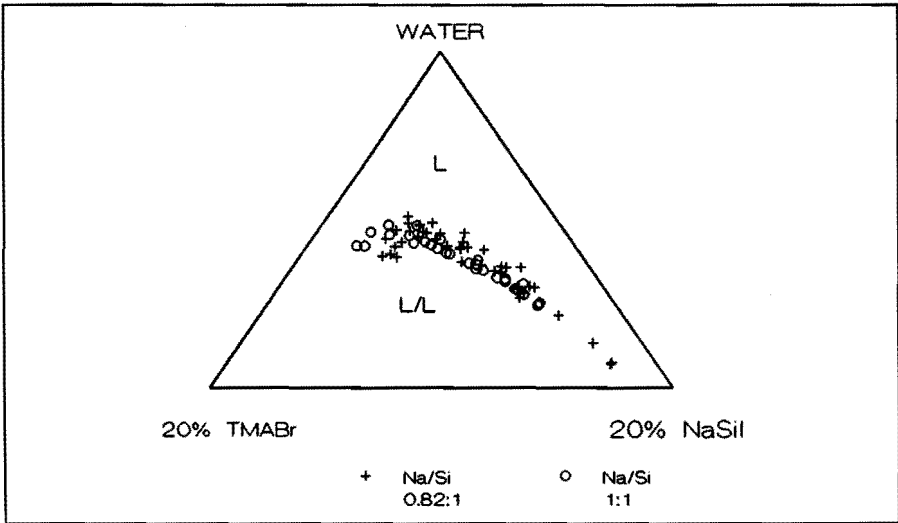


Figure 3.8: Binodals of TMA bromide - 0.82:1 and 1:1 sodium silicate found with titration method.

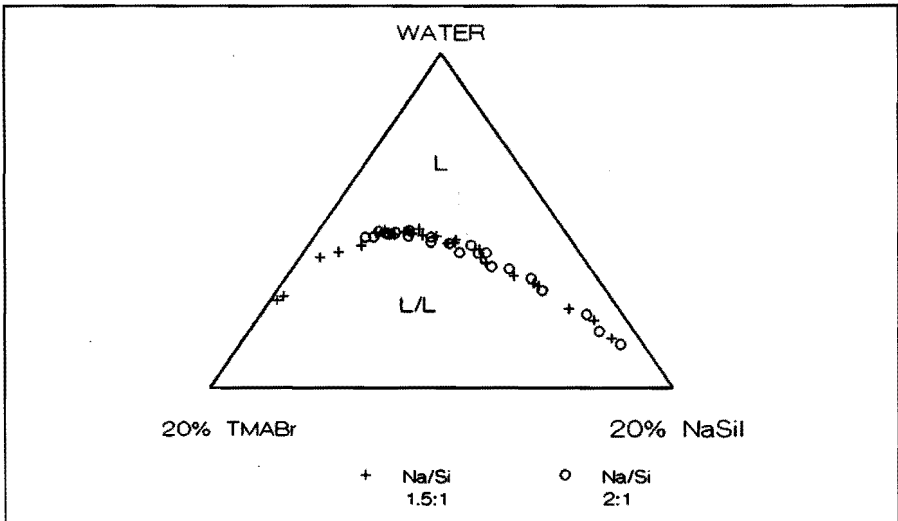


Figure 3.9: Binodals of TMA bromide - 1.5:1 and 2:1 sodium silicate found with titration method.

Chapter III

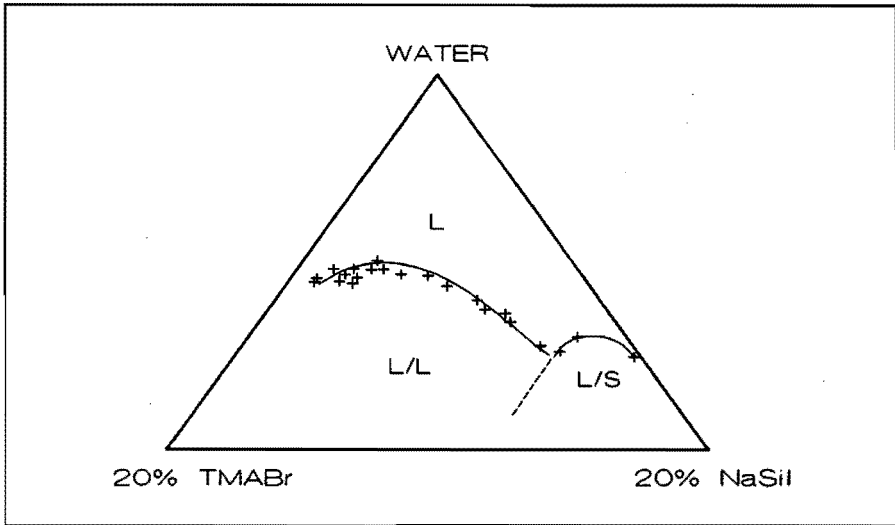


Figure 3.10: Binodal of TMA bromide - 3:1 sodium silicate found with titration method.

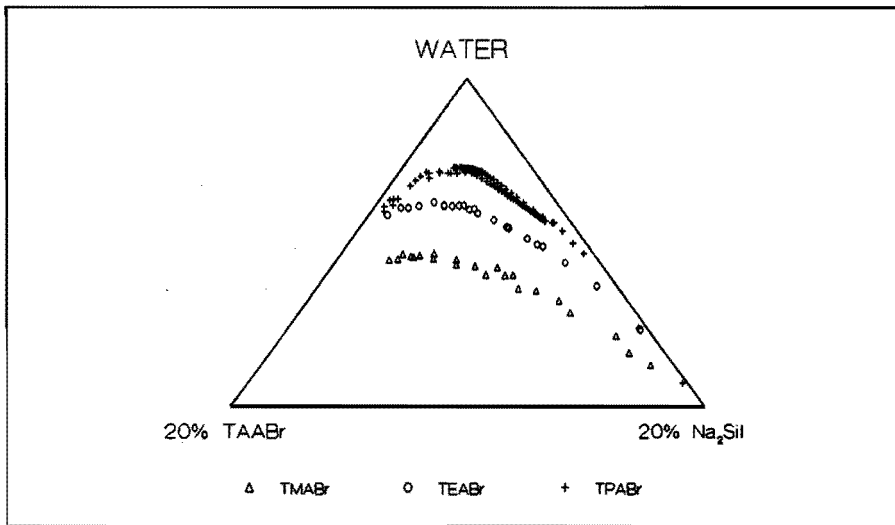


Figure 3.11: Binodals of TMA, TEA and TPA bromide - 2:1 sodium silicate found with titration method.

Chapter III

slightly scattered results. This is ascribed to flocculation of silica which obstructs the determination of the presence of a coacervate. The silica is flocculated because at low sodium / silicate ratios the amount of base is not large enough to charge all silicate ions. The silica will be present as oligomers and when salt is added the oligomers can coagulate. The amount of silica which is flocculated is relatively small. Most of the scattering in the binodal points is ascribed to the influence of the flocculates on the opacity of the solution.

The binodal curve has a sharp bent at the TMA bromide side of the diagram. This is ascribed to the formation of cubic octameric silicate ions under the influence of the TMA which takes place at high TMA concentrations. If cubic octameric silicate ions are present the number of silicate ions (all types) present in solution is about as large as when the silicate ions are present as monomer. The total amount of silica is much larger than when only monomers would be present. This effect is present as the sharp bent in binodal curve.

For the 1:1 sodium/silicate a similar bent was found in the binodal. This is also ascribed to formation of the cubic octamer. For higher sodium/silicate ratios the formation of cubic octamers was less important. The presence of sodium inhibits the formation of the cubic octamer. The sodium-silicate distance is much smaller than the TMA-silicate distance. The effect of the TMA on the silicate is swamped out by sodium because the silicate ions are shielded by the sodium ions against the influences of TMA ions.

In Figure 3.10 the binodal of the 3:1 sodium silicate is shown. At the sodium silicate side of the diagram a solid phase is present. The solid phase disappeared rapidly on the addition of water. From the solids which may be separated from the solutions concerned, TMA bromide is the most probable

Chapter III

one in view of the high solubility of sodium silicate and sodium silicate, and in view of the consideration that the solid was present in the sodium silicate containing phase of the coacervate, in which only small amounts of TMA bromide are soluble.

Figure 3.11 shows that the binodals tend to shift towards higher water contents when the size of the TAA ions is increasing. This shows that the repulsive interaction between TAA and silicate ions is increasing with the size of the cation.

3.4.3 Combination of the analyses of coexisting phases and titration.

3.4.3.1 Contributions of the activity coefficients.

The intersection point of the line through the midpoints of the conodes and the binodal found with the titration procedure gives the plait point and the tangential on the binodal in the plait point. The tangential was drawn by means of a polynomial fit of the experimental binodal points. Nearly all variables of the equations 3.18 and 3.19 are known except for the second and third derivative of the contribution of the activity coefficients to the Gibbs free energy. This contribution can be calculated from the activity coefficients of the pure electrolytes in solution with equation 3.9.

Figure 3.12 shows an example of the contributions of the activity coefficients and the second and third derivative along the tangential through the plait point for TMA bromide - 2:1 sodium silicate as calculated according to equation 3.9.

In this figure the place of the plait point is shown by the vertical line at $i=0.55$. The values of the second and third derivative are taken for equation

Chapter III

3.18 and 3.19 to calculate E_0 and E_1 . This kind of calculations is performed for all coacervates.

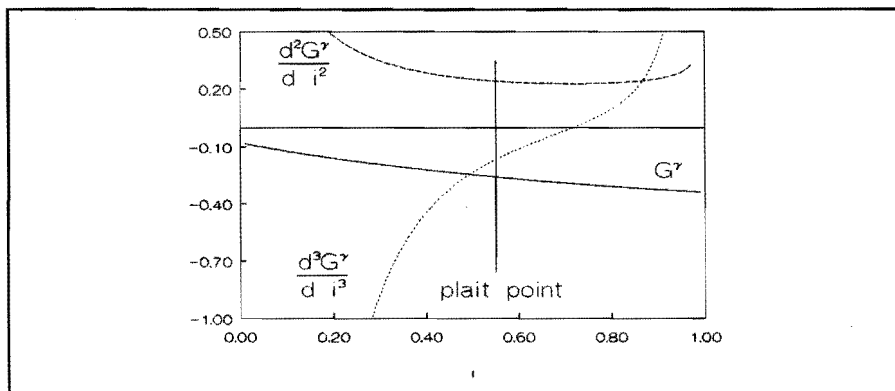


Figure 3.12: Contributions of the activity coefficients along the tangential through the plait point for TMA bromide - 2:1 sodium silicate.

For the activity coefficients of the TAA bromide literature data were provided by Wirth [29] and Lindenbaum and Boyd [30]. Activity coefficients of sodium silicates were not available. As an approximation activity coefficients of other sodium salts were used provided by Robinson and Stokes [31]. For the 2:1 sodium silicate activity coefficients of sodium sulfate were used because of the resemblance between silicate and sulfate in charge and structure. For the 0.82:1 and 1:1 sodium silicates activity coefficients of sodium chloride were used. In the solutions of 0.82:1 sodium silicate the total charge on the silicates is lower than in 1:1 sodium silicate solutions. In view of the Debye-Hückel limiting slope being proportional to $|z_+z_-|$ and the average charge of the silicate ions being -0.82, the Debye-Hückel limiting slope for this ratio should be multiplied with this charge. The B- and R- terms were estimated by the sodium chloride values.

Chapter III

Of course taking the activity coefficients of other sodium salts, than sodium silicate, gives only an approximation of the contribution of the activity coefficients to the Gibbs free energy. Sodium sulfate was used because of the resemblance in structure with a 2:1 sodium silicate. The choice of the sodium chloride is quite arbitrary. Nevertheless, this approximate taking into account of the activity coefficients is better than ignoring them.

3.4.3.2 Comparison of the experiments with the calculated binodal.

In Figure 3.12 to 3.16 the combined data of the titration and the coexisting phases are shown. In these figures the plait points and the tangentials in the plait points at the binodals found with the titration procedure are

TABLE 3.1: Plait points and constants of the excess Gibbs free energy.

Sample		Plait point			Excess constants	
TAA Br	Na/SiO ₂ ratio	x ₁ water	x ₂ TAABr	x ₃ Na ₂ Sil	E ₀ kJ/mole ²	E ₁ kJ/mole ³
TMA	0.82:1	0.8505	0.0284	0.1211	43.15	13.43
TMA	1:1	0.8652	0.0393	0.0955	32.89	17.87
TMA	2:1	0.8725	0.0356	0.0919	29.06	19.72
TEA	2:1	0.9082	0.0272	0.0646	38.35	52.54
TPA	2:1	0.9311	0.0173	0.0516	37.61	141.02

shown. From the plait point, the tangent on the binodal in the plait point and the second and third derivative of the contribution of the activity coefficients, as described in section 3.4.3.1, the E₀ and E₁ can be determined by using equations 3.18 and 3.19. In Table 3.1 the positions of the plait points and the calculated values of the E₀ and E₁ are listed for the coacervates investigated.

Chapter III

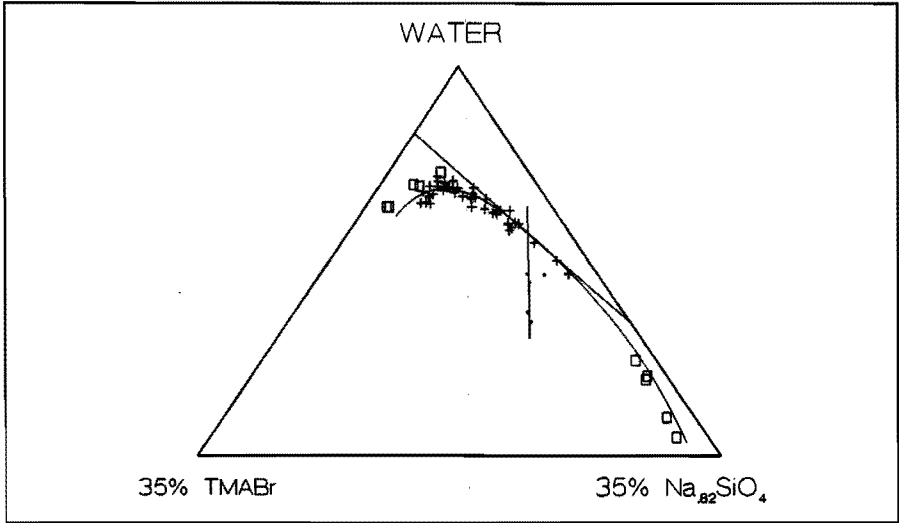


Figure 3.13: Combined data of the coacervate TMA bromide - 0.82:1 sodium silicate.

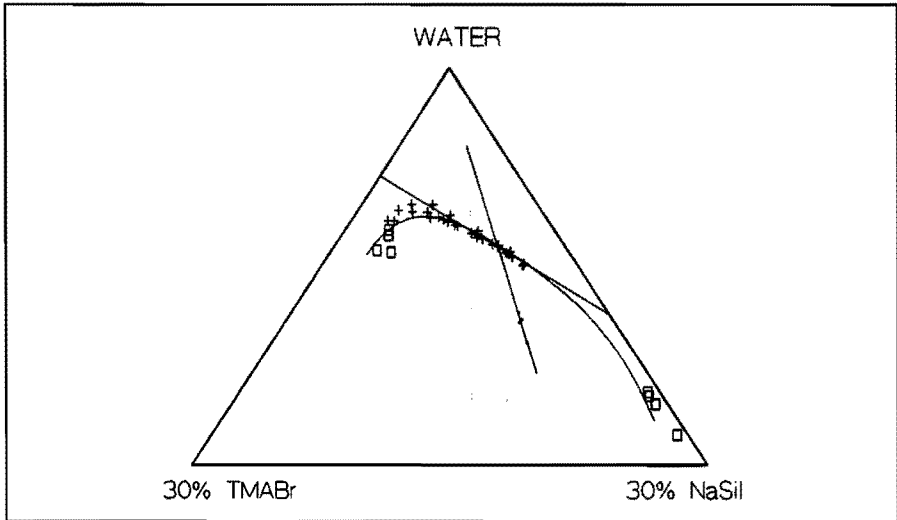


Figure 3.14: Combined data of the coacervate TMA bromide - 1:1 sodium silicate.

Chapter III

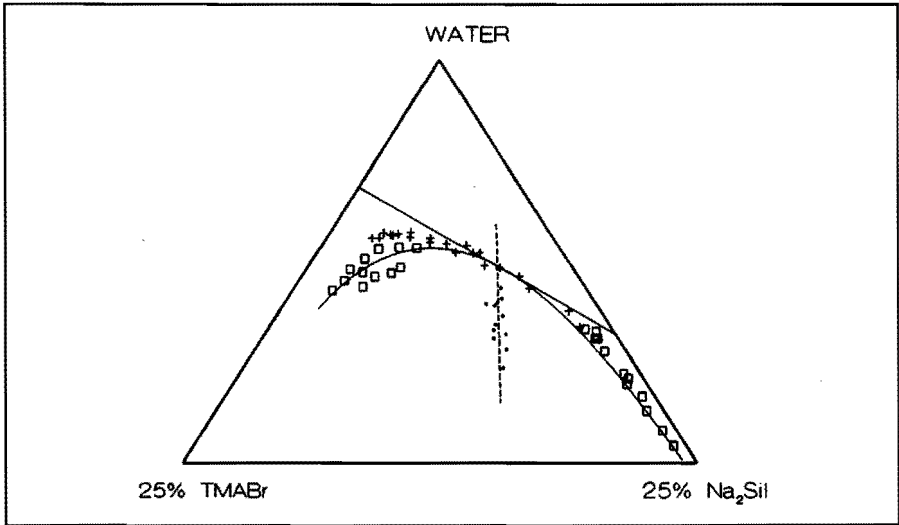


Figure 3.15: Combined data of the coacervate TMA bromide 2:1 sodium silicate.

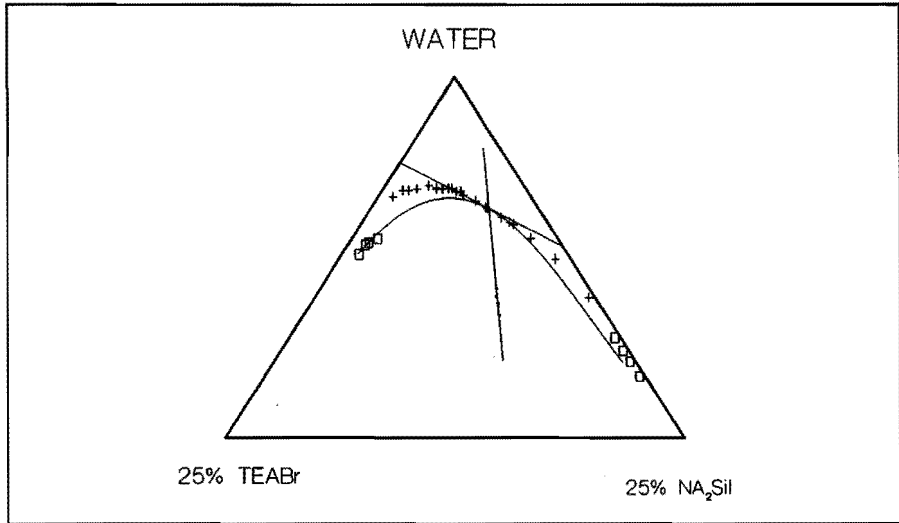


Figure 3.16: Combined data of the coacervate TEA bromide 2:1 sodium silicate.

Chapter III

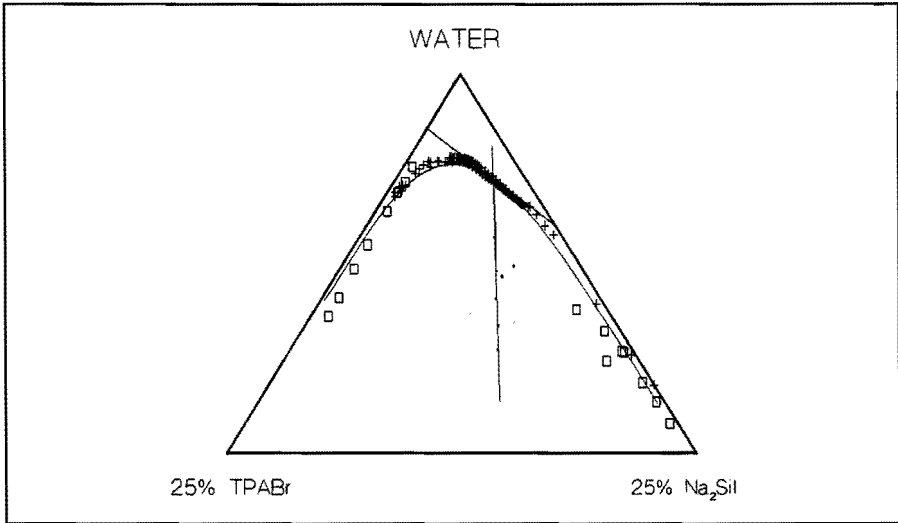


Figure 3.17: Combined data of the coacervate TPA bromide 2:1 sodium silicate.

The constants in TABLE 3.1 are used in the equation for the Gibbs free energy (equation 3.16) and the binodals are calculated. These calculated binodal are presented in the same figures as drawn lines.

In figures 3.13 to 3.17 the calculated binodals are presented as drawn lines. For most coacervates the calculated binodal does give a satisfactory comparison with the experiments. Deviations are seen in figures 3.14 and 3.15 for TMA bromide and TEA bromide 2:1 sodium silicate coacervates. For these systems the binodal found with the titration method are at much higher water contents at the TAA bromide side of the diagram than the composition of the upper layer. This is ascribed to the fact that the system is shown as a ternary system. The titration method gives the binodal for the ternary systems. The compositions of both layers are not ternary, however.

Chapter III

The deviations from the ternary system can be described by two different methods, as shown in Figure 3.18.

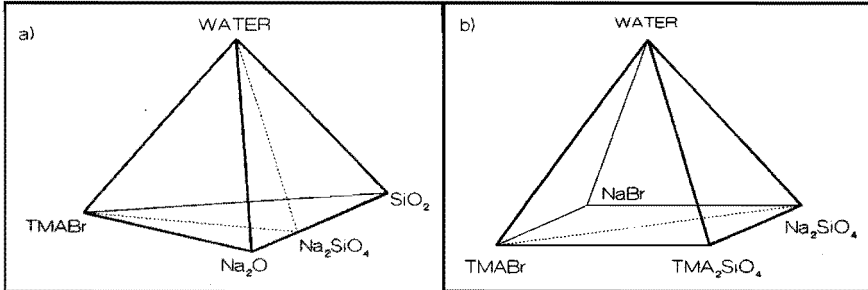


Figure 3.18: Deviations from the ternary plane.

i) The system can be considered as a quaternary system of water, TAA bromide, sodium hydroxide and silica (see figure 3.18 a). Deviations from the ternary system can be caused by different sodium/silicate ratios in the upper and lower phases, respectively. The mean charge of the silicate ions in the upper layers is different from that in the lower layer. The TMA and the bromide are supposed to be distributed in exactly the same way over both layers in this description.

ii) The system can be considered as the quinary system water, TAA bromide, TAA silicate, sodium bromide and sodium silicate (see figure 3.18 b). Deviations from the quinary system can occur when sodium ions are exchanged by TAA ions in one of the layers. The mean charge of the silicate ions is the same in both layers.

The influence of these processes is most clearly present in the distribution coefficients. If the demixing occurs according to the ternary system, TAA bromide - sodium silicate - water, the distribution coefficients of TMA would equal those of bromide and the distribution coefficients of sodium

Chapter III

would equal those of silicate. In process i) the distribution coefficients of TAA and bromide should have the same value. The distribution coefficients of sodium and silicate however may be different. In process ii) all distribution coefficients are different. A simple test whether the description as process ii) may be applied is: If the distribution coefficients of TAA are larger than those of bromide the distribution coefficients of silicate should be larger than those of sodium. The difference between the amount of TAA and bromide present in the one layer should be compensated by a comparable additional amount of silicate or sodium ions. In process ii) the hydroxide should be distributed in the same way as the silicate, since the charge of the silicate is supposed to be constant. However there is no reason why the silicate and the hydroxide distribute the same way. In the figures 3.3-3.7 the distribution coefficients are shown. In most cases the distribution coefficients of TMA and bromide are different. This shows the inadequacy of process i), meaning that the system should be treated according to process ii) at least. For coacervates with TEA and TPA the test does not exclude process ii). But the difference in TAA- and bromide- concentration is not equal to the difference in sodium- and silicate- concentration. With the electroneutrality the concentrations of hydroxylic ions can be calculated. In most cases different silicate / hydroxylic ratios for the two layers are found. This shows the additional presence of process i). In these coacervates the formation of double ring silicate ions interferes with processes i) and ii). Until now we assumed the silicate ions being present as monomers. In practice double ring structures are formed. As double ring formation occurs mainly in the upper layer the distribution coefficients of silicate are in those cases larger than that corresponding to the monomers. Therefore both processes i) and ii) and the formation of double ring silicate ions play a role in the deviations from the

Chapter III

ternary systems TAA bromide - sodium silicate - water.

3.4.3.3 The constants of the excess Gibbs free energy.

In Table 3.1 the constants E_0 and E_1 of the excess Gibbs free energy are tabulated. In graphical form the constants of the TMA bromide coacervates can be linked. The constants for the TMA bromide coacervates show a remarkable connection, as is shown in figure 3.19. The influence of the alkyl chain length on the E_0 is quite small. This coefficient increases slightly with the chain length. More pronounced differences are present in the E_1 . This coefficient increases with the size of the quaternary ammonium ion. A linear correlation of E_1 with the square of the enthalpy of hydrophobic hydration was observed (figure 3.20). The enthalpy of hydrophobic hydration was determined by Heuvelsland [32].

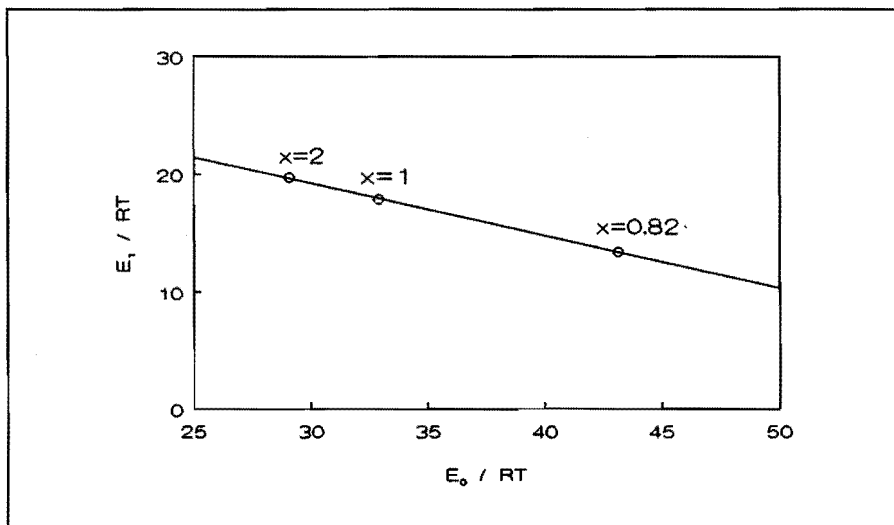


Figure 3.19: Coefficients of the excess energy for TMA bromide - X:1 sodium silicate coacervates.

Chapter III

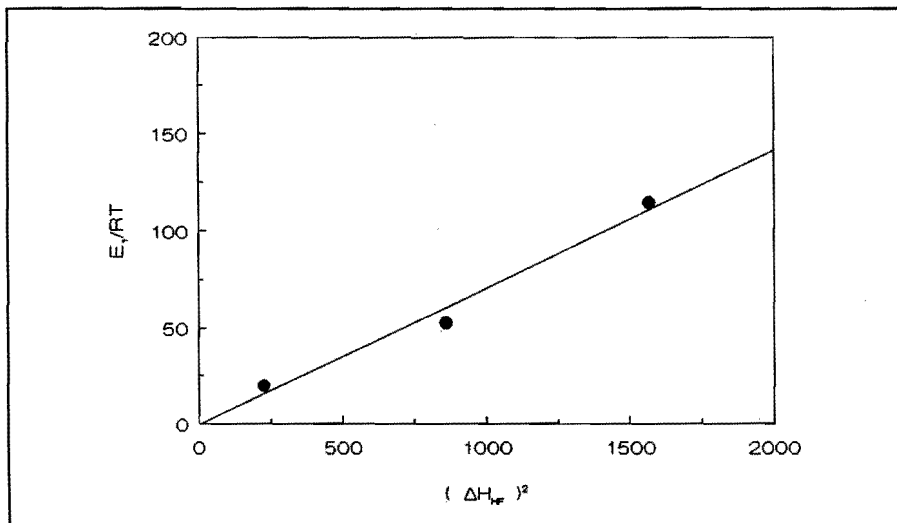


Figure 3.20: E_a of TMA, TEA and TPA as function of the enthalpy of hydrophobic hydration.

At this point the question arises about the molecular mechanism which is the cause of this excess Gibbs free energy. In equation 3.13 the excess Gibbs free energy is described in terms of the Redlich-Kister equation with the contributions of the activity coefficients. As the coacervation is thought to be caused by the interaction between TAA and silicate ions, we leave the contribution of the activity coefficients out of consideration. The Redlich-Kister part of equation 3.13 remains. This term is due to an interaction between the TAA and the silica. These interactions can be regarded as a combination of a Gibbs free interaction enthalpy and an excess entropy. Frequently the excess enthalpy and entropy have the same sign while the absolute values of the interaction enthalpy and the excess entropy (more strictly Ts^E) are about the same. This is frequently found in the following

Chapter III

cases: i) $H^E > 0$ and $s^E > 0$: both due to the cancelling of self association of the pure components during mixing. ii) $H^E < 0$ and $s^E < 0$: on mixing, pronounced complex formation occurs between the compounds. However in some mixtures of polar and apolar compounds the excess entropy can be very small or even negative while the excess enthalpy is positive [33]. This is considered to be due to the formation of networks of hydrogen bonds. In our case we are dealing with hydrophobically and hydrophilically hydrated ions. It is likely that these hydrated regions are still present in the mixtures. H^E will be positive because in a mixture a part of the sodium ions near silicate ions is replaced by TAA ion, and part of the bromide ions near TAA ions are replaced by silicate ions. The positive H^E is then caused by the larger average distance between cations and anions in the mixture, than in the separate solutions of sodium silicate and TAA bromide. It is likely that in this case s^E will be small in absolute sense. Therefore the excess enthalpy will be regarded as the main component of the excess Gibbs free energy. This is in agreement with the model of strictly regular solutions as described by several authors [34,35, 36,37,38].

Several factors influence this interaction enthalpy:

- The type of TAA ion.
- The sodium / silicate ratio.

The interaction enthalpy can be divided into compound-compound interactions (assuming additivity of interaction energies). In equation 3.7 the excess Gibbs free energy was supposed to be caused by the interaction between TAA and silicate ions. The E_0 describes the interaction between one TAA with one silicate ion and the E_1 is a mixed interaction of three ionic units: one term describing the interaction between two TAA ions with one silicate ion and one term describing the interaction between one TAA ion

Chapter III

and two silicate ions. The second term is subtracted from the first as is described in the first extension of the Redlich-Kister equation (equation 3.13).

In figure 3.19 the coefficients of the excess Gibbs free energy of TMA bromide-sodium silicate with three sodium / silicate ratios are shown. At increasing sodium / silicate ratio the contribution of the TMA-silicate interaction energy (E_0) diminishes and the contribution of the three ionic units (E_1) increases. A linear relation was found between the E_0 and the E_1 . In a relatively sense, the decrease in E_0 is more pronounced than the increase of E_1 . On the basis of the hydration of the ions leading to coacervation this can be explained as follows:

At high sodium / silicate ratio the silicate ions will be present predominantly as monomers with a relatively large charge (1,5-2 units) per silicate ion. This charge can be compensated by sodium and TMA ions. When a large amount of sodium is present the charge compensation of the silicate ions will occur predominantly by the sodium ions. At small sodium / silicate ratios charge compensation of the silicate ions will be to a larger extent by TMA ions. Therefore the main contribution to the excess Gibbs free energy, the E_0 , decreases with increasing sodium silicate ratio.

The increase in E_1 with increasing sodium/silicate ratio can also be explained by the differences in charge on the silicate ions. The excess energy can be written as:

$$\begin{aligned} G^E &= x_2 x_3 (E_0 + (x_2 - x_3) E_1) \\ &= x_2 x_3 E_0 + x_2^2 x_3 E_1 - x_2 x_3^2 E_1 \end{aligned} \tag{3.20}$$

Chapter III

Here the first term with E_1 describes the interaction between two TMA ions with one silicate ion and the second term with E_1 describes the interaction of one TMA ion with two silicate ions. In the proportionality constant E_1 the average charge per silicate ion is reflected: If the silicate is doubly charged, the three ionic interaction will be more pronounced than when the silicate is predominantly mono charged.

For the different TAA ions E_0 is nearly constant. The E_1 however does increase with increasing chain length. In figure 3.20 the E_1 is shown as a function of the square of the enthalpy of hydrophobic hydration, which were calculated by Heuvelsland [32]. A linear relation is found. This shows that the interaction between two TAA ions and one silicate ion is the major contribution to the E_1 for these coacervates. The E_1 considered here are those of 2:1 coacervates. As we found for the TMA coacervates with increasing sodium / silicate ratio the contribution of the first term of the E_1 is of increasing importance over the second term for 2:1 sodium silicate. The deviations from the line can be due to the errors both in the E_1 constant and the enthalpy of hydrophobic hydration. The connection between the enthalpy of hydrophobic hydration and the E_1 suggests that the hydrophobic hydration of the quaternary ammonium ions is of particular importance in the coacervation.

Our system has a close resemblance with the systems investigated by Thalberg et.al. [15,16,17,18]. These authors found complex coacervation in systems containing cationic surfactants and anionic polymers. We have a cationic surfactant (TAA ions) and something resembling an anionic polymeric species (monosilicate ions partially form larger silicate ions which can be regarded as polymers). The coacervation is caused by an interaction between

Chapter III

the silicate ions and the TAA ions. Because these ions do not form ion pairs the coacervation cannot be ascribed to complex coacervation. The fact that the coacervation disappears upon dilution can be regarded as an indication that in our system simple coacervation occurs [4].

3.5 Conclusions.

Coacervation takes place in solutions of TAA bromide - sodium silicate - water. The TAA bromide is predominantly present in the upper layer and the sodium silicate is mainly present in the lower layer. The coacervation can be described with the activity coefficients of the two separate salts and an additional excess Gibbs free energy. For this additional excess Gibbs free energy the first two terms of a Redlich-Kister equation are used. One of the terms is linearly dependent on the square of the enthalpy of hydrophobic hydration. The coacervation is ascribed to the following mechanism:

TAA ions are hydrophobically hydrated and silicate ions are hydrophilically hydrated. The structures of the hydration layer are different and can not overlap. In solutions which contain, besides TAA and silicate, a cation (e.g. sodium) and an anion (e.g. bromide) coacervation can occur. At higher concentrations the TAA and the silicate ions will migrate apart. The respective electrical charges will be predominantly neutralized by the other ions present. The sodium will surround predominantly the silicate and the bromide the TAA. Two microstructures are formed in this way. At higher concentration coalescence of these microstructures will occur to macroscopic droplets and gravity will cause the formation of two layers.

Coacervation in the system TAA bromide-sodium silicate-water can be

Chapter III

classified as simple coacervation.

References

- [1] W.Pauli, *Kolloidchem. Beihefte*, 3(1912)382.
- [2] W.Ostwald, *Kolloid-Z.*, 43(1927)131.
- [3] H.G.Bungenberg de Jong and H.R.Kruyt, *Kolloid-Z.*,50(1930)39.
- [4] H.R.Kruyt, "Colloid Science", Elsevier publishing co., Amsterdam, 1949, Volume II, p. 243-256.
- [5] M.J.Voorn, Thesis, Amsterdam, 1956.
- [6] A.M.Mugnier de Trobriant, M.Lucas, J.Steigman and L.Hwang., *J.inorg.nucl.Chem.*,41(1979)1214.
- [7] A.M.Mugnier de Trobriant, M.Lucas, J.Steigman and L.Hwang., *J.Phys. Chem.*,82(1987)418.
- [8] A.M.Mugnier de Trobriant, 1979, Centre d'Etudes Nucléaires de Fontenay-aux-Roses, Rapport CEA-R-5009.
- [9] M.Lucas, *J.Inorg.nucl.Chem.*,32(1970)3692.
- [10] M.Lucas, *J.inorg.nucl.Chem.*,33(1971)543.
- [11] M.Lucas, *J.inorg.nucl.Chem.*,33(1971)1883.
- [12] H.R.Kruyt, "Colloid Science", Volume II,Elsevier publishing co., Amsterdam, 1949, Chap.X.
- [13] A.E.Vassiliades and I.Cohen, *J.Am.Oil Chemists Soc.*, 39(1962)246.
- [14] P.Economou, I.Cohen and A.Libackyj, *J.Phys.Chem.*, 66(1962)1829.
- [15] K.Thalberg and B.Lindman, *J.Phys.Chem.*,93(1989)1478.
- [16] K.Thalberg, B.Lindman and G.Karlström, *J.Phys.Chem.*, 94(1990) 4289.
- [17] K.Thalberg and B.Lindman, *Langmuir*, 7(1991)277.
- [18] K.Thalberg, B.Lindman and G.Karlström, *J.Phys.Chem.*, 95(1991)

Chapter III

3370.

- [19] I.Prigogine and R.Defay, "Chemical Thermodynamics", Longmans, Green and co., London, 1954.
- [20] A.Findlay, "The phase rule and its application", 9th ed.,Dover publ. 1951, p 285.
- [21] R.Koningsveld, Thesis, Leiden, 1967.
- [22] O.Redlich and A.T.Kister, *Ind.Eng.Chem.*,40(1948)345.
- [23] L.A.Robbins, "Liquid-liquid extraction", in R.H.Perry, D.W.Green and J.O.Maloney (eds), *Perry's Chemical Engineers' Handbook*, 1984, 6th ed, p 15-6.
- [24] C.L.M.Holten and H.N.Stein, *Analyst*, 115(1990)1211.
- [25] K.Kato, *Anal.Chim.Acta*, 82(1976)401,
V.W.Truesdale and C.J.Smith, *Analyst*, 100(1975)797.
- [26] D.Hoebbel, G.Garzó, G.Engelhardt and A.Vargha, *Z.Anorg.allg. Chem.*, 494(1982)31.
- [27] D.Hoebbel, A.Vargha, B.Fahlke and G.Engelhardt, *Z.Anorg.allg. Chem.*, 509(1984)85.
- [28] D.Hoebbel, A.Vargha,G.Engelhardt and K.Ujszászy, *Z.Anorg.allg. Chem.*, 521(1985)61.
- [29] H.Wirth, *J.Phys.Chem.*, 71(1967)2922.
- [30] S.Lindenbaum and G.E.Boyd, *J.Phys.Chem.*,68(1964)911.
- [31] R.L.Robinson and R.H.Stokes, "Electrolyte solutions", Butterwoths Scientific Publications, 2nd ed., London, 1959.
- [32] W.J.M.Heuvelsland, Thesis, Amsterdam, 1980.
- [33] J.S.Rowlinson and F.L.Swinton, "Liquids and Liquid Mixtures", Butterworth Scientific, 3rd ed., London, 1982, p. 171.
- [34] A.W.Porter, *Trans. Faraday Soc.*, 16(1920)336.

Chapter III

- [35] J.J. van Laar and R.Lorenz, *Z.anorg.Chem.*, 145(1925)239.
- [36] W.Heitler, *Ann.d.Phys.*, 80(1926)629.
- [37] J.H.Hildebrand, *J.Am.Chem.Soc.*, 51(1929)66.
- [38] G.Scatchard, *Chem.Rev.*, 8(1931)321.

CHAPTER IV: ADSORPTION OF TAA BROMIDE ON SILICA.

4.1 Introduction.

In the previous chapters the interactions between TAA and silicate ions in solutions were discussed. The viscosity and coacervation behaviour was explained by a repulsive interaction between the TAA and silicate ions which is superimposed on the attraction between two oppositely charged ions. The most probable reason for this is the difference in hydration of the ions. The TAA ions are hydrophobically hydrated and the silicate ions are hydrophilically hydrated. These hydration structures are considered to arise from different origins and are supposed not to overlap.

Between macroscopic silica particles and TAA ions such repulsions are not found. Rubio and Goldfarb [1] determined the stability of silica dispersions in the presence of TAA salts and the adsorption of cetyltrimethylammonium bromide (CTAB) on Aerosil 200. The stability of silica dispersions decreased in the presence of TAA salts. This was attributed to the adsorption behaviour of TAA ions. They found that the limiting amount of adsorbed CTAB at large concentration is higher than the number of silanol groups. They contributed this to the formation of a bilayer of CTAB ions. Wijnen [2] found a strong decrease in the dissolution rate of Aerosil 200 in the presence

Chapter IV

of TMA hydroxide. This effect was ascribed to the adsorption of TMA on the silica surface.

In the zeolite syntheses this adsorption behaviour is thought to play a role. In the first step adsorption on the silica/alumina gel takes place, which influences the dissolution behaviour, and in the last step the TAA is present in the cavities of the zeolite and prevents the zeolite-quartz transition. The adsorption mechanism is expected to give important information about the interactions that take place.

Adsorption has an influence on quite a few characteristic features of silica. It may influence the dissolution rate and the colloid chemical stability of silica dispersions. The stability of dispersions is closely related to the charge of the colloid and the size of the region around the particle in which the colloid influences the potential. A powerful tool to study these processes is the ζ potential. This is the potential at the electrokinetic slipping plane. Although the ζ potential is conceptionally different from the Stern potential (Ψ_δ) which enters into the colloid chemical stability calculations according to Derjaguin, Landau, Verweij and Overbeek [3], in practice one obtains in cases of surfaces not covered by polymers a good indication for Ψ_δ by employing the ζ potential in such calculations as was shown by Parfitt and Picton [4] and Horn and Smith [5]. Adsorption of ions changes the charge behind the electrokinetic slipping plane and changes the ζ potential. The charge of the adsorbed ions interferes with the surface silanol groups. This causes a rather complex system. The changes in ζ potential give a quantitative indication of some aspects of the adsorption. For a more detailed study the amount of ions at the surface has to be determined. Both is done in this chapter. The data obtained from ζ potential measurements are combined with data obtained by adsorption experiments in order to obtain a complete picture

Chapter IV

of the charges at the silica/solution interface.

4.2 Theory.

In this section two different kinds of theories will be discussed. i) the theory of charged particles in a dispersion medium, ii) several adsorption mechanisms. These mechanisms will contain general mechanisms and mechanisms developed for the adsorption of organic- and even TAA- ions on silica.

4.2.1 The electrical double layer.

When oxidic materials are dispersed in water alkaline or acidic surface groups are formed. The pH of the solution will determine the dissociation behaviour of these groups and in this way the charge of the particles. The charged particles influence their direct surrounding. The region of influence is called the electrical double layer. An important theory describing the double layer at a flat S/L interface is the Gouy-Chapman theory which is well described by Hunter [6]. This theory is summarized below.

If a charged particle is present in an electrolyte solution the counter ions will be attracted and the coions will be repelled. The concentration of these ions can be expressed in terms of the Boltzman equation:

$$n^+ = n_o \exp\left(-\frac{z_+ e_o \Psi}{kT}\right); n^- = n_o \exp\left(-\frac{z_- e_o \Psi}{kT}\right) \quad (4.1)$$

Chapter IV

In this equation n_0 is the bulk concentration (m^{-3}), z_i the valency including sign of ion i , e_0 charge of proton and Ψ the potential at a certain distance from the S/L plane.

Because of the difference in charge of the co- and counter- ions a space charge, ρ , is present which can be described as:

$$\rho = \sum z_i n_i e_0 = \sum n_0 z_i e_0 \exp\left(-\frac{z_i e_0 \Psi}{kT}\right) \quad (4.2)$$

With the Poisson equation the space charge is related to the local potential in the double layer.

$$\nabla^2 \Psi = -\frac{\rho}{\epsilon_0 \epsilon_r} \quad (4.3)$$

After substituting equation 4.2 in 4.3, some calculations yield for the special case of a plane S/L interface in a solution of a symmetrical electrolyte with ions of valency z , the potential as function of the distance from the particle surface:

$$\Psi = \frac{2kT}{ze_0} \ln \frac{1 + \gamma \exp(-\kappa x)}{1 - \gamma \exp(-\kappa x)} \quad (4.4)$$

The constants γ and κ have the following value:

The Ψ_0 is the surface potential and κ is called the Debye-Hückel length. It can be regarded as the reciprocal double layer thickness.

Chapter IV

$$\gamma = \frac{\exp(ze_o\Psi_o/2kT) - 1}{\exp(ze_o\Psi_o/2kT) + 1} \quad (4.5)$$

$$\kappa = \sqrt{\frac{2z^2e_o^2n_o}{\epsilon_o\epsilon_r kT}}$$

These equations are only valid for plane interfaces. For most colloids this is a good approximation. The size of the double layer is supposed to be relatively small compared to the size of the particle ($\kappa a \gg 1$, a is the particle radius).

With this model the surface charge can be calculated. The surface charge has to be compensated by the charge in the electrical double layer:

$$\sigma_o = -\sigma_{dd} = -\int_0^{\infty} \rho dx \quad (4.6)$$

Substituting equation 4.2 and 4.4 gives:

$$\sigma_o = \sqrt{8n_o\epsilon_o\epsilon_r kT} \sinh\left(\frac{ze_o\Psi_o}{2kT}\right) \quad (4.7)$$

Equation 4.7 would be the surface charge on the solid itself, if the approximations of the Gouy-Chapman theory would be valid up to the phase boundary. Close to the colloid surface deviations occur. The relative permit-

Chapter IV

tivity of the dispersion medium, ϵ_r , has a value different from that in the bulk solution. But the most important approximation is that the ions are supposed to be point charges in this theory. In reality the part of the double layer close to the surface does not contain charges because of the finite size of the ions. In this region the charge density is zero and the potential drops linearly with the distance. The plane to which the ions can approach is called the Stern layer. Frequently the Stern layer is divided in two parts: The Inner Helmholtz Plane (IHP) and the Outer Helmholtz Plane (OHP). The IHP is the distance of closest approach of unhydrated ions and the OHP is the distance of closest approach of hydrated ions. The chemisorbed ions are usually present in the IHP and the electrical double layer starts from the OHP. Close to the solid/liquid interphase the water molecules are fixed to the solid ("no slip" condition, known from hydrodynamics). A little further away from the surface the hydration layer of the colloid becomes less fixed and the surrounding water can move with respect to the particle. The transition plane is called the electrokinetic slipping plane. The potential at this point is called the ζ potential.

In the context of the present chapter the integration of equation 4.6 is thought to start at the slipping plane. In the region outside the slipping plane the approximations of the Gouy-Chapman theory can be relied upon to a much better degree than close to the surface. The charge behind the slipping plane can be calculated with:

$$\sigma_{\zeta} = \sqrt{8n_o \epsilon_o \epsilon_r kT} \sinh \left(\frac{ze_o \zeta}{2kT} \right) \quad (4.8)$$

Chapter IV

in which ζ is the ζ potential. In the derivation of this formula, the validity of the assumptions of the Gouy-Chapman theory is claimed only for the region outward of the electrokinetic slipping plane.

4.2.2 Adsorption models.

4.2.2.1 The Stern model.

The adsorption of gasses on surfaces can generally be described with the Langmuir adsorption isotherm. In some cases the adsorption at S/L interfaces can be treated with similar theories as the solutes usually behaves gas like. The charge in the Stern layer, for symmetrical electrolytes with valency z , can be calculated according to Hunter [6].

$$\sigma_{\beta} = \frac{z e_0 N_s \frac{n_0 V_m}{N_{av}} \exp(-\Delta G_{ads}/kT)}{1 + \frac{n_0 V_m}{N_{av}} \exp(-\Delta G_{ads}/kT)} \quad (4.9)$$

In this equation σ_{β} is the charge in the Stern layer ($C.m^{-2}$), e_0 is the charge of a proton (C), N_s is the number of sites (m^{-2}), V_m is the molar volume of the solvent ($m^3 \text{ mole}^{-1}$), n_0 is the electrolyte concentration (m^{-3}) and N_{av} is the Avogadro number (mole^{-1}). The adsorption energy, ΔG , can be considered to have two components: The electrical energy of the ion in the Stern layer and a chemical adsorption energy.

Chapter IV

$$\Delta G_{ads} = z e_0 \Psi_\beta + E \quad (4.10)$$

where Ψ_β is the Stern potential and E the chemical adsorption energy.

In first approximation the Stern potential can be considered to be equal to the ζ potential. According to Kamo et.al. [7] the number of sites and the adsorption energy, E, can be obtained by rewriting equation 4.9 to:

$$\frac{1}{\Gamma} = \frac{N_{av}}{N_s} \exp\left(\frac{E}{kT}\right) * \frac{55.6}{c_0} \exp\left(\frac{z e_0 \zeta}{kT}\right) + \frac{N_{av}}{N_s} \quad (4.11)$$

In this equation Γ is the amount of adsorbed ions per m^2 . The approximation which are valid for the charge in the Stern plane (equation 4.9) are valid for equation 4.11 as well. The adsorption energy is split into two terms: An electrical term, approximated with the term with the ζ potential, and a constant term described by E.

By plotting the reciprocal amount of adsorbed ions against the reciprocal equilibrium concentration multiplied with the exponential term containing the ζ potential the number of adsorption sites and the chemical adsorption energy can be determined.

The Stern adsorption model is a good description for silver iodide and mercury. Adsorption on oxidic surfaces can be described as well but the Stern adsorption theory can not explain the combination of high surface charge densities with relatively low ζ potentials. Tadros and Lyklema [8] explained this by the presence of a porous gel layer at the S/L interface. This gel layer can be penetrated by counter ions but the pores are considered to be too small to be measured with nitrogen adsorption. Therefore the

Chapter IV

specific area used for the surface charge is too small. This results in a high surface charge.

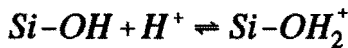
4.2.2.2 The Site-binding model.

In the Gouy-Chapman model the charge is assumed to be distributed homogeneously over the surface. In fact discrete charges are present. These discrete charges can be considered as adsorption sites for potential determining ions, e.g. protons, and counterions. In this model attention is paid to the mechanism of adsorption, which is not done in the Stern model. Therefore this model is called the Site-binding model. In the Site-binding model two layers close to the S/L interface are distinguished:

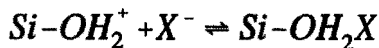
-A layer of ion pairs formed by charged surface groups and counter ions.

-A diffuse layer which can be described with the Gouy-Chapman theory.

The charges arise by adsorption or desorption of protons from the surface groups.



The surface charge is formed according to these reactions. The surface charge consists of discrete charges. These charges can act as sites for the adsorption of counterions to the formation of ion pairs.



Chapter IV

From these reaction equilibria Yates, Levine and Healy [9] derived:

$$-\sigma_{dd} = \sigma_0 + \sigma_c = \frac{N_s e_0}{2} \left[u \left(\frac{1}{\alpha_+} + \frac{1}{\alpha_-} \right) + v \left(\frac{1}{\alpha_+} - \frac{1}{\alpha_-} \right) \right] \quad (4.12)$$

In this equation σ_{dd} is the charge in the diffuse double layer, σ_c is the charge of the adsorbed ions, α_+^{-1} and α_-^{-1} are the fractions of unoccupied positive and negative sites respectively, u is a standard for the number of uncharged surface groups and v is the total fraction of sites which is charged.

The site binding model can explain the large surface charge of oxides. Charged surface groups are neutralised by counter ions. This diminishes the repulsion between the surface and the potential determining ions. Therefore the potential determining ions will be adsorbed more strongly at the surface. Smit and Holten [10] found reliable fits for the ζ potential and the surface charge of α -alumina single crystals. For silica and titania Healy and White [11] however found that the ζ potential and the surface charge could not be described simultaneously with this model. Similarly, Janssen et.al. [12] reported that calculations with the site binding model, based on experimental data and on the assumption that local activity coefficients near the surface are independent of the charge at the interface, lead to conclusions which are at variance with this assumption.

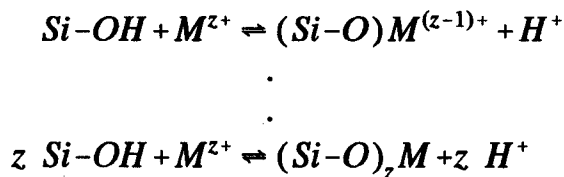
4.2.2.3 The surface-ligand model.

In the Gouy-Chapman model and in the model of Stern and the site binding model the surface potential used is a smeared out potential. On oxidic surfaces this is not a good approximation. The charges present are caused by adsorption of protons or the dissociation of surface acid groups.

Chapter IV

The potential of oxides is better described by a potential caused by discrete charges than by a smeared out potential.

For the adsorption on silica deviations from the site binding model were reported by Schindler et.al. [13]. Some highly charged cations are adsorbed at very low pH values. According to the Site-binding model no adsorption should be possible. In addition the expulsion of surface protons was much stronger than was predicted by the Site-binding model and the saturation of the surface took place at a pH, where according to the Site-binding model negative sites should be present. A good example is the adsorption of iron (III) ions on Aerosil 200 silica. Schindler et.al. found that at pH=1 20 % of the maximum adsorption was obtained. At pH=3.5 the silica surface was saturated. According to the Site binding model the iron should be adsorbed at negative sites. At pH=1 the fraction of negative sites is negligible and at pH=10 only 50 % of the silanol groups were dissociated. This leads to the conclusion that iron can be adsorbed on uncharged sites. According to Schindler et.al. the adsorption of the iron causes a desorption of the protons of the site. The following reactions are thought to occur at the silica solution interface.



The expulsion of the surface protons by the adsorption of the cation can be described by the following relation:

Chapter IV

$$Z = - \frac{d\Gamma_{H^+}}{d\Gamma_{M^{z+}}} \quad (4.13)$$

Γ_{H^+} is the amount of adsorbed protons and $\Gamma_{M^{z+}}$ is the amount of adsorbed M^{z+} .

For the adsorption of iron (III) on silica Schindler et.al. found $Z=1.2$ at $pH=1$, $Z=2$ at the interval of $pH=3$ up to $pH=10$. Schindler et.al. explained this behaviour with formation of a chelate by which one or more covalent bonds are formed. At increasing pH it becomes easier to expel protons from the surface. This explains the increase in Z -parameter with increasing pH . The fact that the Z parameter passes through a maximum value is explained by the steric inhibition on the formation of a threefold bond with the surface.

4.2.2.4 Stimulated adsorption.

Schindler showed that protons can be expelled from the surface by adsorption of cations. He describes it as an ion exchange process. According to Stein and co-workers [14,15,16,17] the difference between desorption of protons and adsorption of hydroxylic ions in aqueous solutions can not be made. For the adsorption of calcium on calcium silicates the stimulated adsorption model was developed in order to explain the increasing adsorption of hydroxylic ions at increasing calcium concentration and the increasing adsorption of Ca^{2+} with increasing hydroxylic ion adsorption. According to this model the adsorption of ions is dominated by the local potential instead of the smeared out potential. By adsorbing a calcium ion the local potential

Chapter IV

at adsorption sites around the calcium ion is changed. This promotes the adsorption of hydroxylic ions in the neighbourhood of the calcium ion. This changes the local potential at other nearby Ca^{2+} sites and more calcium can be adsorbed.

A kind of local potential can be defined by:

$$\phi = \frac{\int \Theta_i(1-\Theta_i)\phi_i dN_i}{\int \Theta_i(1-\Theta_i) dN_i} \quad (4.14)$$

In this equation ϕ_i is the local potential at sites of type i , Θ_i the degree of occupation and N_i the number of sites of type i . According to this definition, the average potential is determined primarily by those sites for which the degree of occupation is about 0.5. However, if sites of different standard adsorption Gibbs free energies are distributed at random over the surface, no difference between this average and the true average potential ($= \int \Theta_i\phi_i dN_i / \int \Theta_i dN_i$) is expected. In practical calculations, mostly a Gauss type distribution of sites N_i as function of the adsorption energy is chosen. This is characterised by an average value (f) and a standard deviation (w).

According to this model the change in local potential with the concentration can be described with:

$$\frac{kT}{e_0} \frac{d\phi}{d \log(\gamma m)} = 2.303 \frac{\frac{d\Gamma}{d \log(\gamma m)}}{\int \Theta_i(1-\Theta_i) dN_i} \quad (4.15)$$

Chapter IV

γ is the activity coefficient and m is the molality of the adsorbing salt.

Two parameters in this distribution are not known a priori in the case discussed here (adsorption of non-lattice ions):

- i) The total number of sites;
- ii) The spread of the adsorption energy values about its average value (w/f , with w =standard deviation, f =average value).

For the application of this model two integrations are necessary:

- 1) $\int \Theta_i dN_i$ for finding a combination of f and w which describes the measured adsorption values;
- 2) $\int \Theta_i(1-\Theta_i) dN_i$ for use in equation 4.15.

4.2.2.5 Model of hydrophobic monolayer/hydrophilic bilayer.

Until now normal electrolytes were involved in all models. The interactions considered were electrostatic and chemical interactions. In this thesis organic ions are investigated. These ions cannot form chelates with opposite charged silanol groups. Therefore the surface-ligand model cannot be applied. For the adsorption of these ions both electrostatic and hydrophobic interactions have to be taken into account. In the previous parts the electrostatic interactions are discussed but the hydrophobic interactions are not.

The first model for the adsorption of organic ions was developed by Somasundaran, Healy and Fürstenau [18]. They measured the ζ potential of quartz with long chain alkylammonium acetates (C_{10} - C_{18}). All salts were able to induce a charge reversal at higher concentrations. This is a positive indication on specific adsorption. Somasundaran et.al. measured the ζ potential as a function of the electrolyte concentration at constant pH. The concentration necessary to reduce the ζ potential to zero, c_0 , was plotted

Chapter IV

against the number of carbon atoms in the alkyl chain. With the help of the Stern model of adsorption the following formula was derived:

$$\ln c_0 = -n \frac{E_1}{kT} + K \quad (4.16)$$

E_1 is the contribution to the adsorption energy of one methylene group of the alkyl chain, n the number of carbon atoms in the chain and K is a constant.

The experiments could be well described with equation 4.16. The alkyl chains have a predominant influence on the adsorption.

Somasundaran et.al. explained the charge reversal with the amphiphilic character of the alkylammonium ions. At low concentrations the alkylammonium ions behave as normal electrolytes. They are adsorbed with their ionic part at the surface at a negative site and with the hydrophobic chain to the solution. In this way a hydrophobic monolayer is formed at the silica surface. On surpassing a certain critical concentration the amphiphilic character is shown by adsorption of additional alkylammonium ions because of the hydrophobic interactions between the hydrocarbon tails. These ions are adsorbed with their alkyl chain towards the hydrophobic monolayer and the ionic part to the solution forming a hydrophilic bilayer.

Some consequences of this have been investigated by Rubio and Goldfarb [1]. They found for quartz with cetyl-trimethylammonium bromide (CTAB) as electrolyte a critical coagulation concentration but they found also that by surpassing a higher concentration the dispersion became restabilized. First, on increasing the CTAB concentration a hydrophobic monolayer is formed. The ζ potential approaches zero and the dispersion is coagulated. At

Chapter IV

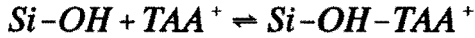
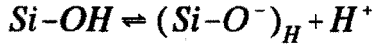
increasing concentrations a hydrophilic bilayer is formed and the dispersion becomes stable again.

However, Rubio and Goldfarb [1] found restabilisation for TAA ions as well. They concluded that the adsorption behaviour of these ions (TMA, TEA and TBA) is comparable to the behaviour of long chain alkylammonium ions. Claesson, Horn and Pashley [19] have shown that only one layer of TAA ions can adsorb onto a mica surface and it is most likely that the adsorption on silica shows the same behaviour. Besides, the amphiphilic character of the small TAA ions is restricted. The concentrations for which charge reversal was observed for TEA and TPA are lower than the cmc of TBA bromide. Therefore it is not very likely that these ions will form a hydrophilic bilayer. Even for long chain trimethylalkylammonium ions the IEP is at a concentration which is $< 0.01 \cdot \text{CMC}$. TAA ions do not adsorb according to this mechanism.

4.2.2.6 Adsorption of TAA according to Rutland and Pashley.

Rutland and Pashley [20] measured ζ potentials of silica in the presence of some TAA ions. They used a model developed by Claesson, Horn and Pashley [19]. This model was originally developed for large, monovalent, hydrated anorganic ions. Claesson et.al. found that a complete monolayer of adsorbed ions was not sufficient to neutralize the surface charge completely. The explanation for this is that the area occupied by the ions is larger than a silanol group. Because of the size of the TAA ions Rutland and Pashley supposed that this theory was valid for the TAA ions as well. The adsorption of TAA ions takes place on two sites: negatively charged sites and neutral sites. The adsorption on negative sites competes with the adsorption of protons. The following reactions at the surface were taken into account:

Chapter IV



$(Si-O^-)_{TAA}$ and $(Si-O^-)_H$ are not the same because a negative site in the neighbourhood of a TAA site can be accessible for protons but not for a TAA ion.

Rutland and Pashley [20] measured the ζ potential as function of the electrolyte concentration. They found a maximum for the numerical ζ potential at electrolyte concentration 10^{-5} M and a minimum for the numerical ζ potential at electrolyte concentration 10^{-3} M. At higher concentration the absolute value of the ζ potential decreased as is to be expected. With their model they could explain this maximum in the ζ potential. At low concentration the adsorption on neutral sites dominates. At a certain concentration saturation of the surface takes place and when that concentration is surpassed the TAA salts act as indifferent electrolyte. At increasing concentration of TAA salts dissociation of silanol groups will occur according to the Gouy-Chapman model. As the adsorption does not increase, the charge on the silica surface will increase and the potential will increase as well.

According to Rutland and Pashley the maximum in the ζ potential explains the results of Rubio and Goldfarb [1]. At low concentrations the ζ potentials found by Rutland and Pashley [20] are strongly negative. At increasing concentration the ζ potential becomes less negative and coagulati-

Chapter IV

on takes place. At a further increase of the concentration the ζ potential decreases again (i.e. the numerical value becomes less negative) and the dispersion is restabilized again. Some points of this explanation, however, are not satisfactory. Wiese and Healy [21] found rapid coagulation when $|\zeta| \leq 14$ mV. This critical ζ potential was independent of the type of disperse phase (alumina or titania) and of the way the ζ potential was diminished (pH change or addition of salt). Rutland and Pashley found ζ potentials between -52 to -40 mV in the maximum of the curve. This ζ potential is high enough to stabilize the dispersion. Rapid coagulation will not take place. In addition, the concentration range where Rubio and Goldfarb found coagulation is different from the maximum in the ζ - concentration curve of Rutland and Pashley. The maximum was at 10^{-5} M for pH=5.7. Rubio and Goldfarb found, at this pH, rapid coagulation for TMA chloride in the concentration range 0.01-0.5 M. At 0.01 M Rutland and Pashley found a ζ potential of about -10 mV. This is in agreement with the critical ζ potential values reported by Wiese and Healy [21].

Other explanations for the measurements of Rutland and Pashley are possible. They use micron sized silica particles. At very low concentrations the double layer is very extended and has about the same size as the particle ($\kappa a \approx 7$). If $\kappa a \approx 1$ the double layer diminishes the electrophoretic mobility. This is called the relaxation effect. According to Wiersema, Loeb and Overbeek [22] for 1:1 electrolytes at given ζ potential, the electrophoretic mobility is minimal if $\kappa a \approx 1$. At increasing κa values the electrophoretic mobility increases rapidly. Rutland and Pashley did not take into account this relaxation effect. They calculated the ζ potential from the electrophoretic mobility with von Smoluchowski's relation [23] (valid for $\kappa a \gg 1$). For very low electrolyte concentration the double layer thickness is

Chapter IV

approximately constant because of the proton concentration which is about $3 \cdot 10^{-6}$ M. At increasing concentration the double layer thickness diminishes and the electrophoretic mobility increases rapidly. By using von Smoluchowski's relation this increase in mobility is translated into an increase in ζ potential.

4.3 Experimental.

4.3.1 Materials.

Degussa Aerosil 200.

TMA bromide, Merck, >99%.

TEA bromide, Janssen chimica, >99%.

TPA bromide, Merck, > 99%.

Potassium bromide, Merck, >99,5%.

Potassium hydroxide, Merck Titrisol, 1 M.

Nitric acid, Merck Titrisol, 0.1 M.

Hydrochloric acid, Merck Titrisol, 0.1 and 1 M.

Sodium tetraphenylborate, Janssen chimica, 98%.

4.3.2 Measurement of the ζ potential.

The ζ potential was determined as a function of the pH. For this purpose a Malvern Zetasizer III was coupled to a titration vessel. The vessel was stirred, thermostated at 25 °C, flushed with nitrogen, electrically grounded and connected with a van Laar salt bridge [24] to a reference vessel. The pH was measured with a glass electrode in the titration vessel and a

Chapter IV

saturated calomel electrode in the reference vessel both connected to a Radiometer Copenhagen PHM 84 Research pH meter. The pH was adjusted with 0.1 M hydrochloric acid or 0.1 M nitric acid using a Radiometer Copenhagen Abu 80 Autoburette. The pH-meter and the burette were connected to a computer (Figure 4.1). The computer was programmed to change the pH at constant time intervals with constant pH differences by controlled addition of acid. Not shown in this figure is the reference vessel with reference electrode and the salt bridge.

The Malvern Zetasizer III uses an electrophoretic light scattering method. In a coherent crossbeam the silica particles migrate under an applied electrical field. The fringes in the crossbeam move with a frequency of 1000 Hz. The moving particles scatter light with a different frequency. The velocity of the particles can be calculated from the Doppler shift and from this velocity the ζ potential is calculated using von Smoluchowski's relation [23].

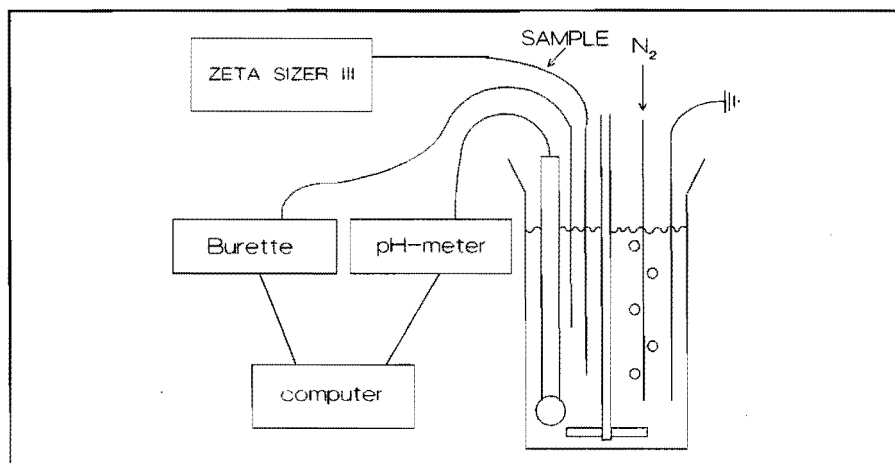


Figure 4.1: Apparatus for the determination of the ζ potential.

Chapter IV

In this way the pH-steps from pH=8 to pH=3 can be made with intervals of 0.5 pH-units. The pH changes were separated by 90 minute intervals in order to obtain equilibrium. The zetasizer III was programmed to take a sample just before the next acid addition and to measure the ζ potential twice.

The ζ potential was measured with 300 ml suspensions of 0.1 w/w% silica in a solution of an electrolyte. As electrolytes were used: Potassium nitrate, potassium bromide, TMA bromide, TEA bromide and TPA bromide with concentrations of 10^{-3} and 10^{-2} M. With these electrolyte concentrations we obtain κa values of 50 and 150 ($a \approx 500$ nm). For the use of von Smoluchowski's relation [23] the κa value of 50 is rather low. During the experiment the electrolyte concentration remained nearly constant and the ζ potentials were quite low. This reduces the relaxation effect and von Smoluchowski's relation can be used.

4.3.3 Determination of the surface charge.

The surface charge, σ_0 , was determined with a titration procedure carried out with the Matec ESA 8000 system. In the context of the present discussion, σ^0 is the surface charge due to the adsorption of the potential determining ions (H^+ and OH^-) to the surface. In the titration vessel about 250 ml of silica dispersion (Degussa Aerosil 200, 1.5 w/w%) was titrated with 1 M HCl and KOH. The vessel was flushed under nitrogen to avoid the effects of CO_2 . During the experiments the added amount of base or acid was registered as function of the pH. The amount of base or acid found for the titration of the dispersion media was subtracted from the titration curves

Chapter IV

of the silica dispersions.

4.3.4 Adsorption of TAA ions on silica.

A precise volume of 100 ml or 150 ml of a TAA bromide solution was added to 5 g Aerosil 200. The concentrations of the solutions were 10^{-3} , $3 \cdot 10^{-3}$, 10^{-2} , $3 \cdot 10^{-2}$ and 10^{-1} M of the TMA, TEA or TPA bromide. The pH was adjusted at pH=3 and pH=5 with hydrochloric acid or sodium hydroxide solutions and shaken overnight at 25 °C. During the night the pH shifted 0.3 pH units at most. Again the pH was adjusted and the suspension was centrifuged. The supernatants and the original solutions were analyzed with a potentiometric titration with sodium tetrphenylborate using an Orion 940/960 Autochemistry system with a TAA sensitive electrode developed by Holten and Stein [25]. From the concentration difference, the amount of silica, the volume of the solution and the specific area (200 m²/g) the adsorption in mole per square meter was calculated.

4.4 Results and discussion.

4.4.1 ζ Potentials of silica.

The ζ potential of silica was determined as a function of the pH for several electrolytes. In the figures 4.2 to 4.6 the results are shown.

The ζ potential-pH curves of silica in potassium nitrate solutions are shown in Figure 4.2. At low pH the ζ potential is around zero and at increasing pH it becomes increasingly negative. At high electrolyte concen

Chapter IV

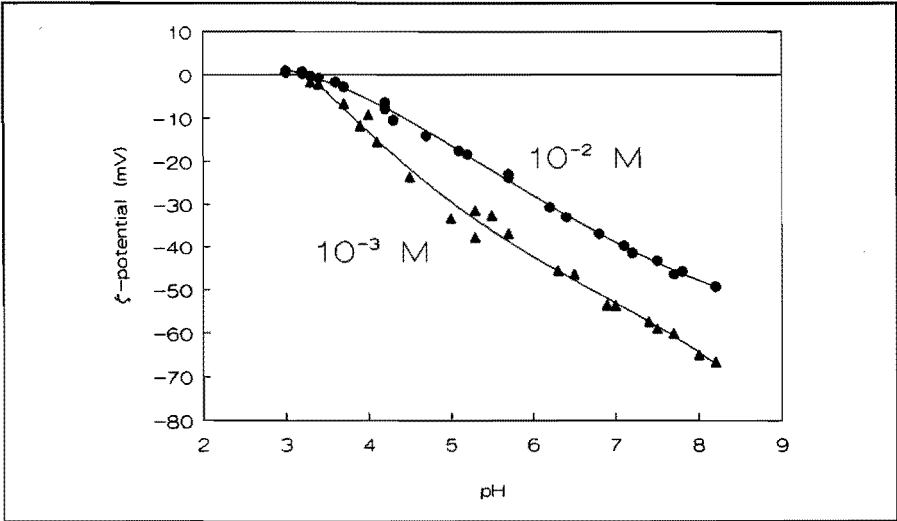


Figure 4.2: ζ Potential of silica in solution of potassium nitrate.

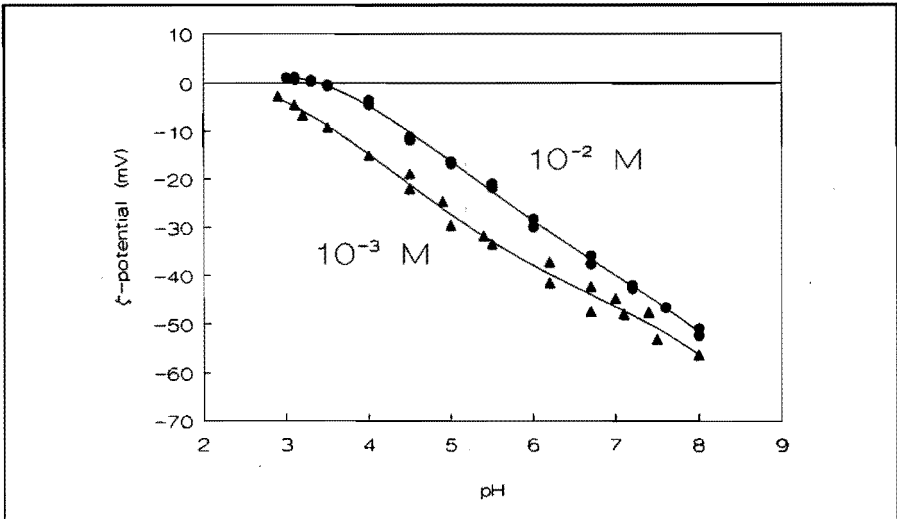


Figure 4.3: ζ Potential of silica in solutions of potassium bromide.

Chapter IV

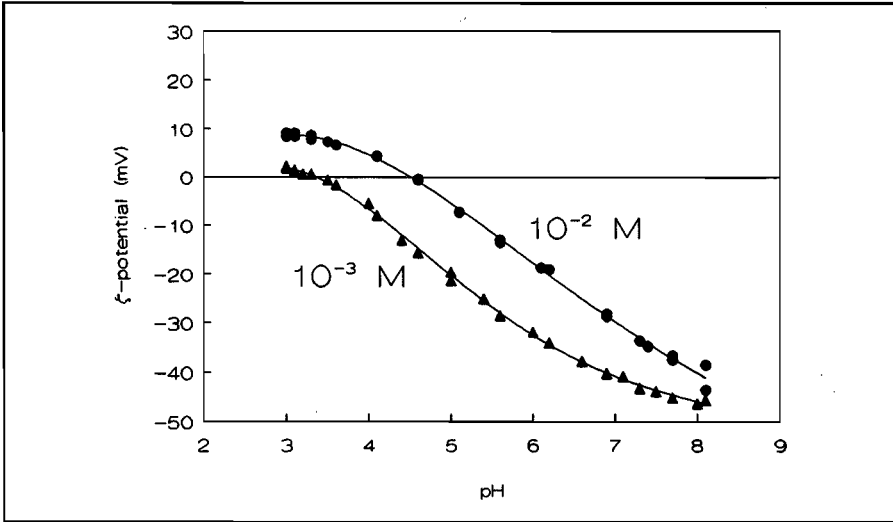


Figure 4.4: ζ Potential of silica in solutions of TMA bromide.

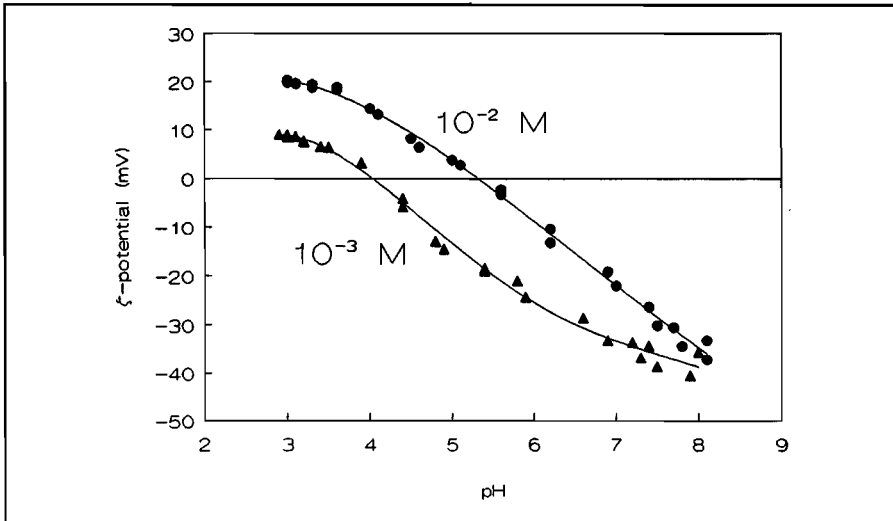


Figure 4.5: ζ Potential of silica in solutions of TEA bromide.

Chapter IV

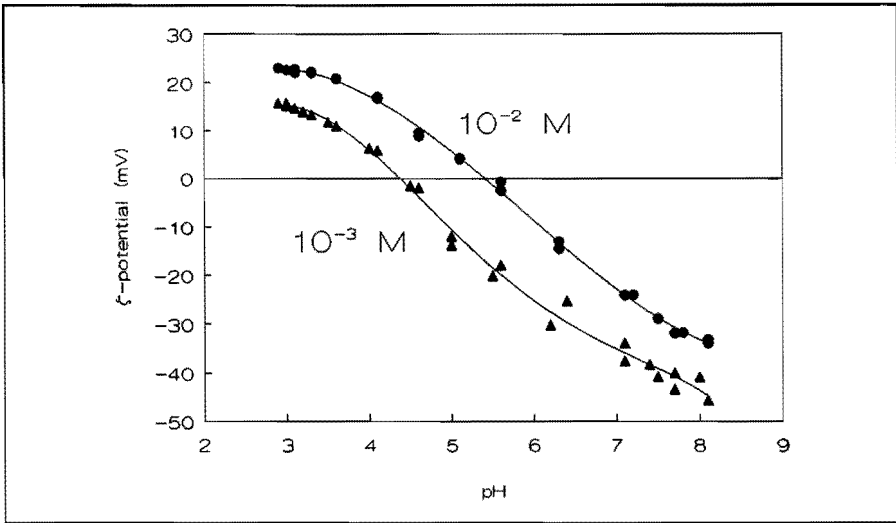


Figure 4.6: ζ Potential of silica in solutions of TPA bromide.

tration the absolute value of the ζ potential decreases. This is to be expected because at high concentration the charge of counterions present behind the slipping plane is higher. The isoelectric point (IEP) is at $\text{pH}=3.2$. When only indifferent electrolytes are present the IEP should coincide with the point of zero charge (PZC). According to Iler [26^a] the PZC of silica may vary between $\text{pH}=2$ and $\text{pH}=3$. Our value is rather high. This could be due to the preparation of the silica. The aerosil silica is a pyrogenic silica. For this type of silica the PZC can shift to higher values [26^b].

For potassium bromide (figure 4.3) the curves differ a little from those of potassium nitrate. The TAA bromides have a more distinct influence on the ζ potentials in the low pH range (figures 4.4 to 4.6). All ζ potentials shift to positive or less negative values. The IEP shifts to higher pH values.

Chapter IV

The charge reversal is a positive indication on the specific adsorption of TAA on silica. It shows that the adsorption is not only due to the electrostatic attractions between a negatively charged surface and the positively charged TAA ions, but that in addition another kind of interaction plays a key role. The shift in IEP is shown in Figure 4.7 as function of the chain length of the TAA ions.

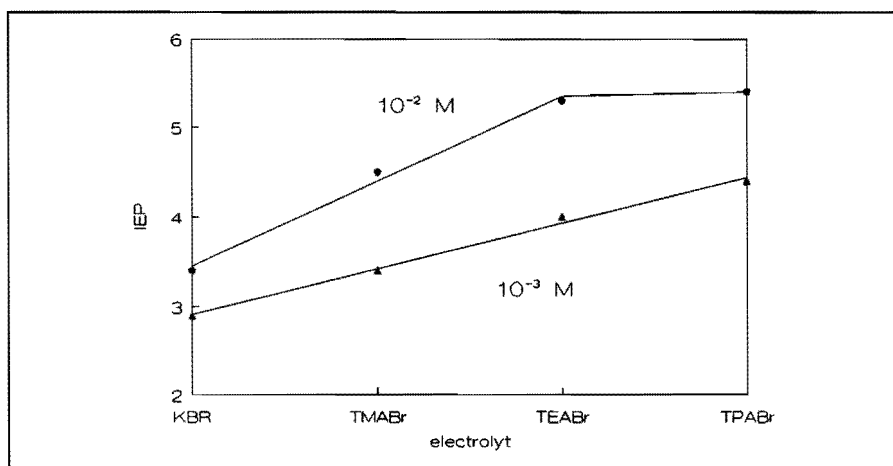


Figure 4.7: IEP shifts for some TAA ions.

For the 10^{-3} M suspensions the shifts in IEP depend linearly on the chain length. The amount of adsorbed TAA ions increases with increasing chain length. As with increasing chain length the hydrophobic effect increases, the influence of the chain length on the IEP shift indicates that the interactions between the TAA ions and the silica are of hydrophobic origin. The amphiphilic character of the TAA ions is much too small for the formation of a bilayer as described by Somasundaran (see section 4.2.2.5). For the 10^{-2} M suspensions the shift is linear up to TEA. The ζ potential-pH

Chapter IV

curves for the 10^{-2} M TEA and TPA bromide suspensions are almost the same. The adsorption behaviour of TEA and TPA apparently is comparable at 10^{-2} M. This can be ascribed to saturation of the surface.

The ζ potentials found in the present investigation can give an explanation to the stability behaviour reported by Rubio and Goldfarb [1]. In the presence of an indifferent electrolyte the ζ potential is strongly negative at $\text{pH} > 4$. In the presence of low concentrations of TAA ions the ζ potentials are negative too at high pH. But at higher concentrations and lower pH's the ζ potential will be less negative. In most cases of aqueous suspensions of oxides, it has been reported by Wiese and Healy [21] that the suspensions will be stable as long as: $|\zeta| \geq 14$ mV. The concentration-pH ranges which are mentioned by Rubio and Goldfarb [1] match the values were we find: $|\zeta| \leq 14$ mV. In this case rapid coagulation is observed. At higher concentrations the amount of adsorbed cations can induce charge reversal. At increasing concentration the critical ζ potential of 14 mV will be surpassed and the dispersion becomes stable again. In fact we found ζ potentials over +20 mV. Our results show low ζ potentials, $|\zeta| \leq 14$ mV, in the range where Rubio and Goldfarb found rapid coagulation and high ζ potentials, $|\zeta| \geq 14$ mV, in the range where they found stable dispersions.

4.4.2 Surface charge of silica.

In figures 4.8-4.11 the relative surface charge of silica in the presence of several electrolytes is shown. This relative charge is the charge relative to the charge at $\text{pH}=3$. The relative charge is mentioned here instead of the surface charge proper, because the position of the PZC for the silica used here has not been fixed unambiguously.

Chapter IV

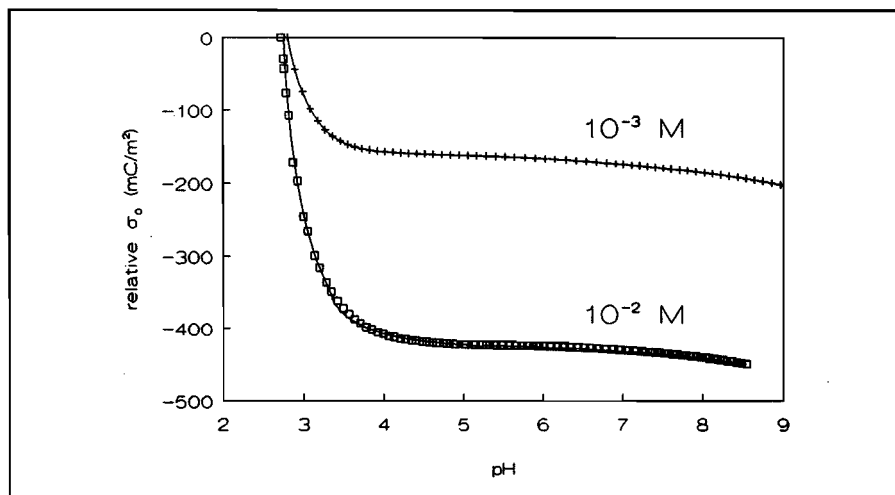


Figure 4.8: Relative surface charge of silica in solutions of potassium bromide.

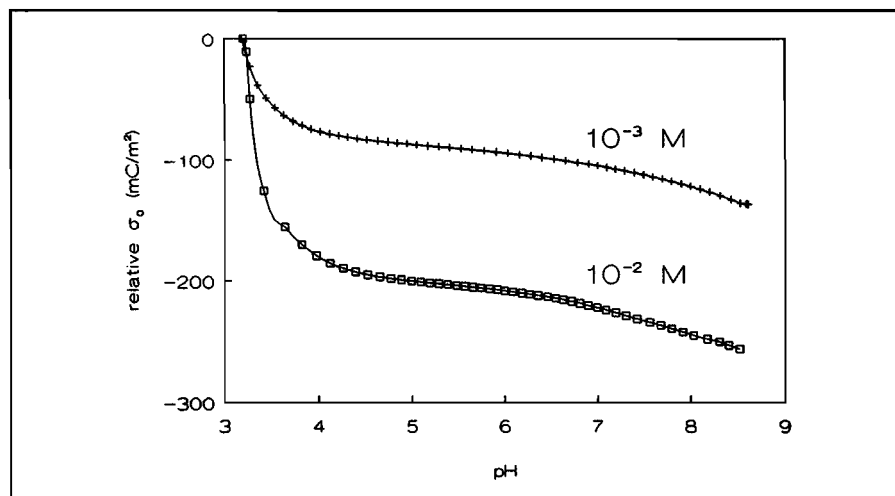


Figure 4.9: Relative surface charge of silica in solutions of TMA bromide.

Chapter IV

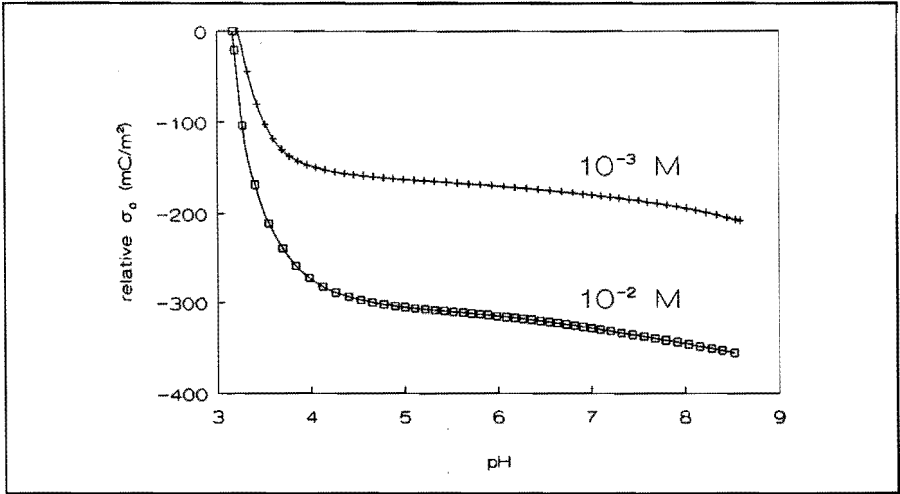


Figure 4.10: Relative surface charge of silica in solutions of TEA bromide.

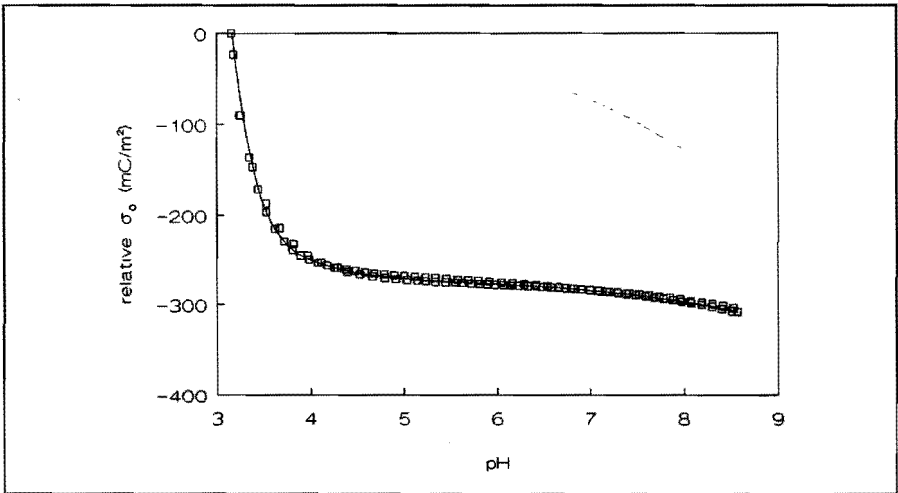


Figure 4.11: Relative surface charge of silica in solutions of 10^{-3} M TPA bromide.

Chapter IV

With the titration procedure as described in section 4.3.3 it is in principle possible to determine the surface charge. However the value of the PZC is not known. As the surface charge is dependent on the amount of electrolyte the titration has to be carried out at constant ionic strength. The IEP of Aerosil 200 was at $\text{pH}=3.2$ as was observed from the curves of the ζ potentials with potassium nitrate as electrolyte (figure 4.2). In the case of indifferent electrolytes the PZC is at the intersection point of titration curves with different salt concentrations. In the case of silica it is impossible to obtain titration curves at electrolyte concentrations $\leq 10^{-3}$ M to pH values lower than 3, with constant salt concentration. The electrolyte concentration increases during a titration procedure. When the pH becomes smaller than $\text{pH}=3$ the electrolyte concentration increases by at least 10^{-3} M. If the initial electrolyte concentration is 10^{-3} M the surface charge will be at least $\sqrt{2}$ times too high. Therefore the PZC cannot be obtained for 10^{-3} M solutions. However, for the determination of the Z-parameter, as mentioned in equation 4.13, knowledge of the absolute value of the surface charge is not necessary. When we assume that all charge between the electrokinetic slipping plane and the silica surface is chemisorbed, the charge behind the electrokinetic slipping plane (σ_f) can be considered to be the sum of the surface charge and the charge of the ions adsorbed at the surface. Equation 4.13 can be rewritten as:

Chapter IV

$$Z = - \frac{\frac{d\sigma_0}{d\text{pH}}}{\frac{d(\sigma_\zeta - \sigma_0)}{d\text{pH}}} \quad (4.17)$$

This equation is only valid for the adsorption of monovalent ions. In equation 4.13 changes in amounts of ions are used and in equation 4.17 changes in charges. This is only compatible if the charge of the ions, which are adsorbed, is equal to the charge of a proton.

The first derivative of the surface charge to the pH is experimentally accessible from the titration experiments (see figures 4.8 to 4.11). The σ_ζ can be calculated from the ζ potentials with equation 4.8. The first derivative of the σ_ζ is easy to determine. The Z-parameter calculated in this way is different from the Z-parameter as defined by Schindler et.al. [13], see equation 4.13. The adsorption in the Stern plane which is caused by electrostatic interactions is incorporated in equation 4.17 while it is not incorporated in equation 4.13.

The physical meaning of the Z-parameter is the amount of protons which is desorbed from the surface divided by the amount of cations which is adsorbed at the surface when the pH changes slightly. It can be interpreted as a standard for the expulsion of protons from the surface according to the Surface-ligand model (see section 4.2.2.3) or adsorption of hydroxylic ions on the surface by adsorbing cations according to the stimulated adsorption model (see section 4.2.2.4). In the Surface-ligand model the adsorbed ions

Chapter IV

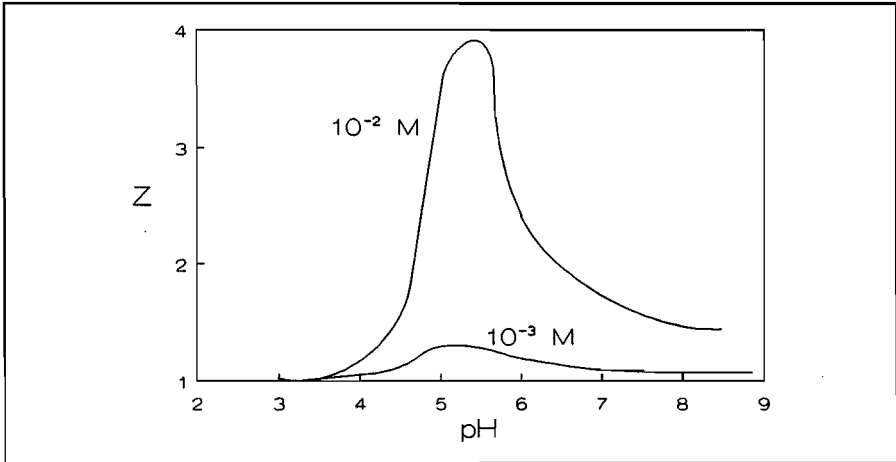


Figure 4.12: Z-parameter of silica with potassium bromide solutions.

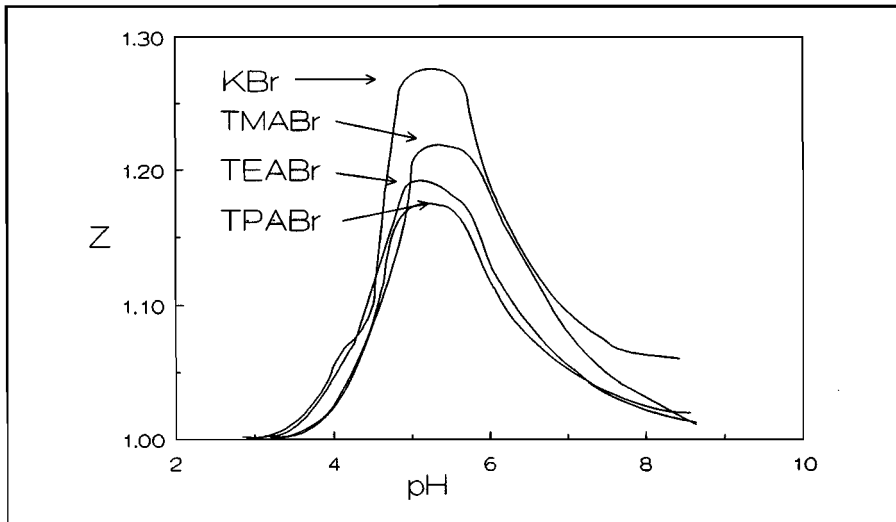


Figure 4.13: Z-parameter of silica with 10^{-3} M solutions.

Chapter IV

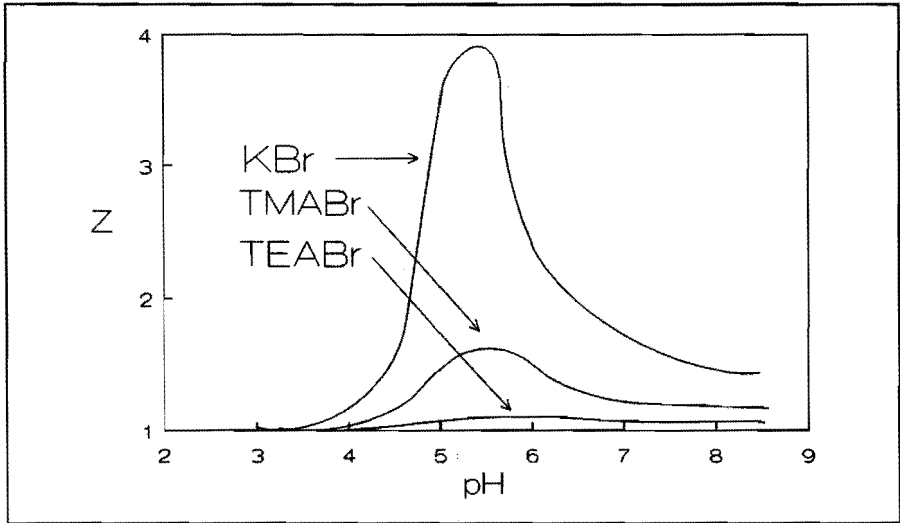


Figure 4.14: Z-parameter of silica with 10^{-2} M solutions.

form covalent bonds with the surface. TAA ions cannot form covalent bonds. But their adsorption can cause expulsion of surface protons (or adsorption of hydroxylic ions) by their influence on the local potential. For indifferent electrolytes the amount of cations which is specifically adsorbed at the surface should be zero and so would the change of specifically adsorbed cations ($d\Gamma_M$ in equation 4.13). The Z-parameter according to Schindler et.al. [13] should be infinitely large. The curves in figure 4.12 show finite Z-parameters, but this can be understood because some potassium ions are present in the Stern layer because of the electrostatical interactions. The amount of ions will be proportional to the concentration of ions in the slipping plane which can be calculated from the Boltzman equation.

Chapter IV

$$\Gamma_{M^+} = C n_0 e^{-\frac{ze_0\zeta}{kT}} \quad (4.18)$$

The first derivative of the adsorbed amount to the pH is:

$$\frac{d\Gamma_{M^+}}{dpH} = -\frac{C n_0 z e_0}{kT} e^{-\frac{ze_0\zeta}{kT}} \frac{d\zeta}{dpH} \quad (4.19)$$

With the ζ potentials in figure 4.3 $d\Gamma/dpH$ can be calculated for the two electrolyte concentrations. It should be remarked that this must be regarded as a first approximation, since the local potential at a site may differ considerably from the ζ potential [14,15,16,17]. For the 10^{-2} M potassium bromide concentration equation 4.17 yields a $d\Gamma/dpH$ value which is 9 times higher than for the 10^{-3} M concentration. In figure 4.12 the maximum of the Z-parameter of the 10^{-2} M solution is 3 times higher than the Z-parameter of the 10^{-3} M. This implies that the change in surface charge of the silica in the 10^{-2} M solution should be 27 times higher than that of silica in the 10^{-3} M solution.

According to the Gouy-Chapman theory the surface charge should scale with the square root of the concentration. The first derivative of the surface charge to the pH should scale with the square root of the concentration too. As a consequence of this the change in surface charge of silica in the 10^{-2} M solution should be $\sqrt{10}$ times higher than the change in surface charge of the 10^{-3} M solution. This is about 9 times lower than what was calculated in the preceding paragraph. For silica/water surfaces in the presence of indifferent electrolytes the Gouy-Chapman theory is not fit for

Chapter IV

the description of $d\Gamma_{M^+}$ as a function of the pH.

From the surface charges as shown in the figures 4.8 to 4.11 the first derivatives can be calculated. In figures 4.15 and 4.16 the first derivatives of the surface charge to the pH are shown as a function of the cation for pH=3 and pH=5.

At pH=3 the change in charge behind the slipping plane (including the surface charge) is small compared to the change in surface charge. Therefore the Z-parameter is near to 1. At pH=5 the change in surface charge is about 30-40 times smaller than at pH=3, while the change in charge behind the

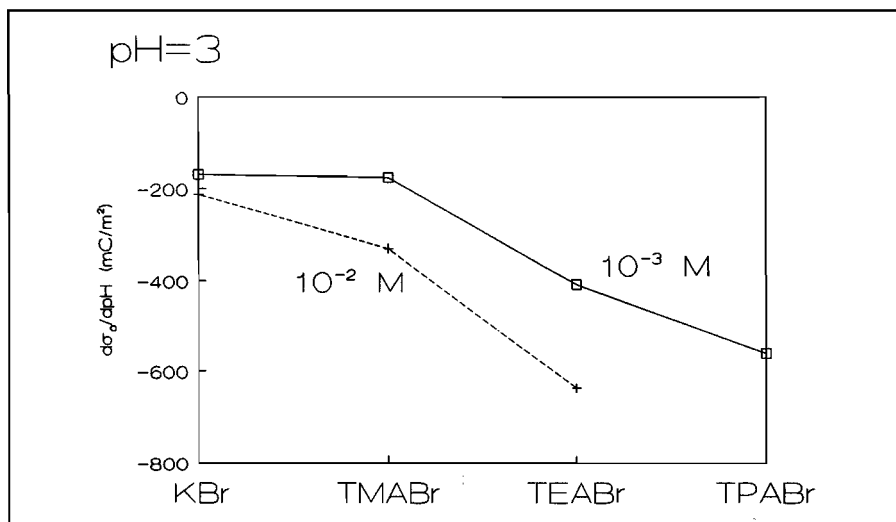


Figure 4.15: First derivative of the surface charge as function of the cation type at pH=3.

Chapter IV

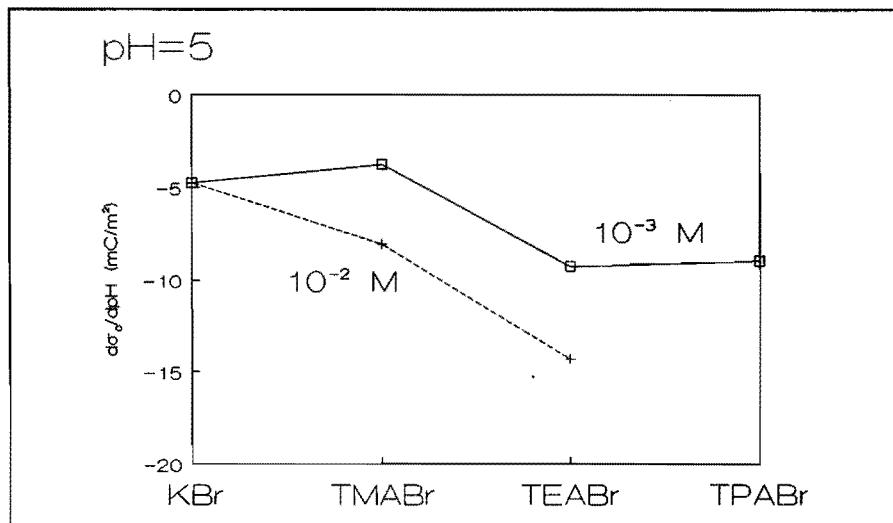


Figure 4.16: First derivative of the surface charge as function of the cation type at pH=5.

slipping plane is nearly constant. At pH=5 a maximum is present in the Z-parameter-pH curve. The first derivative of the surface charge to the pH is the same for solutions of 10^{-3} M and 10^{-2} M potassium bromide. As the Z-parameter in the 10^{-3} M solution is 3 times smaller than in the 10^{-2} M solution the change in adsorbed ions in the Stern plane must be 3 times higher in the 10^{-3} M solution than in the 10^{-2} M solution. This is in contradiction with the figures calculated with equation 4.17.

In our approach the expulsion of surface protons by an chemisorbing cation is mixed with electrostatic adsorption in the Stern plane. If ions are chemisorbed two processes take place: i) protons are expelled from the surface because of the influence on the local potential. This results in a more negative $d\sigma_0/dpH$. ii) because of the adsorption the ζ potential diminishes and

Chapter IV

$d(\sigma_f - \sigma_0)/dpH$ increases. In figure 4.16 is shown that the change in the surface charge is more negative for TMA, TEA and TPA than for potassium bromide at $pH=5$ in 10^{-2} M solutions. In 10^{-3} M solution the difference between potassium bromide and TMA bromide is small. Some protons are expelled from the surface by the TAA ions.

As the Z-parameters in solutions of the TAA salts are smaller than in solutions of potassium bromide this cannot be explained with the first process alone, The second effect takes place as well.

The curve for 10^{-3} M potassium bromide in figure 4.13 is only slightly higher than the curves for the other cations at this concentration. The Z-parameters of the indifferent potassium bromide are thought to be caused by the pH change and adsorption in the Stern plane rather than chemisorption on the silica surface. The change in surface charge at $pH=5$ (maximum Z) in solutions of the TAA ions is for TMA bromide comparable with that of potassium bromide and for TEA and TPA bromide about 2 times more negative. As the Z-parameters of the other cations have about the same value this shows that at a concentration of 10^{-3} M the change in adsorbed ions is for TMA bromide comparable with potassium bromide. For TEA and TPA the change in adsorbed ions must be more than 2 times higher than for potassium bromide. At this concentration (10^{-3} M) the influence of the TMA bromide which is adsorbed in the Stern plane is more important than the TMA bromide chemisorbed at the surface. As the change in adsorption for TEA and TPA is about 2 times higher than for the indifferent potassium bromide the importance of TEA/TPA bromide adsorbed in the Stern plane is about as important as the chemisorption of TAA bromide at the silica surface.

For the 10^{-2} M electrolytes (see figure 4.14) the differences between

Chapter IV

the TAA salts and the bromide are much more pronounced. At pH=5 (maximum Z) the change in surface charge is for TMA is about 2 times and for TEA 3 times higher than for potassium. With the maximum Z-value as shown in figure 4.14 the change in adsorbed ions can be calculated. For TMA the change in adsorbed ions is 5 times higher than for potassium and for TEA 9 times. This shows that at this concentration the chemisorption of TAA ions on the silica surface is more important than the electrostatic adsorption in the Stern plane.

4.4.3 Adsorption of TAA ions on silica.

The amount of TAA ions which is adsorbed at the silica surface can be determined with a procedure described in section 4.3.4. The adsorption is investigated at two pH values: pH=3 and pH=5. In figure 4.17 and 4.18 the results, corrected for the amount present in the double layer, are shown.

No saturation is seen for TEA and TPA and for TMA at a concentration of $5 \cdot 10^{-2}$ M. According to the model of Rutland and Pashley [20] (see section 4.2.6) saturation should take place at 10^{-5} M for both TMA and TPA. Our results are in contradiction with the assumptions of Rutland and Pashley.

The adsorption was determined by calculating the decrease in concentration on the addition of silica. The TAA ions will be present at the surface (behind the electrokinetic slipping plane) but they will be present in the electrical double layer as well. The amount present in the double layer can be calculated using equation 4.20.

Chapter IV

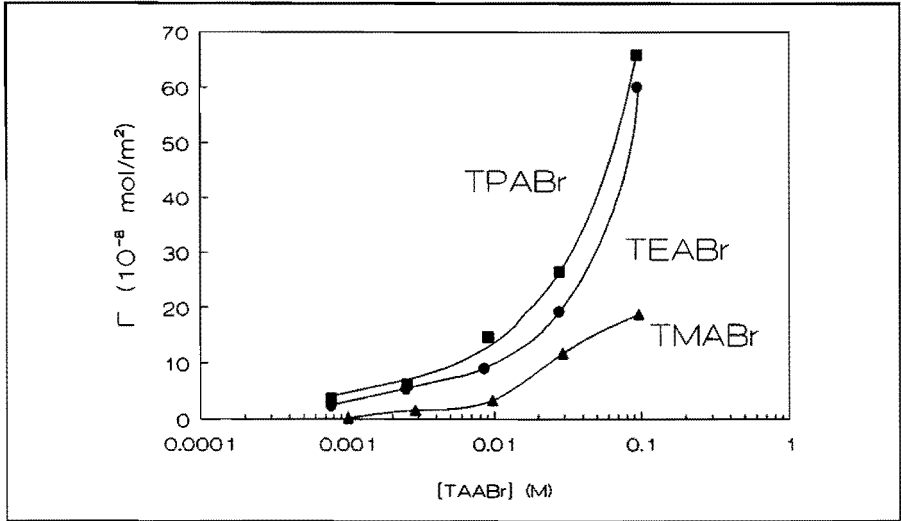


Figure 4.17: Adsorption of TAA ions on silica at pH=3.

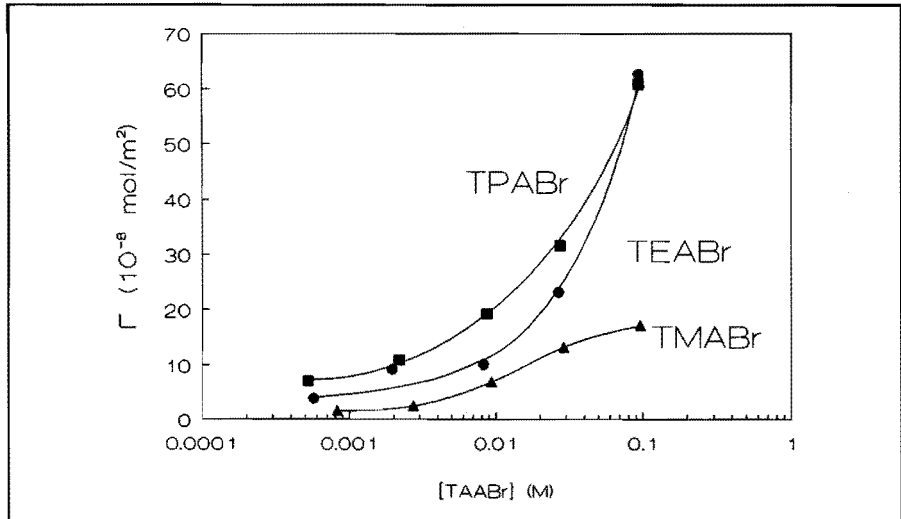


Figure 4.18: Adsorption of TAA ions on silica at pH=5.

Chapter IV

$$\Gamma_{dd} = \int_{\delta}^{\infty} (n^+ - n_0) dx \quad (4.20)$$

In this equation n^+ is the average TAA concentration at a certain distance from the particle, n_0 is the bulk concentration and δ is the distance of the electrokinetic slipping plane from the surface. The average concentration is dependent on the mean potential at a certain distance from the surface. By using, in the region outside the electrokinetic slipping plane, the potential as calculated from the Gouy-Chapman theory (equation 4.4) the equation for the additional amount of cations present in the double layer can be derived.

$$\Gamma_{dd} = \frac{2n_0}{\kappa} \left\{ \exp\left(-\frac{ze_o\zeta}{2kT}\right) - 1 \right\} \quad (4.21)$$

κ is the reciprocal thickness of the double layer and ζ is the ζ potential. The ζ potential is used because in the absence of polymers near the surface, the Stern plane and the slipping plane are nearly the same as described by Parfitt and Picton [4] and Horn and Smith [5].

In the figures 4.17 and 4.18 the adsorption of TAA ions, corrected for the electrical double layer with equation 4.21, are shown for pH=3 and pH=5. The difference in adsorption between the two pH-values is quite small (mean difference $2 \cdot 10^{-8}$ mole/m²). According to the figure 4.8 to 4.11 the surface charge increases considerably if the pH changes from pH=3 to

Chapter IV

pH=5. As the adsorption remains constant it can be concluded that the adsorption is hardly dependent on the surface charge. A consequence of this is that the adsorption of TAA ions doesn't take place on the charged groups of the silica. This is in agreement with the results of chapter II and III. In these chapters was found that, besides the electrostatic attraction between silicate and TAA ions, a repulsive force was present between these ions. Silicate ions mainly consist of protonated and deprotonated silanol groups. Therefore it is not likely that the TAA ions will adsorb on silanol groups of the surface. This is in contradiction with the Site-binding model (section 4.2.2.2), the model of hydrophobic monolayer/hydrophilic bilayer (section 4.2.2.5) and the model of Rutland and Pashley (section 4.2.2.7).

The charge of the adsorbed ions can be compensated in several ways:

- a) If the solid is a (semi)conductor, the charge of an adsorbed ion can be compensated through charges in the solid phase. In our case this is excluded because silica is an insulator.
- b) Compensation by counter ions in the double layer.
- c) Compensation by adsorption on adjacent sites for ions of opposite charge or by expulsion of protons from surface hydroxyl groups.

The two effects b) and c) both effect the adsorption in a qualitatively similar way: If effect b) is important, then an effect on neighbouring sites is expected especially at low electrolyte concentration in the bulk liquid: under these conditions the thickness of the double layer is large, and if it surpasses the distance between two adjacent sites, the charge of an adsorbed ion is compensated only partially by counter ions at the adjacent site. This is indicated schematically in the right part of figure 4.19. At large electrolyte concentration, however, the thickness of the double layer is smaller than the distance between adjacent sites, and the charge of an adsorbed ion will be

Chapter IV

compensated nearly totally at the distance of a neighbouring site (see left hand part of figure 4.19). The effect will be apparent from a relatively low adsorption at low electrolyte concentration, because the charge of an adsorbed ion is shielded only partially at the distance of an adjacent site.

If effect c) is important, the influence of adsorbed ions on neighbouring sites is especially pronounced at high electrolyte concentration

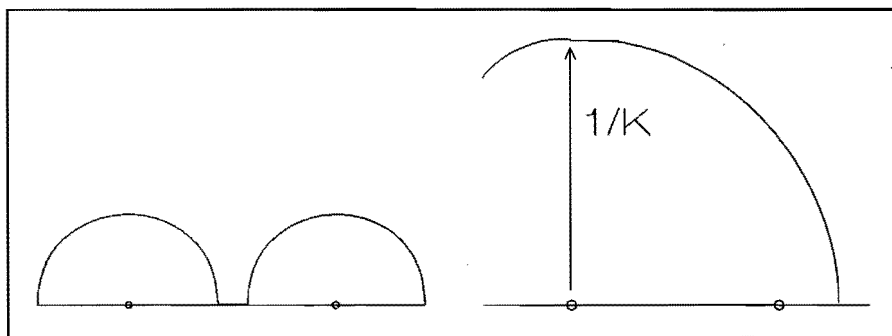


Figure 4.19: The influence of the double layer thickness on the influence of adjacent adsorption sites.

and large surface coverages. This will be apparent by a specially large adsorption at high concentration. This was found for TEA and TPA bromide but not for TMA bromide.

Some aspects of the adsorption are not described by compensation by counter ions in the double layer. If the adsorption of TEA and TPA bromide at high concentration is caused by the decreasing shielding the Adsorption of TMA bromide should be large as well. This was not found. Another point against this theory is that the surface is charged in most cases. If the surface

Chapter IV

charge and the charge of the adsorbed ion are opposite of sign, as in our case, the double layer in the direction perpendicular to the surface is different from the double layer in the direction parallel to the surface. The double layer perpendicular to the surface is dependent on the bulk concentration. The double layer parallel of the surface is more dependent on the surface charge. At $\text{pH}=5$ for low concentrations the ζ potential is negative. This means that the surface charge is larger than the charge of the adsorbed ions. The average distance between a site and an adjacent charged surface group is smaller than the distance between two sites and much smaller than the double layer thickness. This shows that at low electrolyte concentration the compensation of the surface charge by counter ions in the solution does not influence adsorption on nearby sites.

The main interaction leading to adsorption is assumed to be an overlap of the hydrophobically induced water structures around the TAA ions and some surface groups. Kamo et.al. [7] showed that the Stern model for adsorption can be used to describe the adsorption of anionic surfactants at liposome surfaces in spite of the assumptions in the theory being far from satisfactorily defensible (the most debatable of these assumptions are the equal adsorption energy for all sites and the absence of mutual interactions between adsorbed species). By splitting the adsorption energy into two parts according to equation 4.10: an electrical energy, approximated by the ζ potential, and a constant adsorption energy term, due to hydrophobic interactions, the assumption of the equal adsorption energies is not an obstacle any more. Therefore the results are fitted to equation 4.11. This appears to be a plot of the reciprocal adsorption against the reciprocal concentration (see figure 4.20 and 4.21). The exponential term on the legend of the ordinate can be regarded as a consequence of a Boltzman like distribu

Chapter IV

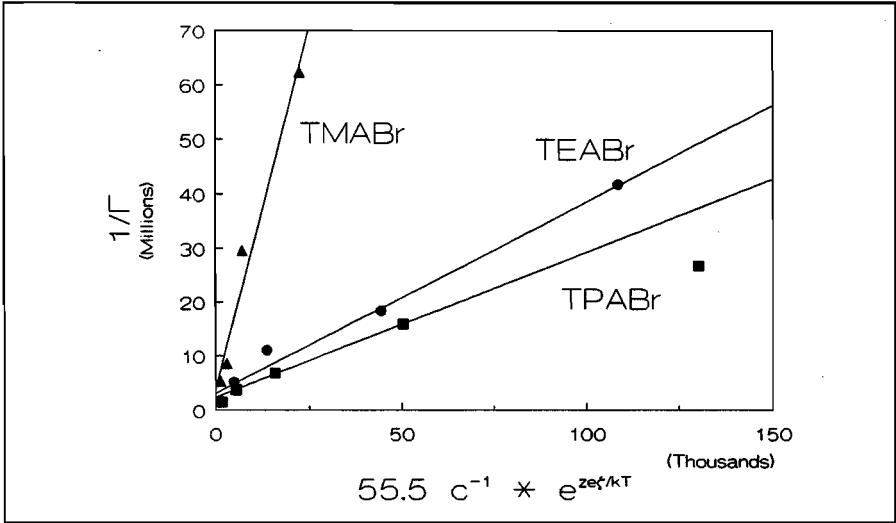


Figure 4.20: Fit of adsorption data at pH=3.

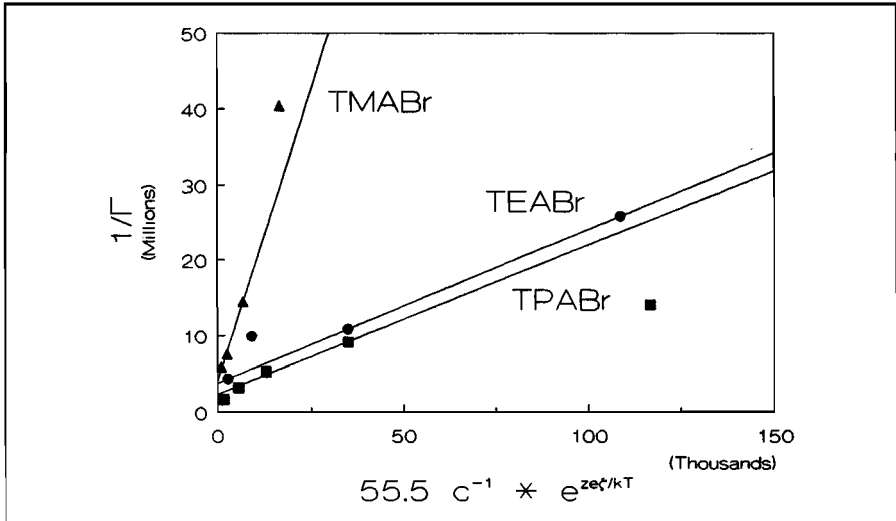


Figure 4.21: Fit of adsorption data at pH=5.

Chapter IV

tion of the ions outside the electrokinetic slipping plane. It gives the reciprocal value of the concentration of the cations at the electrokinetic slipping plane.

On the basis of the results presented in previous chapters of this thesis, we expect that the driving force of chemisorption of TAA ions is an attraction between hydrophobically hydrated parts of the silica surface and hydrophobically hydrated alkyl chains, rather than a special attraction between TAA ions and negatively charged silanol groups, which should lead to other viscosity data and to other distribution coefficients in coacervation than those found experimentally. Thus the driving force for chemisorption is in the system investigated here different from the type of system which is the basis of the surface-ligand model. In this model a type of covalent bond is postulated between an adsorbed ion and the oppositely charged site itself.

In order to obtain an impression of the factors involved in adsorption (number of sites and adsorption energies) we first applied the simplest model, the one described by Kamo et.al. [7] (equation 4.11). In this model the influence between adjacent sites is assumed to be electrically only and is approximated by the ζ potential. Figures 4.19 and 4.20 present the adsorption data they should have according to equation 4.11 would be obeyed. These figures show definite deviations from the linear course: At large concentrations $1/\Gamma$ is lower than expected from a linear course especially in the case of TEA and TPA bromide, meaning that Γ is at high concentration larger than expected from equation 4.11. It would be erroneous to ascribe this fact to an influence by the size of the double layer, since in this case the effect would be equal for all types of ions.

In order to obtain a rough idea of the number of adsorption sites per unit surface area, and of the adsorption energies involved, we fitted the

Chapter IV

adsorption data to equation 4.11. The results are mentioned in table 4.1.

One of the boundary conditions of equation 4.11 is: all sites are characterized by a constant adsorption energy (E). Sites with adsorption energies which are out of a certain range (e.g. very low adsorption energies) are not taken into account.

Table 4.1: Fitting parameters of the adsorption equation.

pH=3			pH=5		
TAA	$N_s \cdot 10^7$ (mole/m ²)	E (kJ/mole)	TAA	$N_s \cdot 10^7$ (mole/m ²)	E (kJ/mole)
TMA	2.59	-18.1	TMA	2.52	-19.5
TEA	3.16	-22.6	TEA	2.67	-24.3
TPA	4.14	-22.6	TPA	4.32	-23.2

The data presented in table 4.1 show a striking feature: The adsorption energies are nearly the same for all types of cations, the number of adsorption sites per unit surface area is approximately constant at two pH values and increases with increasing chain length.

The fact that the number of adsorption sites is not dependent on the pH shows that the adsorption does not take place on charged silanol groups.

An explanation for this behaviour is the following: On the silica surface small hydrophobically hydrated sites are present originating from siloxane bridge-like sites. These groups have to be distinguished from the hydrophilic silanol groups. The area of these hydrophobically hydrated sites are small compared to the area of the ions. The overlap area determines the adsorption energy. Probably the site area is smaller than the dimensions of

Chapter IV

the TEA and TPA ions (including the water layer bound hydrophobically to the ion). Therefore the hydrophobic hydration layers around TEA and TPA have similar overlap areas with the hydrophobically hydrated sites on siloxane bridges. TMA is smaller and more compact. By steric effects the overlap, and thus the adsorption energy, could be smaller.

The dependence of the number of sites on the chain length can be explained in two ways:

- i) The TMA ion has a relatively small hydrophobically hydrated layer compared to TEA and TPA ions. The sites are surrounded by hydrophilic silanol groups. Between the TAA ions and silanol groups a repulsion is present. Some sites will be partially shielded by silanol groups. In these cases the hydrophobic hydration of TMA may be not strong enough to cause adsorption on these sites. The stronger the hydrophobic hydration of the TAA ions the better partially shielded sites can be used for adsorption.
- ii) The TAA ions can be regarded as bulky ions with tiny alkyl chains sticking into the solution. The adsorption can be regarded as the overlap of the hydrophobically hydrated regions of the site and the alkyl chains. Some sites will be at a flat S/L interface. These sites are accessible for all TAA

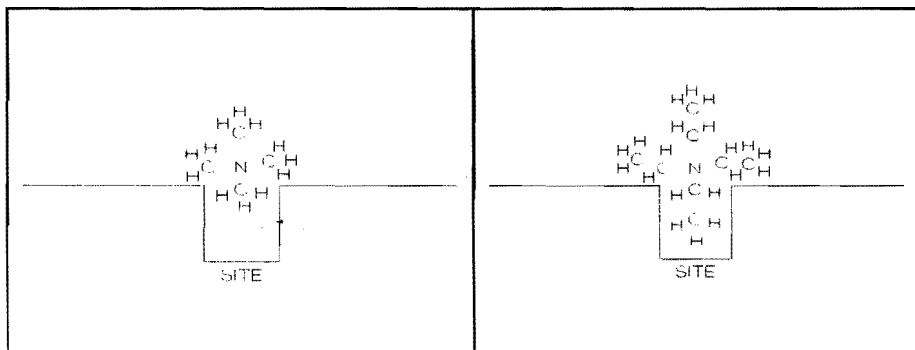


Figure 4.22: Adsorption site in a cleft.

Chapter IV

In the present investigation we are dealing with the adsorption of non-lattice ions (TAA on silica). In figure 4.23 adsorption at a particular site (e.g. A) is expected to be so favourable that at low TAA concentrations adsorption takes place. An adsorbed ion at site A will influence the local potential at site B such as to promote their dissociation. This in turn makes TAA adsorption on adjacent site C possible, etc..

Prerequisite to such a mechanism to occur is, that the Z value should be >1 . This is, in a rather broad pH range, the case in all solutions investigated. However the very large Z values found in 10^{-2} M potassium bromide solutions are not found for 10^{-2} M TAA bromide solutions. This difference can be ascribed to the chemisorption of the TAA ions: on changing the pH, in the case of potassium bromide only electrostatic adsorption of potassium ions takes place behind the electrokinetic slipping plane; $d(\sigma_f - \sigma_0)/dpH$ is small, and this leads to large Z values.

In the case of TAA bromide solutions, the net charge behind the electrokinetic slipping plane changes because of cation adsorption both caused by electrostatic attraction, and because of overlap of similar water structures. Thus, $d(\sigma_f - \sigma_0)/dpH$ is here larger than in the case of potassium bromide, and Z remains between 1 and 2. But the fact that $Z > 1$ confirms the expulsion of protons from adjacent surface groups on the adsorption of TAA ions.

In the case of TAA ions on silica, no crystal structure considerations giving a value for the total number of adsorption sites per unit area are available. The calculations are therefore restricted to the adsorption of TMA, because only in this case a satisfactory plateau adsorption at large concentration was found. Two different values were chosen: The value found with the fit to equation 4.11 (see Table 4.1) and the plateau value obtained from

Chapter IV

figures 4.17 and 4.18 ($2.0 \cdot 10^{-7}$ mole/m²). For the spread of the adsorption energy about its average two values were chosen: $w/f=0.1$ and $w/f=0.5$ (w =spread and f =average adsorption energy), corresponding with a rather narrow and a rather broad distribution, respectively. The integrations were performed numerically, using Simpson's method, between adsorption energies ranging between $-5w$ and $+5w$. For the activity coefficients values were calculated from the Debye-Hückel equation, since it is known from the work of Lindenbaum and Boyd [27] and Wirth [28] that for the symmetrical TAA bromides deviations from the theoretical activity coefficients are not prohibitively large up to concentrations of 0.1 M. In the calculations the total concentration of electrolyte, including the amount of electrolyte necessary for obtaining the pH values concerned, was introduced.

Among the data necessary for employing the formulas mentioned, especially $d\Gamma / d\log(\gamma c)$ is only known with a limited accuracy. We approximated this by using $\Delta\Gamma / \Delta\log(\gamma c)$ for the adjacent $\log(\gamma m)$ step in the case of the lowest and highest concentrations investigated. For intermediate $\log(\gamma m)$ values $d\Gamma / d\log(\gamma c)$ was found by linear interpolation between the $\Delta\Gamma / \Delta\log(\gamma c)$ values of the adjacent $\log(\gamma m)$ steps.

Table 4.2 contains the results. The values reported refer to a total number of sites = $2.0 \cdot 10^{-7}$ mole/m²: but similar results were obtained for a total number of sites equal to the values described in table 4.1.

For the lowest concentrations investigated the results are rather uncertain, owing to the difficulty in estimating $d\Gamma / d\log(\gamma c)$ for these cases. If we leave these values out of consideration, it is seen that, as in previous publications, generally $d\phi / d\log(\gamma c)$ is negative, with the trend that its

Chapter IV

Table 4.2: Stimulated adsorption model calculations for TMA bromide on silica.

[TMA bromide] (10 ⁻³ M)	Adsorbed amount (10 ⁻⁸ mole/m ²) ¹⁾	$e_0/kT \cdot d\phi/d\log(\gamma m)$	
		w/f=0.1	w/f=0.5
pH=3:			
0.997	0.22	-11.95	-13.37
2.862	1.61	0.08	-1.60
9.687	3.38	-5.51	-1.60
29.09	11.75	-1.31	-4.98
96.11	18.83	-11.58	---- ²⁾
pH=5:			
0.823	1.63	1.17	-0.46
2.713	2.48	-0.09	-2.06
9.318	6.93	-0.28	-2.91
28.88	13.24	-0.25	-3.67
96.31	17.13	-1.11	-5.82

¹⁾ Value corrected for the amount present in the diffuse part of the double layer.

²⁾ Large value for average adsorption energy required for explaining the experimentally measured adsorbed amount. In this case, the integrals could not be calculated for the broad range of adsorption energies between $-5w$ and $+5w$.

absolute value increases with increasing concentration. The local potential at adsorption sites therefore changes in a direction opposite found for the ζ potential. This confirms the central issue of the stimulated adsorption model, viz. that the ζ potential is not a good approximation for the local potential at

Chapter IV

the adsorption sites. In calculating electrical repulsions, however, it is a good approximation for the Stern potential, since here we are dealing with a potential averaged over the Stern plane.

The fact that the absolute value of $d\phi / d\log(\gamma c)$ increases with increasing TMA concentration is to be expected since at large concentrations the average distance between adsorbed ions is small, resulting in a more pronounced influence on the total adsorption energy at a site being occupied, from neighbouring sites. Thus the model appears to be consistent with adsorption data of ions even in the case when we are dealing with non-lattice ions.

For the adsorption of TEA and TPA bromide the stimulated adsorption model cannot be used because the adsorption does not level off at large concentrations, which makes a reasonably accurate estimate of the total number of available sites impossible. The adsorption data, especially the large adsorption for TEA and TPA at high concentration compared to adsorption for TMA, can be understood as follows:

At low concentrations of TAA bromide, only the interaction of individual ions with the silica surface is important: the hydrophobically hydrated regions around adsorbed ions do not overlap to a significant degree. With TMA bromide, the limiting adsorption is reached in this stage. With larger ions such as TEA and TPA, when this limiting stage of adsorption of individual ions is reached, additional sites become energetically attractive because parts of the adsorbed ions are close enough for the hydrophobically hydrated layer around an additional ion to have some form of overlap with hydration layers around previously adsorbed ions. The overlap of the hydration layers is not thought to be due to the formation of a bilayer but it makes relatively unattractive adsorption sites energetically acceptable.

Chapter IV

At this transition of adsorption of individual ions to adsorption of cooperative ions, the adsorption density is about $3 \cdot 10^{-7}$ mole/m². This corresponds with an average mutual distance between adsorbed ions of the order of 2.5 nm (assuming homogeneous distribution of adsorbed ions over the surface), which is still quite large compared with the radii of TEA and TPA ions. These radii are estimated to be of the order of 0.5-0.6 nm when the first hydration layer is included. However, when the possibility of non-homogeneous distribution of the adsorbed ions over the surface is envisaged, then it is possible that the distances between some sites are in the order of twice their radius (1-1.2 nm). In this case these sites can be occupied by the overlap of the hydration layers of the ions. The transition of ideally dispersed ions to clustered ions causes a change in adsorption energy (E in equation 4.10). This is a second reason why the stimulated adsorption model cannot be used for TEA and TPA bromide.

We stress that the idea represented in the last paragraph is at present a working hypothesis rather than an established theory.

4.5 Conclusions.

TAA ions have an influence on the ζ potentials of silica. The IEP shifts to higher pH. This can be regarded as the result of adsorption of TAA ions on the silica surface. The shifts in IEP were linearly dependent on the chain length. This shows that hydrophobic interactions are important for the adsorption. By describing the adsorption in terms of the Stern model of adsorption mean adsorption energies of -18.8 kJ/mole for TMA and -23.1 kJ/mole for TEA and TPA are found. The number of adsorption sites increases from $2.5 \cdot 10^{-7}$ mole/m² for TMA to $4.2 \cdot 10^{-7}$ mole/m² for TPA. The

Chapter IV

influence of the surface charge on the adsorption was small. This leads to the conclusion that the TAA ions do not adsorb on the charged silanol groups. This is in agreement with the conclusions of the chapter II and III.

The adsorption data for TMA are consistent with stimulated adsorption by cations and anions, even in this case where we are dealing with the adsorption of non-lattice ions. For TEA and TPA these theories cannot be used because the total number of sites cannot be estimated from the experimental results. The high adsorption for TEA and TPA bromide at high concentrations is considered to take place because the distances between some sites are in the order of twice the ionic radius. In that case the overlap of hydration layers makes relatively unattractive adsorption sites energetically acceptable.

The results of the adsorption can be explained by assuming that the adsorption sites consist of small siloxane like hydrophobically hydrated places on the silica surface. It is possible that these siloxane groups are stabilized by the adsorption of TAA ions. This could be an explanation for the slow dissolution rate of silica in TMA hydroxide solutions as found by Wijnen [2].

References.

- [1] J.Rubio and J.Goldfarb, *J.Coll.Int.Sci.*, 36(1971)289.
- [2] P.Wijnen, thesis, Eindhoven, 1990.
- [3] E.J.W.Verwey and J.Th.G.Overbeek, "Theory of the stability of lyophobic colloids", Elsevier, Amsterdam, 1948, p.60.
- [4] G.D.Parfitt and N.H.Picton, *Trans.Faraday Soc.*, (1968)1955-1964.
- [5] R.G.Horn and D.T.Smith, *J.Non-Cryst.Solids*, 120(1990)72.
- [6] R.J.Hunter, "Zeta potential in Colloid Science", Academic press,

Chapter IV

London, 1981, p362.

- [7] N.Kamo, T.Aiochi, K.Kurihara and Y.Kobastake, *Coll.Polym.Sci.*, 256(1978)31.
- [8] T.F.Tadros and J.Lyklema, *J.Electroanal.Chem.*, 17(1976)9.
- [9] D.E.Yates, S.Levina and T.W.Healy, *J.Chem.Soc.,Faraday I*, 70 (1974)1807.
- [10] W.Smit and C.L.M.Holten, *J.Coll.Int.Sci.*, 78(1980)1.
- [11] T.W.Healy and L.R.White, *Adv.Coll.Sci.*, 9(1978)303.
- [12] M.J.G.Janssen and H.N.Stein, *J.Coll.Int.Sci.*, 111(1986)112-118.
- [13] P.W.Schindler, B.Fürst, R.Dick and P.U.Wolf, *J.Coll.Int.Sci.*, 55 (1976)469.
- [14] C.A.M.Siskens, H.N.Stein and J.M.Stevens, *J.Coll.Int.Sci.*, 52(1975) 251.
- [15] A.J.G. van Diemen and H.N.Stein, *J.Coll.Int.Sci.*, 67(1978)213.
- [16] A.J.G. van Diemen and H.N.Stein, *Sci. of Ceramics*, 9(1977)264-271.
- [17] H.N.Stein, *Adv.Coll.Sci.*, 11(1979)67.
- [18] P.Somasundaran, T.W.Healy and D.W.Fürstenau, *J.Phys.Chem.*, 68(1964)3562.
- [19] P.Claesson, R.G.Horn and R.M.Pashley, *J.Coll.Int.Sci.*, 100(1984) 250.
- [20] M.W.Rutland and R.M.Pashley, *J.Coll.Int.Sci.*, 130(1989)448.
- [21] G.R.Wiese and T.W.Healy, *J.Coll.Int.Sci.*, 51(1975)34.
- [22] P.H.Wiersema, A.L.Loeb and J.Th.G.Overbeek, *J.Coll.Int.Sci.*, 22(1966)78.
- [23] M. von Smoluchowski, *Handbuch der Elektrizität und des Magnetismus* (L.Graetz), vol II, Barth, Leipzig, 1921, p.336.

Chapter IV

- [24] J.A.W. van Laar, thesis, Utrecht, 1952.
- [25] C.L.M.Holten and H.N.Stein, *Analist*, 115(1990)1211.
- [26] R.K.Iler, "The Chemistry of Silica", John Wiley and sons, New York, 1979. ^a p. 186., ^b p. 660.
- [27] S.Lindenbaum and G.E.Boyd, *J.Phys.Chem.* 68(1964)911-917.
- [28] H.E.Wirth, *J.Phys.Chem.* 71(1967)2922.

CHAPTER V:

CONCLUSIONS

In zeolite syntheses organic templates are used. The role of these templates has until now not been fully understood. Specific interactions between the templates and the zeolite precursor phase are thought to be the main reason for the action of the template. In this thesis interactions between a special class of templates, the symmetrical TAA ions, and a zeolite precursor, silica, are investigated. The formation of specific double ring silicate structures, which takes place, can be considered as a result of the presence of the interactions between the TAA ions and silicate ions in solutions. These double ring silicate ions are thought to be important intermediates in the zeolite syntheses. This thesis reports some evidence on these interactions.

In chapter II the dependence of the viscosity on the concentration is described with the extended Jones-Dole equation. The Jones-Dole equation is the only theory which describes the viscosity of electrolyte solutions as a function of the concentration in terms of interaction parameters, the Jones-Dole coefficients A, B and D. The A coefficient describes the electrostatic interactions. For TMA silicate the A coefficient was approximately 2½ times higher than for sodium silicate and 3 times higher than for potassium silicate. For mixtures of TMA silicate with sodium or potassium silicate the influence of the alkali silicates on the A coefficient was much higher than of TMA silicate. Especially the difference in A coefficient between TMA silicate and sodium silicate can not be explained by current theories as TMA and sodium ions have the same mobility. An explanation is that the TMA silicate distance is larger than the equilibrium distance predicted by the Debye-

Chapter V

Hückel theory.

The B coefficient, which describes solute solvent interactions, is in agreement with the additivity rule for mixtures of TMA silicate with alkali metal silicates for all solutions except for TMA silicate. The large values of the B coefficient for silicate solutions can be considered as a result of the presence of a strongly ordered hydration layer around the silicate and the TMA.

The D coefficient is not well defined. It should contain high order terms of the A and B coefficients and solute-solute interactions. In our systems a high D coefficient was found for TMA silicates. This D coefficient was much higher than for TMA bromide and alkali metal silicate. This should be an indication on the presence of additional interactions between the TMA and silicate ions.

The molecular picture we obtained from these results is that besides the electrostatic attraction, an additional interaction is present between the TMA and the silicate ions. An additional attraction between TMA and silicate ions would have been visible as a decrease in the A coefficient and a high influence of TMA ions in mixtures. We found a high A coefficient for TMA silicate solutions. It is very likely that the interaction between TMA and silicate ions is a repulsion. This explains the high value of the A coefficient and the strong influence of the alkali metal ions. In solutions with only TMA and silicate ions present the distance between TMA and silicate ions is larger than predicted by the Debye-Hückel theory. In mixtures of TMA silicate and alkali metal silicate the alkali metal ions can approach the silicate ions more closely than the TMA ions. Therefore the alkali metal ions will be preferentially closer to the silicate ions. This results in an ion cloud which does not differ much from the Debye-Hückel ion cloud and the A coefficient does not differ much from the alkali metal silicate value. This behaviour is thought to

Chapter V

be caused by the difference in hydration of the TMA and the silicate ions. The silicate ions are hydrophilically hydrated and the TMA ions are hydrophobically hydrated. As these hydration layers are caused by different effects it is likely that a structural difference is present between both highly structured regions. This means that these regions cannot overlap and a repulsive interaction is present.

In chapter III the coacervation behaviour of the system water- TMA bromide- sodium silicate is described. Coacervation is the demixing of aqueous solutions into two different layers. In order to obtain coacervation it is necessary to have the combination of TAA halogenide or nitrate with alkali metal silicate. In our systems the TAA bromide was present in the upper layer and the sodium silicate in the lower. This is an indication that the coacervation is caused because of a repulsion between the TMA and the silicate ions. This is in agreement with the results of the viscosity measurements.

The coacervation was described using partial miscibility theories. For this the excess Gibbs free energy was calculated. The excess Gibbs free energy was split into pair interactions. The pair interactions of the salts with water were described with the activity coefficients and the TMA-silicate interaction term was described with the Redlich-Kister equation. From the Redlich-Kister equation only the first two terms were used. With this Gibbs free energy the binodals were calculated. These calculated binodals were in reasonable agreement with the experimental binodals.

The excess Gibbs free energy is the combination of an interaction enthalpy and an excess entropy. The excess entropy (strictly Ts^E) is thought to be much smaller than the excess enthalpy and is therefore neglected. By using the Redlich-Kister equation for the excess Gibbs free energy the interaction

Chapter V

enthalpy has two contributions: i) one TAA ion with one Silicate ion and ii) two TAA ions with one silicate ion and one TAA ion with two silicate ions. The two contributions were dependent on the type of organic cation and the sodium/silicate ratio. At increasing sodium/silicate ratio the interaction enthalpy of two TAA ions with one silicate ion increases. This is thought to be an effect of the charge of the silica which increases with increasing sodium/silicate ratio. The interaction enthalpy of one TAA ion with one silicate ion decreases with increasing sodium/silicate ratio. This is thought to be due to the diminished charge compensation of the silica by the TAA.

For several different TAA ions the interaction enthalpy of one TAA ion with one silicate ion increases slightly with increasing chain length. The interaction enthalpy of two TAA ions with one silicate ion increases with the square of the hydrophobic hydration enthalpy. This shows that the coacervation is dependent on the hydrophobic hydration of the TAA ions. This supports the origin of the repulsive interaction between TAA ions and silicate ions which was reported in chapter II.

This leads to the following mechanism of the coacervation:

TAA ions are hydrophobically hydrated and silicate ions are hydrophilically hydrated. The structures of these hydration layers are different and can therefore not overlap. In solutions which contain, besides TAA and silicate ions, a cation (e.g. sodium) and an anion (e.g. bromide) coacervation can occur. At higher concentrations the TAA and silicate ions will migrate apart because of the repulsion. The respective charges will be predominantly neutralized by the other ions present. The sodium will surround the silicate and the bromide the TAA. This way two microstructures are formed. At higher concentration coalescence of these microstructures will occur to macroscopic droplets and gravity will cause the formation of both layers.

Chapter V

In chapter IV the adsorption of TAA ions on silica is described. Although repulsive interactions are present between TAA- and silicate- ions adsorption of TAA ions on silica does occur. The repulsion between silicate ions and TAA ions is most likely to take place between the charged groups of the silicate ions and the TAA ions. Silica surface have beside the silanol groups at the surface also other groups, like siloxane bridges. With the help of ζ potentials the adsorption was studied. The IEP of silica shifted for the TAA ions to higher values. This is an indication of the specific adsorption of TAA on the silica surface. The shifts in IEP were linearly dependent on the chain length. This is an indication that hydrophobic interactions play an important role in the adsorption.

With the help of the Stern model of adsorption the adsorption energy and the number of adsorption sites were determined at pH=3 and pH=5. All adsorption energies were between -18 and -25 kJ/mole. For TMA the adsorption energy was about 20 % smaller than for TEA and TPA. The number of adsorption sites increased with increasing chain length. These adsorption sites are thought to be hydrophobic sites. The adsorption takes place because the hydration layer of the TAA ion can overlap with the hydration layer of the site. The size of these sites is quite small. This explains the small differences in adsorption energy between TMA, TEA and TPA. The size of the site is so small that TEA and TPA cover the complete site and have the same overlap. The smaller TMA covers most of the site and the adsorption energy is a little smaller than for TEA and TPA. For the dependence of the number of sites on the chain length two explanations are possible:

i) The sites are small and most probably surrounded by silanol groups. Between the silanol groups and the TAA ions a repulsion is present (see

Chapter V

chapters II and III). Some sites will be shielded by the silanol groups. The stronger the hydrophobic hydration the easier these sites can be used for adsorption. Therefore the number of sites increases with increasing chain length.

ii) Some sites are present at a flat S/L interface. These sites can be occupied by all TAA ions. Other sites are present in clefts. If the cleft is narrow it may be impossible for the ion to enter it, while a separate alkyl chain can enter these clefts. The longer the alkyl chains the better they can enter the clefts. Therefore the number of sites increases with increasing chain length.

The adsorption of TAA ions influences the local potential and more hydroxylic ions can adsorb. This influences the local potential on adjacent adsorption sites and more TAA can adsorb. For TMA the local potential decreased with increasing concentration. This is an indication that stimulated adsorption takes place. For TEA and TPA bromide these theories cannot be used because the total number of sites cannot be estimated from the experimental results. The high adsorption for TEA and TPA bromide at high concentrations is considered to take place because the distances between some sites are in the order of twice the ionic radius. In that case the overlap of hydration layers makes relatively unattractive sites energetically acceptable.

Overall in systems with TAA ions and silica repulsions and attractions are present. Repulsions are present between silanol groups and TAA ions and attractions between hydrophobic parts of the silica and the TAA ions. This dualistic behaviour is offered here as an explanation for the formation of double ring silicates in solutions of TAA silicates. These structures have relatively few silanol groups per silicate unit and a lot of siloxane bridges. Our results indicate that the hydration structures of these siloxane bridges have more in common with the hydrophobic hydration of the TAA ions than

Chapter V

the hydration layer of the silanol groups. Similarly zeolites contain mostly siloxane bridges and the zeolite formed may have a hydration structure which is comparable with the hydration structure of the template. Adsorption of TAA ions on the zeolite is expected to stabilize these siloxane bridges, which explains the inhibition of quartz formation when TAA ions are used.

APPENDIX A: VISCOSITIES OF SILICATE SOLUTIONS.

In this appendix the viscosities are given of the silicate solutions of chapter II. In that chapter only the Jones-Dole coefficients are shown in graphical form.

TABLE A.1.

TMA silicate	
concentration	$\eta_r (\pm 0.01 \%)$
0.0296	1.0115
0.0694	1.0246
0.0995	1.0351
0.1403	1.0502
0.2806	1.1031
0.4250	1.1620
0.5645	1.2297
0.6969	1.3037

TABLE A.2.

K Silicate	
concentration	$\eta_r (\pm 0.01 \%)$
0.0300	1.0066
0.0513	1.0110
0.1005	1.0210
0.1793	1.0376
0.2767	1.0593
0.3825	1.0843
0.4871	1.1087
0.6485	1.1519

TABLE A.3.

TMA / K silicate 1/3	
concentration	$\eta_r (\pm 0.01 \%)$
0.0297	1.0073
0.0502	1.0119
0.1087	1.0262
0.1759	1.0435
0.2756	1.0690
0.3820	1.0974
0.5156	1.1373
0.6523	1.1808

TABLE A.4.

TMA / K silicate 1/1	
concentration	$\eta_r (\pm 0.01 \%)$
0.0301	1.0089
0.0701	1.0199
0.1404	1.0406
0.2173	1.0606
0.3050	1.0864
0.3715	1.1065
0.5489	1.1624
0.6951	1.2123

TABLE A.5.

TMA / K silicate 3/1	
concentration	$\eta_r (\pm 0.01 \%)$
0.0299	1.0093
0.0512	1.0167
0.1003	1.0329
0.1808	1.0591
0.2900	1.0974
0.3945	1.1341
0.5495	1.1923
0.6845	1.2510

TABLE A.6.

Na silicate	
concentration	$\eta_r (\pm 0.01 \%)$
0.0349	1.0121
0.1050	1.0327
0.1494	1.0461
0.2235	1.0684
0.4534	1.1494
0.6336	1.2151
0.9751	1.3562
1.3016	1.5124

TABLE A.7.

TMA/Na silicate 54/146	
concentration	$\eta_r (\pm 0.01 \%)$
0.0189	1.0074
0.0197	1.0167
0.1023	1.0334
0.1806	1.0597
0.2653	1.0882
0.3822	1.1299
0.5192	1.1815
0.6732	1.2448

TABLE A.8.

TMA/Na silicate 1/1	
concentration	$\eta_r (\pm 0.01 \%)$
0.0300	1.0111
0.0700	1.0231
0.1006	1.0362
0.1398	1.0508
0.2836	1.1059
0.3455	1.1300
0.5189	1.2053
0.6998	1.2917

TABLE A.9.

TMA:Na silicate 138:62	
concentration	$\eta_r (\pm 0.01 \%)$
0.0311	1.0124
0.0511	1.0196
0.0993	1.0364
0.1817	1.0665
0.2802	1.1040
0.3963	1.1515
0.5377	1.2152
0.6992	1.2925

APPENDIX B: MOLAR FRACTIONS OF ELECTROLYTES.

A normal way of calculating the composition of mixtures in terms of molarfractions is given in equation B.1.

$$x_i = \frac{n_i}{\sum n_j} \quad (\text{B.1})$$

In this equation is x_i the molarfraction of compound i and n_i the amount of compound i in moles. For electrolytes the dissociation has to be incorporated in the molarfractions (equation B.2).

$$x_i = \frac{v_i n_i}{\sum v_j n_j} \quad (\text{B.2})$$

In this equation v_i is the amount of ions in one molecule of compound i .

The main point of this notation is that the activity coefficient of the solute has to be one at infinite dilution. In this appendix we will prove that this is the case for this definition of the molarfraction.

Considering a binary mixture of water with salt S ($A_{v+}B_{v-}$) we can describe the system with molarfractions:

$$x_0 = \frac{n_0}{n_0 + n_+ + n_-}, x_+ = \frac{n_+}{n_0 + n_+ + n_-}, x_- = \frac{n_-}{n_0 + n_+ + n_-} \quad (\text{B.3})$$

The G-function can be described as:

$$G = x_0 \mu_0^0 + x_+ \mu_+^0 + x_- \mu_-^0 + RT \{ x_0 \ln \gamma_0 x_0 + x_+ \ln \gamma_+ x_+ + x_- \ln \gamma_- x_- \} \quad (\text{B.4})$$

The amounts of ions can be rewritten in terms of amount S:

$$n_+ = v_+ n_S, n_- = v_- n_S, v = v_+ + v_- \quad (\text{B.5})$$

The molarfractions become:

$$x_S = \frac{v n_S}{n_0 + v n_S}, x_+ = \frac{v_+}{v} x_S, x_- = \frac{v_-}{v} x_S \quad (\text{B.6})$$

Combination B.6 with B.4 yields:

$$G = x_0 \mu_0^0 + x_S \frac{v_+ \mu_+^0 + v_- \mu_-^0}{v} + RT \left\{ x_0 \ln \gamma_0 x_0 + \frac{v_+ x_S}{v} \ln \frac{\gamma_+ v_+ x_S}{v} + \frac{v_- x_S}{v} \ln \frac{\gamma_- v_- x_S}{v} \right\} \quad (\text{B.7})$$

Rewriting gives:

$$G = x_0 \mu_0^0 + x_s \frac{v_+ \mu_+^0 + v_- \mu_-^0}{v} +$$

$$RT \left\{ x_0 \ln x_0 + x_s \ln x_s + x_s \ln \frac{v_+^{v_+} v_-^{v_-}}{v^v} + \right. \quad (\text{B.8})$$

$$\left. x_0 \ln \gamma_0 + x_s \ln \gamma_+^{v_+} \gamma_-^{v_-} \right\}$$

$$G = x_0 \mu_0^0 + x_s \left(\frac{v_+ \mu_+^0 + v_- \mu_-^0}{v} + K \right) +$$

$$RT \left\{ x_0 \ln x_0 + x_s \ln x_s + x_0 \ln \gamma_0 + x_s \ln \gamma_{\pm} \right\} \quad (\text{B.9})$$

Equation B.9 is very similar to equation B.4. The differences are that equation B.9 deals with a two component system instead of a three component system. Equation B.9 contains a molarfraction and an activity coefficient which are based on the amount of salt S. By using the molarfraction as described in equation B.6 the activity coefficient approaches unity at infinite dilution.

APPENDIX C: ADDITION OF A LINEAR FUNCTION TO THE G-CURVE.

In chapter III is stated that the contributions of the Gibbs free energies of the pure components and of the components in their standard state to the G-function are a function linear to the distance coordinate and therefore they do not influence the phase separation in coacervates. By calculating the G-function along a conode the composition of the two layers are the intercepts of the G-function with the double tangent. In the following derivation will be shown that by addition of a function linear in the distance coordinate the intercepts of the double tangent do not change.

Consider G-curve $G(i)$ with double tangent $Si+A$. There is a function $G^+(i)$:

$$G^+(i) = G(i) + Ki \quad (C.1)$$

$G^+(i)$ has a double tangent $Ci+B$. For the intercepts is:

$$G^+(i) = Ci + B \quad (C.2)$$

$$G(i) + Ki = Ci + B \quad (C.3)$$

$$G(i) = (C-K)i + B \quad (C.4)$$

A and B are the same and for every K there will be a possible C that makes:

$$S=C-K \quad (C.6)$$

Therefore the intercepts don't change by adding a function, linear in i , to the G-curve.

SUMMARY.

In zeolite syntheses tetraalkylammonium (TAA) ions are used as template. The operation is based on specific interactions between the template and the precursor phase. In order to obtain insight in these interactions viscosity measurements were performed and coacervation in solutions of TAA and silicate ions and adsorption of TAA ions on silica were investigated.

The viscosities of silicate solutions were described with the Jones-Dole equation. It appeared that the ion cloud of tetramethylammonium (TMA) silicate behaved in a different way from the ion cloud of sodium silicate. The hydration of the TMA- and silicate- ions is from a different origin (hydrophobic and hydrophilic hydration) and the regions with characteristic water structures cannot overlap. This causes an enlargement of the distance of closest approach between these ions.

In solutions of TAA bromide and sodium silicate demixing into two aqueous layers occurs. The TAA bromide was predominantly present in one layer and the sodium silicate in the other. The demixing, coacervation, was described with the activity coefficients of the separate salts and an excess Gibbs free energy. Some terms of the Gibbs free energy were dependent on the enthalpy of hydrophobic hydration of the TAA ions. This leads to the following mechanism for coacervation:

Because of the difference in hydration TAA and silicate ions cannot approach. If sodium and bromide ions are present then the bromide will surround the TAA ions preferentially and the sodium ions the silicate ions. This way two microstructures are present. At high concentration coalescence occurs and two layers are formed.

However, on solid silica specific adsorption of TAA ions takes place.

Hydrophobic interactions play an important role. The difference between the behaviour of the silicate ions and the solid silica is ascribed to the presence of hydrophobic siloxane like groups, while the silanol groups have a hydrophilic character. The sites are small hydrophobic places on the surface with a mean Gibbs free energy of adsorption of -18 KJ/mole for TMA and -23 KJ/mole for TEA and TPA. The sites are thus small that the overlap region of the site with TEA and TPA are the same. This explains the similar Gibbs free energy of adsorption for these ions.

SAMENVATTING.

Bij de synthese van zeolieten worden tetraalkylammoniumionen (TAA) gebruikt als template. De werking berust op specifieke interacties tussen de template en de precursor fase. Om inzicht te verkrijgen in deze interacties werden viscositeitsmetingen verricht, coacervatie in oplossingen met TAA en silikaat ionen en de adsorptie van TAA op silika onderzocht.

De viscositeiten van silikaat oplossingen werden beschreven met de Jones-Dole vergelijking. Het bleek dat de ionenwolk van tetramethylammonium (TMA) silikaat zich anders gedroeg dan de ionenwolk van natrium silikaat en kalium silikaat. De hydratatie van de TMA en silikaat ionen is van verschillende origine (hydrofoob en hydrofiel) en de gebieden met de typische waterstructuren kunnen daardoor niet overlappen. Dit veroorzaakt een vergroting van de afstand van dichtste nadering tussen deze ionen.

In oplossingen van TAA bromide en natrium silikaat treedt ontmenging in twee waterige lagen op. Het TAA bromide bevond zich voornamelijk in de ene laag en het natrium silikaat in de andere. De ontmenging, ook coacervatie genoemd, werd beschreven in termen van mengentropie en excess Gibbs vrije energie. Sommige termen van de excess Gibbs vrije energie gedroegen waren afhankelijk van de enthalpie van hydrofobe hydratatie van de TAA ionen. Hieruit volgt voor het mechanisme van coacervatie: Door het verschil in hydratatie kunnen TAA en silikaat ionen elkaar niet naderen. Als er natrium en bromide ionen aanwezig zijn zullen de bromide ionen de TAA ionen preferent omringen en de natrium ionen de silikaat ionen. Op deze wijze ontstaan twee microstructuren. Bij hoge concentratie treedt coalescentie op en worden twee lagen gevormd.

Op vast silika treedt echter wel specifieke adsorptie van TAA ionen op. Hydrofobe interacties spelen een grote rol. Het verschil tussen het

gedrag van silikaat ionen en vast silika wordt daaraan toegeschreven, dat siloxaan groepen een hydrofoob karakter hebben en de silanol groepen een hydrofiel karakter. De sites zijn kleine hydrofobe plaatsen op het oppervlak met een gemiddelde Gibbs vrije energie van adsorptie van -18 KJ/mol voor TMA en -23 KJ/mol voor TEA and TPA. De sites zijn zo klein dat TEA en TPA een gelijke overlap hebben met de site zodat een gelijke adsorptie energie gevonden werd.

CURRICULUM VITAE.

Jacques Cor Johan van der Donck werd geboren op 25 September 1965 te Oranjestad (Aruba). In 1977 ging hij naar Het Rhedens Lyceum te Rozendaal (Gld). Alwaar hij in 1983 het diploma VWO behaalde.

In datzelfde jaar begon hij met de studie Scheikunde aan de Rijksuniversiteit Utrecht. In 1984 slaagde hij voor het propaedeutisch examen. Als specialisaties koos hij colloidchemie and de anorganische chemie (katalyse). In 1987 studeerde hij af bij Prof. Dr. ir. J.W.Geus in anorganische chemie.

Van 1 September 1987 tot 1 December 1991 was hij als assistent in opleiding in dienst van de Technische Universiteit Eindhoven. Bij de vakgroep colloidchemie en thermodynamica werd gedurende die tijd, onder supervisie van Prof. Dr. H.N. Stein, het in dit proefschrift beschreven onderzoek uitgevoerd.

DANKWOORD.

Hoewel er op dit proefschrift slechts een naam staat hebben velen aan het tot stand komen van dit proefschrift bijgedragen. Deze mensen wil ik graag bedanken voor hun inspanningen. Een aantal wil ik persoonlijk noemen.

Op de eerste plaats wil ik mijn promotor Prof.Dr. H.N. Stein bedanken voor de vele discussies, evaluaties die we samen gehad hebben en alle tijd die hij voor me heeft vrij gemaakt. Prof.Dr. R.A. van Santen ben ik erkentelijk voor de plezierige wijze waarop hij de voltooiing van dit proefschrift heeft begeleid. Alle studenten die met hun inspanningen iedere keer weer een stapje verder kwamen, in het bijzonder: Martin van den Heuvel, Dirk Kuijken en Jan Vaessen. Verder dank ik de medewerkers van de vakgroep Colloidchemie en Thermodynamica voor de collegialiteit en vriendschap die gedurende mijn promotie een steun en stimulans was om dit werk tot een goed eind te brengen. Hier wil ik speciaal noemen P-P van Mierlo, Peter Baets, Gert Tuin en Jan Vaessen.

IOP-katalyse en STIPT wil ik graag bedanken voor de financiële ondersteuning. Degussa Nederland B.V. dank ik voor het volkomen belangeloos ter beschikking stellen van monsters Degussa Aerosil 200 waaraan de in hoofdstuk 4 beschreven experimenten zijn uitgevoerd.

Als laatste dank ik mijn familie, die met raad en daad hebben bijgedragen aan dit proefschrift, en in het bijzonder dank ik Angela voor alle geduld en ondersteuning welke gedurende het onderzoek en schrijven vaak op de proef werden gesteld.

Stellingen

behorende bij het proefschrift van

J.C.J. van der Donck

1. Het vervangen van experimentele A-coëfficiënten door theoretische waarden door Crudden et al. gebeurt op oneigenlijke gronden.
J.Crudden, G.M.Delaney, D.Feakins and D.J. O'Reilly, J.Chem.Soc., Faraday 1, 82(1986)2195-2206.
2. Het door Somasundaran et al. veronderstelde adsorptie-mechanisme van alkylammonium-ionen op silika is strijdig met de in dit proefschrift gevonden resultaten (zie H.4).
P.Somasundaran, T.W.Heally and D.W.Fürstenau, J.Phys. Chem., 68(1964)3562.
3. Het is niet aannemelijk dat de temperatuur-afhankelijke term van de B-coëfficiënt gecorreleerd kan worden met de activerings-energie voor de coördinatie van watermolekulen aan een ion.
J.Crudden, G.M.Delaney, D.Feakins and D.J. O'Reilly, J.Chem.Soc., Faraday 1, 82(1986)2195-2206.
4. Rutland and Pashley berekenen ten onrechte de ζ -potentiaal uit mobiliteit met de von Smoluchowski vergelijking.
M.W.Rutland and R.M.Pashley, J. Colloid Interface Sci., 130(1989) 448.
5. Gorski verwaarloost ten onrechte het buitengesloten volume van ionen.
N.Gorski, Z.phys.Chemie, Leipzig, 264(1983)640-644.

6. Werblan geeft in vergelijking 8 een onjuist beeld van de A-coëfficiënt van de Jones-Dole vergelijking.
L.Werblan, BULLETIN DE L'ACADEMIE POLONAISE DES SCIENCES, Serie de sciences chimiques Volume XXVII, No. 11, 1979.
7. De bewering van Rutland en Pashley dat de snelle coagulatie van silika-dispersies, zoals gevonden door Rubio en Goldfarb, verklaard kan worden met het door hen gevonden minimum in de ζ -potentiaal - concentratie curve is onjuist.
M.W.Rutland and R.M.Pashley, J.Colloid Interface Sci., 130(1989)-448.
J.Rubio and J.Goldfarb, J.Colloid Interface Sci., 36(1971)289.
8. Wanneer de werking van homeopathische middelen berust op hormesis zou het gebruik van deze middelen slechts symptoombestrijding zijn.
9. Zolang er tegenstellingen bestaan tussen Xhsosas en Zulus is het niet terecht dat in de Nederlandse pers alleen aandacht wordt besteed aan het ANC.
10. Gezien de geringe kwaliteit van de Nederlandse televisieprogramma's is het betalen van de omroepbijdragen tevergeefs.
11. Veel stellingen wekken de indruk dat degene die de stelling poneert dieper inzicht heeft in de materie dan de auteur waarover de stelling gaat.